National Library of Canada
Bibliothèque nationale du Canada

Canadian Theses Service
Service des thèses canadiennes

Ottawa, Canada
K1A 0N4

NOTICE

The quality of this microform is heavily dependent upon the quality of the original thesis submitted for microfilming. Every effort has been made to ensure the highest quality of reproduction possible.

If pages are missing, contact the university which granted the degree.

Some pages may have indistinct print especially if the original pages were typed with a poor typewriter ribbon or if the university sent us an inferior photocopy.

Reproduction in full or in part of this microform is governed by the Canadian Copyright Act, R.S.C. 1970, c. C-30, and subsequent amendments.

AVIS

La qualité de cette microforme dépend grandement de la qualité de la thèse soumise au microfilmage. Nous avons tout fait pour assurer une qualité supérieure de reproduction.

S'il manque des pages, veuillez communiquer avec l'université qui a conféré le grade.

La qualité d'impression de certaines pages peut laisser à désirer, surtout si les pages originales ont été dactylographiées à l'aide d'un ruban usé ou si l'université nous a fait parvenir une photocopie de qualité inférieure.

La reproduction, même partielle, de cette microforme est soumise à la Loi canadienne sur le droit d'auteur, SRC 1970, c. C-30, et ses amendements subséquents.

NL-339 (r. 86/04) c

Canada

National Library of Canada
Bibliothèque nationale du Canada

Canadian Theses Service
Service des thèses canadiennes

Ottawa, Canada
K1A 0N4

The author has granted an irrevocable non-exclusive licence allowing the National Library of Canada to reproduce, loan, distribute or sell copies of his/her thesis by any means and in any form or format, making this thesis available to interested persons.

L'auteur a accordé une licence irrévocable et non exclusive permettant à la Bibliothèque nationale du Canada de reproduire, prêter, distribuer ou vendre des copies de sa thèse de quelque manière et sous quelque forme que ce soit pour mettre des exemplaires de cette thèse à la disposition des personnes intéressées.

The author retains ownership of the copyright in his/her thesis. Neither the thesis nor substantial extracts from it may be printed or otherwise reproduced without his/her permission.

L'auteur conserve la propriété du droit d'auteur qui protège sa thèse. Ni la thèse ni des extraits substantiels de celle-ci ne doivent être imprimés ou autrement reproduits sans son autorisation.

ISBN 0-315-55625-0

Canada

THE UNIVERSITY OF ALBERTA

REACTIONS OF DICHLORO- AND DIBROMOSILYLENE

by

Vinod SANDHU

A THESIS

SUBMITTED TO THE FACULTY OF GRADUATE STUDIES AND RESEARCH IN

PARTIAL FULFILMENT OF THE REQUIREMENTS FOR THE DEGREE OF

DOCTOR OF PHILOSOPHY

DEPARTMENT OF CHEMISTRY

EDMONTON, ALBERTA.

(FALL 1989)

University of Alberta
Edmonton
Canada T6G 2G2

Department of Chemistry
Faculty of Science
E3-44 Chemistry Bldg., Tel. (403) 492-3254 Fax (403) 492-8231

September 21, 1989

Mr. Vinod Sandhu
Department of Chemistry
University of Alberta
Edmonton, Alberta
T6G 2G2

Dear Mr. Sandhu:

I hereby grant you permission to reproduce the following material for your Ph.D. thesis:

Figure I.2, "Absorption Spectrum of $SiCl_2$", which appeared in:
B.P. Ruzsicska, A. Jodhan, I. Safarik, O.P. Strausz and T.N. Bell,
Chem. Phys. Lett., 113 (1985) 67

and

Figure I.3, "Absorption Spectrum of $SiBr_2$", which appeared in:
B.P. Ruzsicska, A. Jodhan, I. Safarik, O.P. Strausz and T.N. Bell,
Chem. Phys. Lett., 139 (1987) 72.

Very sincerely,

Otto P. Strausz
Professor of Chemistry

OPS/lde

THE UNIVERSITY OF ALBERTA

RELEASE FORM

NAME OF AUTHOR: Vinod SANDHU

TITLE OF THESIS: Reactions of Dichloro- and Dibromosilylene

DEGREE: Doctor of Philosophy

YEAR THIS DEGREE GRANTED: 1989

Permission is hereby granted to THE UNIVERSITY OF ALBERTA LIBRARY to reproduce single copies of this thesis and to lend or sell such copies for private, scholarly or scientific research purposes only.

The author reserves other publication rights, and neither the thesis nor extensive extracts from it may be printed or otherwise reproduced without the author's written permission.

(Signed) Vinod Sandhu

PERMANENT ADDRESS:

c/o Prof. O.P. Strausz

Department of Chemistry, University of Alberta

Edmonton, Alberta, CANADA T6G 2G2

Date: Sept. 27, 1989

THE UNIVERSITY OF ALBERTA

FACULTY OF GRADUATE STUDIES AND RESEARCH

The undersigned certify that they have read, and recommend to the Faculty of Graduate Studies and Research for acceptance, a thesis entitled:

REACTIONS OF DICHLORO- AND DIBROMOSILYLENE

submitted by

Vinod SANDHU

in partial fulfilment of the requirements for the degree of Doctor of Philosophy.

O.P. Strausz – Supervisor

J.E. Bertie – Committee Chairman

G. Kotovych

D.D. Tanner

J. Gray – Physics

T.N. Bell – External Examiner

Date: Sept. 22, 1989

To Mom and Dad

ABSTRACT

Absolute rate constants of the room-temperature gas-phase reactions of dichlorosilylene, $SiCl_2$, with O_2, NO, CO, N_2O and 1,3-butadiene, and those of dibromosilylene, $SiBr_2$, with O_2 and NO have been measured using the flash photolysis-kinetic absorption spectroscopic technique.

$SiCl_2$ and $SiBr_2$ were generated by flash-photolysing Si_2Cl_6 and $SiBr_4$, respectively, and their absorption spectra were used to monitor their decay. Absolute rate constants were obtained from the increase in their decay rate in the presence of a substrate relative to the background decay. All the reactions investigated have been found to follow second-order kinetics — first-order in silylene and first-order in substrate concentration, and the following rate constants were obtained:

$SiCl_2$: $k_{O_2} = (3.4 \pm 0.2) \times 10^9\ M^{-1}s^{-1}$, $k_{NO} = (1.6 \pm 0.1) \times 10^9\ M^{-1}s^{-1}$, $k_{CO} = (6.3 \pm 0.7) \times 10^8\ M^{-1}s^{-1}$, $k_{N_2O} = (5.7 \pm 0.3) \times 10^8\ M^{-1}s^{-1}$, $k_{C_4H_6} = (5.4 \pm 0.3) \times 10^8\ M^{-1}s^{-1}$;

$SiBr_2$: $k_{O_2} = (5.6 \pm 0.4) \times 10^8\ M^{-1}s^{-1}$ and $k_{NO} = (2.8 \pm 0.4) \times 10^8\ M^{-1}s^{-1}$.

The reactions of $SiCl_2$ are faster than those of $SiBr_2$. Towards NO, $SiCl_2$ is less reactive than SiH_2 but towards CO it is more reactive than SiH_2. On the other hand, $^1CH_2$ reacts faster than CCl_2 with both NO and CO. Both $SiCl_2$ and $SiBr_2$ react with O_2 much faster than SiF_2. A similar trend has been observed for the CCl_2 *vs* CF_2 reactions with O_2.

Like its reactions with other unsaturated hydrocarbons, $SiCl_2$ was found to react as an electrophile with 1,3-butadiene. With unsaturated hydrocarbons its reactivity is

lower than that of SiH_2 and its selectivity among olefins is higher than that of SiH_2. This trend is similar to the relative selectivity of $^1CH_2$ *vs* CCl_2.

Mechanisms for each of the SiX_2 + S (X = Cl, Br; S = inorganic substrates) reactions investigated have been proposed on the basis of the rate constant measurements, thermochemical considerations, and previously reported qualitative data on the similar reactions of analogous species. Arrhenius parameters for all the primary reactions have also been estimated.

ACKNOWLEDGEMENTS

Upon completing this thesis I would like to express my sincere gratitude to Professor O.P. Strausz for his constant guidance and support throughout the project.

I am also deeply indebted to Dr. E.M. Lown for her helpful suggestions and tremendous assistance in the preparation of the manuscript.

I am equally grateful to Mr. Andrew Jodhan for giving me the benefit of his technical skills. I very much appreciate the heroic efforts of the technical staff, especially Mr. E. Feschuk and Mr. G. Streefkerk for maintaining the instrumentation.

Many thanks are also due Drs. I. Safarik, R.K. Gosavi, M. Torres and P. Mahaffy for their commentary and critical advice.

I would also like to convey many thanks to the members of the photochemistry group, the general office staff and especially to Mrs. Lillian Eastman for making my stay here a warm and memorable experience.

Last but not least, it is my pleasure to acknowledge the moral support (?) of all my friends at the U of A Dance Club, especially Elwood, Kitty, Spike and the gang.

TABLE OF CONTENTS

Page

ABSTRACT v

ACKNOWLEDGEMENTS vii

TABLE OF CONTENTS viii

LIST OF TABLES xii

LIST OF FIGURES xix

Chapter I INTRODUCTION 1

I.1. Physical Properties of Carbenes 1

I.2. Reactivity of Carbenes 6

I.3. Carbenes *vs* Silylenes 14

I.4. Generation of Dichloro- and Dibromosilylene 30

I.4.1. Thermochemical Generation 30

I.4.2. Photochemical Generation 32

I.4.3. Other Modes of Generation 34

I.5. Spectroscopy and Molecular Geometry of Dichloro- and Dibromosilylene 35

I.5.1. Spectrum of $SiCl_2$ 35

I.5.2. Spectrum of $SiBr_2$ 48

I.5.3. Molecular Geometries of $SiCl_2$ and $SiBr_2$ 51

I.6. Heats of Formation of $SiCl_2$ and $SiBr_2$.....55

I.7. Reactivities of Ground State Dichloro- and Dibromosilylene.....57

I.7.1. Qualitative Investigations.....57

I.7.1a. Insertion Reactions.....57

I.7.1b. Addition Reactions.....61

I.7.2. Quantitative Investigations.....64

I.8. Synthetic and Industrial Applications.....66

I.9. Aim of the Present Investigation.....73

Chapter II EXPERIMENTAL.....75

II.1. Apparatus.....76

II.1.1. The Vacuum System.....76

II.1.2. The Flash Photolysis-Absorption Spectroscopic System.....78

II.1.2a. The Reaction Vessel and the Reflective Housing.....78

II.1.2b. The Photolysis Lamp.....79

II.1.2c. The Spectroscopic Lamp.....82

II.1.2d. The Spectrograph.....84

II.1.3. The Microdensitometer.....84

II.2. Operational Procedure.....87

II.2.1. Operation of the Flash Photolysis System.....87

II.2.2. Preparation of the Gas Mixtures.....90

II.2.3. Developement of Photographic Plates.....91

II.3. Materials.....92

Chapter III RESULTS.....94

III.1. Background Decay of the Dihalosilylene Spectra as a Function of Time.....94

III.2. Background $SiCl_2$ Decay as a Function of Argon Pressure.....99

III.3. Reactions of Dihalosilylenes.....104

III.4. Reactions of $SiCl_2$.....105

III.4.1. The $SiCl_2 + O_2$ Reaction.....106

III.4.2. The $SiCl_2$ + NO Reaction.....113

III.4.3. The $SiCl_2$ + CO Reaction.....122

III.4.4. The $SiCl_2 + N_2O$ Reaction.....131

III.4.5. The $SiCl_2$ + 1,3-Butadiene Reaction.....141

III.4.6. The $SiCl_2$ + Isobutane Reaction.....150

III.5. Reactions of $SiBr_2$.....153

III.5.1. The $SiBr_2 + O_2$ Reaction.....153

III.5.2. The $SiBr_2$ + NO Reaction.....162

Chapter IV DISCUSSION.....172

IV.1. Argon Pressure Dependence of the Background Decay of $SiCl_2$.....172

IV.2. Mechanistic Aspects of the Reactions of $SiCl_2$ and $SiBr_2$.....173

IV.2.1. Reactions with Oxygen.....173

IV.2.2. Reactions with Nitric Oxide.....178

IV.2.3. Reaction with Carbon Monoxide.....183

IV.2.4. Reaction with Nitrous Oxide.....188
IV.2.5. Reaction with 1,3-Butadiene.....190

IV.3. Chemical Reactivities of Ground State Singlet
$SiCl_2$ and $SiBr_2$.....195
IV.3.1. Reactions with Inorganic Substrates.....195
IV.3.2. Reactions with Unsaturated Hydrocarbons.....201

SUMMARY AND CONCLUSIONS.....203

REFERENCES.....208

APPENDIX A.....221

APPENDIX B.....223

APPENDIX C.....226

APPENDIX D.....228

APPENDIX E.....233

LIST OF TABLES

Table		Page
I.1.	Equilibrium Ground State Geometries of CX_2 Species	5
I.2.	Absolute Rate Constants of the Reactions of CH_2 ($^1A_1$) and SiH_2 ($^1A_1$)	19
I.3.	Singlet–triplet Energy Separation (ΔE_{ST}) of Carbenes, CX_2, and Silylenes, SiX_2	21
I.4.	Absolute Rate Constants for the Gas-phase Reactions of SiX_2 and CX_2 (X = H, F)	28
I.5.	Assignment of the Absorption Spectrum of $SiCl_2$	44
I.6.	Fundamental Vibrational Frequencies of $SiCl_2$ in the $\tilde{X}\ ^1A_1$ and $\tilde{A}\ ^1B_1$ Electronic States	45
I.7.	Electronic Transition Energy, T_{00} {$\tilde{A}\ ^1B_1(0,0,0) \leftarrow \tilde{X}\ ^1A_1(0,0,0)$} of $SiCl_2$	46
I.8.	Vibrational Frequencies of $SiBr_2$ ($^1A_1$) and Vertical Excitation Energy, T_e (cm^{-1}), of its $\tilde{A}\ ^1B_1 \leftarrow \tilde{X}\ ^1A_1$ Transition	51
I.9.	$\tilde{A}\ ^1B_1 \leftarrow \tilde{X}\ ^1A_1$ Electronic Energies of Group IV A Dihalides MX_2 (M = C, Si, Ge, Sn and Pb)	52
I.10.	Molecular Parameters of $SiCl_2$ ($^1A_1$ and $^1B_1$) and $SiBr_2$ ($^1A_1$)	54

I.11. Heats of Formation of $^1SiCl_{2\,(g)}$ and $^1SiBr_{2\,(g)}$, ΔH_f°, kcal mol^{-1}.....56

I.12. Absolute Rate Constants for the Gas-phase Reactions $SiCX_2 + R \rightarrow$ Products, (X = H, Cl).....65

II.1. Materials and Purification.....93

III.1. Peak Heights as a Function of Time for the Decay of $SiCl_2$.....96

III.2. Peak Heights as a Function of Time for the Decay of $SiBr_2$.....96

III.3. Decay Rate Constants for $SiCl_2$ as Obtained from Peak Height and Peak Area Measurements.....100

III.4. Decay Rate Constants for $SiCl_2$ in Presence of Different Amounts of Argon [$SiCl_2$] = 0.20 Torr.....101

III.5. Dependence of $SiCl_2$ Decay Rate Constants on Ar Pressure.....103

III.6. Peak Heights as a Function of Time for the Reaction of $SiCl_2$ with 0.03 Torr Oxygen.....107

III.7. Peak Heights as a Function of Time for the Reaction of $SiCl_2$ with 0.05 Torr Oxygen.....107

III.8. Peak Heights as a Function of Time for the Reaction of $SiCl_2$ with 0.06 Torr Oxygen.....108

III.9. Peak Heights as a Function of Time for the Reaction of $SiCl_2$ with 0.07 Torr Oxygen.....108

III.10. Dependence of the Pseudo First-order Rate Constants of the $SiCl_2 + O_2$ Reaction on Oxygen Concentration.....111

III.11. Peak Heights as a Function of Time for the Reaction of $SiCl_2$ with 0.024 Torr Nitric Oxide.....114

III.12. Peak Heights as a Function of Time for the Reaction of $SiCl_2$ with 0.05 Torr Nitric Oxide.....114

III.13. Peak Heights as a Function of Time for the Reaction of $SiCl_2$ with 0.066 Torr Nitric Oxide.....115

III.14. Peak Heights as a Function of Time for the Reaction of $SiCl_2$ with 0.078 Torr Nitric Oxide.....115

III.15. Peak Heights as a Function of Time for the Reaction of $SiCl_2$ with 0.09 Torr Nitric Oxide.....116

III.16. Dependence of the Pseudo First-order Rate Constants of the $SiCl_2$ + NO Reaction on Nitric Oxide Concentration.....120

III.17. Peak Heights as a Function of Time for the Reaction of $SiCl_2$ with 0.10 Torr Carbon Monooxide.....123

III.18. Peak Heights as a Function of Time for the Reaction of $SiCl_2$ with 0.12 Torr Carbon Monoxide.....123

III.19. Peak Heights as a Function of Time for the Reaction of $SiCl_2$ with 0.14 Torr Carbon Monoxide.....124

III.20. Peak Heights as a Function of Time for the Reaction of $SiCl_2$ with 0.15 Torr Carbon Monoxide.....124

III.21. Peak Heights as a Function of Time for the Reaction of $SiCl_2$ with 0.16 Torr Carbon Monoxide.....125

III.22. Dependence of the Pseudo First-order Rate Constants of the $SiCl_2$ + CO Reaction on Carbon Monoxide Concentration.....129

III.23. Peak Heights as a Function of Time for the Reaction of $SiCl_2$ with 0.06 Torr Nitrous Oxide.....132

III.24. Peak Heights as a Function of Time for the Reaction of $SiCl_2$ with 0.10 Torr Nitrous Oxide.....132

III.25. Peak Heights as a Function of Time for the Reaction of $SiCl_2$ with 0.12 Torr Nitrous Oxide.....133

III.26. Peak Heights as a Function of Time for the Reaction of $SiCl_2$ with 0.16 Torr Nitrous Oxide.....133

III.27. Peak Heights as a Function of Time for the Reaction of $SiCl_2$ with 0.20 Torr Nitrous Oxide.....134

III.28. Peak Heights as a Function of Time for the Reaction of $SiCl_2$ with 0.25 Torr Nitrous Oxide.....134

III.29. Dependence of the Pseudo First-order Rate Constants of the $SiCl_2$ + N_2O Reaction on Nitrous Oxide Concentration.....138

III.30. Peak Heights as a Function of Time for the Reaction of $SiCl_2$ with 0.04 Torr Butadiene.....142

III.31. Peak Heights as a Function of Time for the Reaction of $SiCl_2$ with 0.08 Torr Butadiene.....142

III.32. Peak Heights as a Function of Time for the Reaction of $SiCl_2$ with 0.12 Torr Butadiene.....143

III.33. Peak Heights as a Function of Time for the Reaction of $SiCl_2$ with 0.16 Torr Butadiene.....143

III.34. Peak Heights as a Function of Time for the Reaction of $SiCl_2$ with 0.20 Torr Butadiene.....144

III.35. Dependence of the Pseudo First-order Rate Constants of the $SiCl_2 + C_4H_6$ Reaction on Butadiene Concentration.....148

III.36. Peak Heights as a Function of Time for the Reaction of $SiCl_2$ with 6.0 Torr Isobutane.....151

III.37. Peak Heights as a Function of Time for the Reaction of $SiBr_2$ with 0.06 Torr Oxygen.....154

III.38. Peak Heights as a Function of Time for the Reaction of $SiBr_2$ with 0.09 Torr Oxygen.....154

III.39. Peak Heights as a Function of Time for the Reaction of $SiBr_2$ with 0.12 Torr Oxygen.....155

III.40. Peak Heights as a Function of Time for the Reaction of $SiBr_2$ with 0.16 Torr Oxygen.....155

III.41. Peak Heights as a Function of Time for the Reaction of $SiBr_2$ with 0.20 Torr Oxygen.....156

III.42. Dependence of the Pseudo First-order Rate Constants of the $SiBr_2 + O_2$ Reaction on Oxygen Concentration.....160

III.43. Peak Heights as a Function of Time for the Reaction of $SiBr_2$ with 0.16 Torr Nitric Oxide.....163

III.44. Peak Heights as a Function of Time for the Reaction of $SiBr_2$ with 0.20 Torr Nitric Oxide.....163

III.45. Peak Heights as a Function of Time for the Reaction of $SiBr_2$ with 0.24 Torr Nitric Oxide.....164

III.46. Peak Heights as a Function of Time for the Reaction of $SiBr_2$ with 0.28 Torr Nitric Oxide.....164

III.47. Peak Heights as a Function of Time for the Reaction of $SiBr_2$ with 0.30 Torr Nitric Oxide.....165

III.48. Dependence of the Pseudo First-order Rate Constants of the $SiBr_2$ + NO Reaction on Nitric Oxide Concentration.....169

III.49. Absolute Rate Constants for the Gas-phase Reactions of $SiCl_2$ and $SiBr_2$ with Different Substrates R.....171

IV.1. Absolute Rate Constants of Reactions of Divalent Species MX_2 with Various Inorganic Substrates.....196

IV.2. Absolute Rate Constants of Reactions of Divalent Species MX_2 with Various Unsaturated Hydrocarbons.....202

D.1. Thermochemical Data used in the Present Study.....229

D.2. Heats of Reaction ($\Delta H^{\circ}_{rxn.}$) for SiX_2 + S Systems (X = Cl, Br; S = O_2, NO, CO, N_2O, 1,3-C_4H_6).....231

E.1. Molecular Radii used in the Estimation of *A*-factors.....234

E.2. Arrhenius Parameters for SiX_2 + S Reactions.....236

LIST OF FIGURES

Figure		Page
I.1.	Electronic Configuration of Triplet and Singlet Carbenes	3
I.2.	Absorption Spectrum of $SiCl_2$	39
I.3.	Absorption Spectrum of $SiBr_2$	50
I.4.	Chemical Vapor Deposition Reactors	68
II.1.	The Main Vacuum System	77
II.2.	The Flash Photolysis System	80
II.3.	The Reaction Vessel and the Reflective Housing	81
II.4.	The Spectroscopic Lamp	83
II.5.	The Littrow Prism and Mounting	85
II.6.	Schematic Diagram of the Microdensitometer	86
II.7.	Circuit Diagram of the Flash Photolysis System	88
II.8.	Oscilloscope Trace	89
III.1.	Background Decay Curves of [$SiCl_2$]	97
III.2.	Background Decay Curves of [$SiBr_2$]	98
III.3.	Dependence of the Decay of $SiCl_2$ on Argon Pressure	102

III.4. Decay Curves for [$SiCl_2$] in the Absence and Presence of 0.03 Torr Oxygen.....109

III.5. Decay Curves for [$SiCl_2$] in the Absence and Presence of 0.05 Torr Oxygen.....109

III.6. Decay Curves for [$SiCl_2$] in the Absence and Presence of 0.06 Torr Oxygen.....110

III.7. Decay Curves for [$SiCl_2$] in the Absence and Presence of 0.07 Torr Oxygen.....110

III.8. Dependence of the Pseudo First-order Rate Constants of the $SiCl_2 + O_2$ Reaction on the Oxygen Concentration.....112

III.9. Decay Curves for [$SiCl_2$] in the Absence and Presence of 0.024 Torr Nitric Oxide.....117

III.10. Decay Curves for [$SiCl_2$] in the Absence and Presence of 0.05 Torr Nitric Oxide.....117

III.11. Decay Curves for [$SiCl_2$] in the Absence and Presence of 0.066 Torr Nitric Oxide.....118

III.12. Decay Curves for [$SiCl_2$] in the Absence and Presence of 0.078 Torr Nitric Oxide.....118

III.13. Decay Curves for [$SiCl_2$] in the Absence and Presence of 0.09 Torr Nitric Oxide.....119

III.14. Dependence of the Pseudo First-order Rate Constants of the $SiCl_2$ + NO Reaction on the Nitric Oxide Concentration.....121

III.15. Decay Curves for [$SiCl_2$] in the Absence and Presence of 0.10 Torr Carbon Monoxide.....126

III.16. Decay Curves for [$SiCl_2$] in the Absence and Presence of 0.12 Torr Carbon Monoxide.....126

III.17. Decay Curves for [$SiCl_2$] in the Absence and Presence of 0.14 Torr Carbon Monoxide.....127

III.18. Decay Curves for [$SiCl_2$] in the Absence and Presence of 0.15 Torr Carbon Monoxide.....127

III.19. Decay Curves for [$SiCl_2$] in the Absence and Presence of 0.16 Torr Carbon Monoxide.....128

III.20. Dependence of the Pseudo First-order Rate Constants of the $SiCl_2$ + CO Reaction on the Carbon Monoxide Concentration.....130

III.21. Decay Curves for [$SiCl_2$] in the Absence and Presence of 0.06 Torr Nitrous Oxide.....135

III.22. Decay Curves for [$SiCl_2$] in the Absence and Presence of 0.10 Torr Nitrous Oxide.....135

III.23. Decay Curves for [$SiCl_2$] in the Absence and Presence of 0.12 Torr Nitrous Oxide.....136

III.24. Decay Curves for [$SiCl_2$] in the Absence and Presence of 0.16 Torr Nitrous Oxide.....136

III.25. Decay Curves for [$SiCl_2$] in the Absence and Presence of 0.20 Torr Nitrous Oxide.....137

III.26. Decay Curves for [$SiCl_2$] in the Absence and Presence of 0.25 Torr Nitrous Oxide.....137

III.27. Dependence of the Pseudo First-order Rate Constants of the $SiCl_2 + N_2O$ Reaction on the Nitrous Oxide Concentration.....140

III.28. Decay Curves for [$SiCl_2$] in the Absence and Presence of 0.04 Torr Butadiene.....145

III.29. Decay Curves for [$SiCl_2$] in the Absence and Presence of 0.08 Torr Butadiene.....145

III.30. Decay Curves for [$SiCl_2$] in the Absence and Presence of 0.12 Torr Butadiene.....146

III.31. Decay Curves for [$SiCl_2$] in the Absence and Presence of 0.16 Torr Butadiene.....146

III.32. Decay Curves for [$SiCl_2$] in the Absence and Presence of 0.20 Torr Butadiene.....147

III.33. Dependence of the Pseudo First-order Rate Constants of the $SiCl_2 + C_4H_6$ Reaction on the Butadiene Concentration.....149

III.34. Decay Curves for [$SiCl_2$] in the Absence and Presence of 6.0 Torr Isobutane.....152

III.35. Decay Curves for [$SiBr_2$] in the Absence and Presence of 0.06 Torr Oxygen.....157

III.36. Decay Curves for [$SiBr_2$] in the Absence and Presence of 0.09 Torr Oxygen.....157

III.37. Decay Curves for [$SiBr_2$] in the Absence and Presence of 0.12 Torr Oxygen.....158

III.38. Decay Curves for [$SiBr_2$] in the Absence and Presence of 0.16 Torr Oxygen.....158

III.39. Decay Curves for [$SiBr_2$] in the Absence and Presence of 0.20 Torr Oxygen.....159

III.40. Dependence of the Pseudo First-order Rate Constants of the $SiBr_2 + O_2$ Reaction on the Oxygen Concentration.....161

III.41. Decay Curves for [$SiBr_2$] in the Absence and Presence of 0.16 Torr Nitric Oxide.....166

III.42. Decay Curves for [$SiBr_2$] in the Absence and Presence of 0.20 Torr Nitric Oxide.....166

III.43. Decay Curves for [$SiBr_2$] in the Absence and Presence of 0.24 Torr Nitric Oxide.....167

III.44. Decay Curves for [$SiBr_2$] in the Absence and Presence of 0.28 Torr Nitric Oxide.....167

III.45. Decay Curves for [$SiBr_2$] in the Absence and Presence of 0.30 Torr Nitric Oxide.....168

III.46. Dependence of the Pseudo First-order Rate Constants of the $SiBr_2$ + NO Reaction on the Nitric Oxide Concentration.....170

A.1. Trace of SiX_2 absorption band.....221

B.1. Measurement of the peak height of the absorption profile of $SiCl_2$.....224

B.2. Decay curves for [$SiCl_2$] in the absence and presence of 0.06 Torr oxygen.....224

B.3. Dependence of the pseudo first-order rate constant of $SiCl_2 + O_2$ reaction on the oxygen concentration.....225

Chapter I

INTRODUCTION

The divalent species "silylenes" are the silicon analogs of carbenes. Carbene chemistry has been extensively investigated by both organic and physical chemists and several excellent reviews have been written on the subject [1].

I.1. Physical Properties of Carbenes.

The simplest carbene, methylene, has been studied very extensively since its involvement as an intermediate in the photolysis of diazomethane and ketene was reported more than 50 years ago [2, 3]. Its absorption spectrum was first reported by Herzberg and Shoosmith [4] in 1959 from the flash photolysis of diazomethane, CH_2N_2, in a large excess of N_2. The spectrum featured a diffused band near 141.5 nm and by isotopic labeling experiments it was attributed to methylene, CH_2, in its lowest triplet state. For CHD and CD_2 this absorption band showed a fine structure and from rotational analysis was assigned to the $^3\Sigma_u^- \leftrightarrow {}^3\Sigma_g^-$ transition of CH_2. This assignment was based on the assumption that CH_2 is nearly linear or linear in both the lower and upper state, *i.e.* the $\angle$ HCH angle is between 140° and 180°.

The geometry of CH_2 in its triplet ground state and the energy difference between its ground and the lowest singlet states have been controversial subjects for many years. In the ground state, values of the $\angle$ HCH angle ranging from 109° to 180° have been proposed [5]. It is now well established that CH_2 is bent in its ground state ($^3B_1$) and not linear ($^3\Sigma_g^-$). Its well-accepted geometrical parameters are: r(C–H) = 1.078Å, $\angle$ HCH = 136°, first reported by Herzberg and Johns [6] from analysis of the UV spectrum. The electronic configurations in the ground ($^3B_1$) and lowest singlet

($^1A_1$) states are $(1a_1)^2\ (2a_1)^2\ (1b_2)^2\ (3a_1)\ (1b_1)$ and $(1a_1)^2\ (2a_1)^2\ (1b_2)^2\ (3a_1)^2$, respectively.

For the singlet ($^1A_1$) – triplet ($^3B_1$) splitting ($\Delta E_{ST} = E_{Singlet} - E_{Triplet}$), values in the range –23 to 54 kcal mol^{-1} have been suggested on the basis of theoretical calculations and experimental observations [5]. It is now well accepted that the value of ΔE_{ST} is ~ 9.1 kcal mol^{-1} [7, 8].

Upon replacing the hydrogens of methylene by different substituents, the spin state of the resulting ground state species is not always triplet. The carbene carbon in CX_2 (X is any substituent including H) has two non-bonding electrons which can be accomodated in two non-bonding orbitals, a σ- and a p-orbital. The spin multiplicity of the ground state of the carbene depends on the relative energy of these two orbitals. If the energy difference between the σ- and p-orbitals is less than the increase in energy due to electron-electron repulsion when two non-bonding electrons are brought together in the same spatial orbital, then the two non-bonding electrons will occupy different orbitals giving a (σp) configuration and, in accordance with Hund's rule, their spins will be parallel and thus the ground state of the carbene will be triplet (*cf.* Figure I.1a). On the other hand, if the energy difference between the two non-bonding orbitals is too large, the two electrons will rather occupy the same orbital (the lowest energy orbital) with opposite spin and thus the carbene will have a singlet ground state (*cf.* Figure I.1b).

For the relative energies of σ- and p-orbitals of substituted carbenes, Harrison *et al.* [9] proposed a theory based on the electronegativity of the substituent, which suggest that the electronegativity is a decisive factor in determining the spin multiplicity

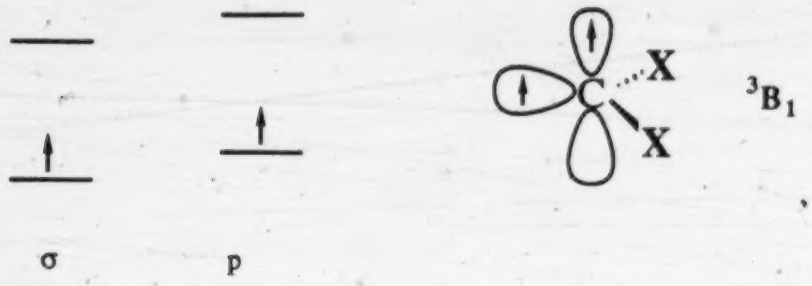

(a) Triplet ground state

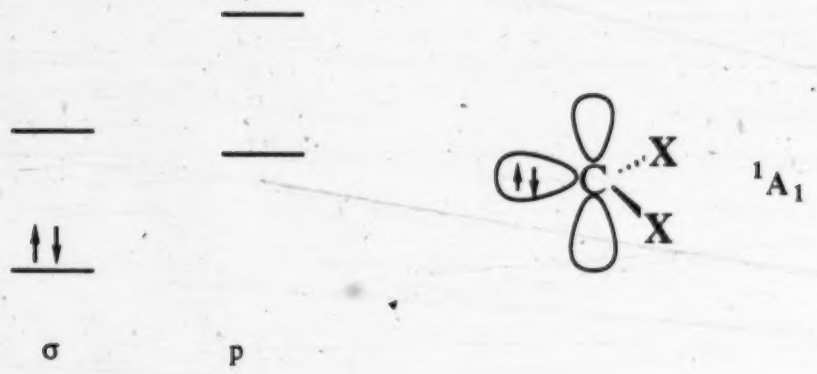

(b) Singlet ground state

Figure I.1. Electronic configurations of triplet (a) and singlet (b) carbenes.

of the ground state of the substituted carbene. As the substituent becomes more electronegative relative to the carbene carbon, the s-character of the σ-orbital increases, thus its energy decreases and this favors the singlet ground state for the carbene. On the other hand, a more electropositive substituent relative to carbon would result in electron transfer from the substituent to the carbon, *i.e.* the σ-orbital will lose its s-character and at some point the σ- and p-orbitals will become close in energy, giving rise to a triplet ground state. Thus halo- and dihalocarbenes, CHX and CX_2 (X = F, Cl, Br), have singlet ground states ($^1A_1$) whereas LiCH and CLi_2 are triplet in their ground states ($^3B_1$). Theoretical estimates of the singlet – triplet energy gaps (ΔE_{ST}), calculated using *ab initio* methods, are – 8 kcal mol^{-1} for CBr_2 [10], – 25.9 kcal mol^{-1} for CCl_2 [8] and – 57.5 kcal mol^{-1} for CF_2 [8]. These data are in excellent agreement with Harrison *et al.*'s theory, *i.e.* as the electronegativity of the substituent increases, the singlet ground state becomes more stable.

Harrison *et al.* have also suggested that by replacing carbon in carbenes with a less electronegative atom, *e.g.* silicon, while keeping the substituents unchanged, the relative energies of the σ- and p-orbitals would be affected in a similar way as by substituting the carbene with more electronegative atoms, *i.e.* the σ-orbital will become more stable than the p-orbital. Thus on going from carbenes to the corresponding silylenes, the singlet ground state would become more favorable than the triplet ground state. This explains the singlet ground state of silylene, SiH_2, in contrast to the triplet ground state of its carbon analog, methylene. The singlet ground state for SiH_2 was first predicted by Jordan [11].

The equilibrium geometries of dihalocarbenes in their ground electronic states have been investigated experimentally and theoretically using *ab initio* methods. The molecular parameters thus obtained are compiled in Table I.1.

Table I.1. Equilibrium ground state geometries of CX_2 species.

X	Ground Electronic State	Calculated Geometry [10][a]		Experimental Geometry	
		r, Å	θ, °	r, Å	θ, °
H	$^3B_1$	1.075	128.8	1.078 [6]	136 [6]
F	$^1A_1$	1.305	104.3		104.9 [12]
Cl	$^1A_1$	1.756	109.2		106 ± 5 [13]
Br	$^1A_1$	1.875	110.1	1.740 [14]	114 [14]

[a] In this and the following Tables, numbers in brackets are reference numbers.

The data exhibit good agreement between theoretical and experimental values. All dihalocarbenes as well as methylene are bent in their ground electronic state and have C_{2v} symmetry:

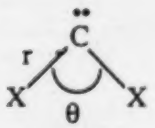

X = H, Br, Cl, F

I.2. Reactivity of Carbenes.

The two main types of reactions carbenes generally undergo are insertion and addition. A vast body of research has been devoted to the reactivity of carbenes, as is evident from the number of reviews on carbene chemistry [1], therefore, only a brief description of these two types of reactions of carbenes is given here.

In their addition and insertion reactions, carbenes of different multiplicity follow different reaction paths. Singlet carbenes are capable of insertion into the C—H bonds in a concerted process whereas triplet carbenes react *via* H abstraction giving radical products.

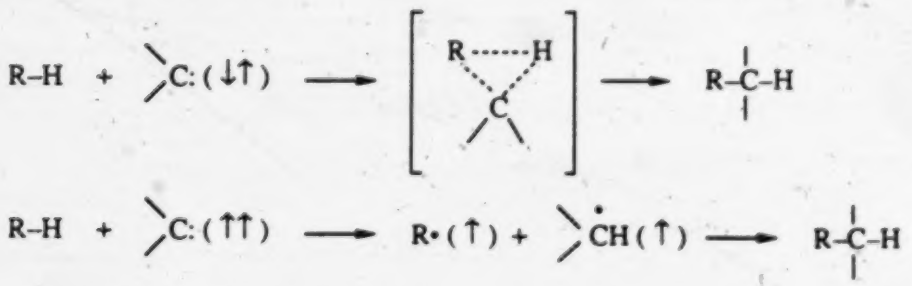

In their addition reactions, singlet carbenes add to unsaturated bonds in a one-step stereospecific process in accordance with the rules of conservation of orbital

symmetry. The addition proceeds *via* a π-approach transition state (A) in which the p-orbital of the carbene impinges on the π-system of the unsaturated bond. This approach is commonly accepted in view of the electrophilic character of carbene; only the p-orbital of a singlet carbene is able to accept additional electrons, thus the most efficient overlap would occur in a transition state resembling (A):

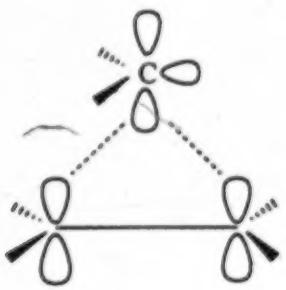

(A)

The general scheme for stereospecific addition of a singlet carbene to an olefinic bond is:

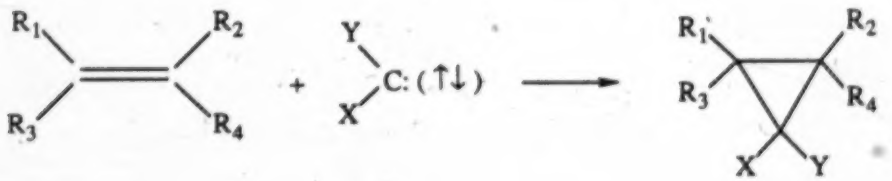

The addition reactions of triplet carbenes to unsaturated systems proceed *via* a non-stereospecific two-step mechanism. In accordance with the spin conservation rule, the initial step gives a triplet diradical intermediate. Spin inversion is much slower than any molecular process and rotation about the C—C bond in this intermediate is fast compared to ring closure. The general mechanism for the addition of triplet carbenes to olefins is as follows:

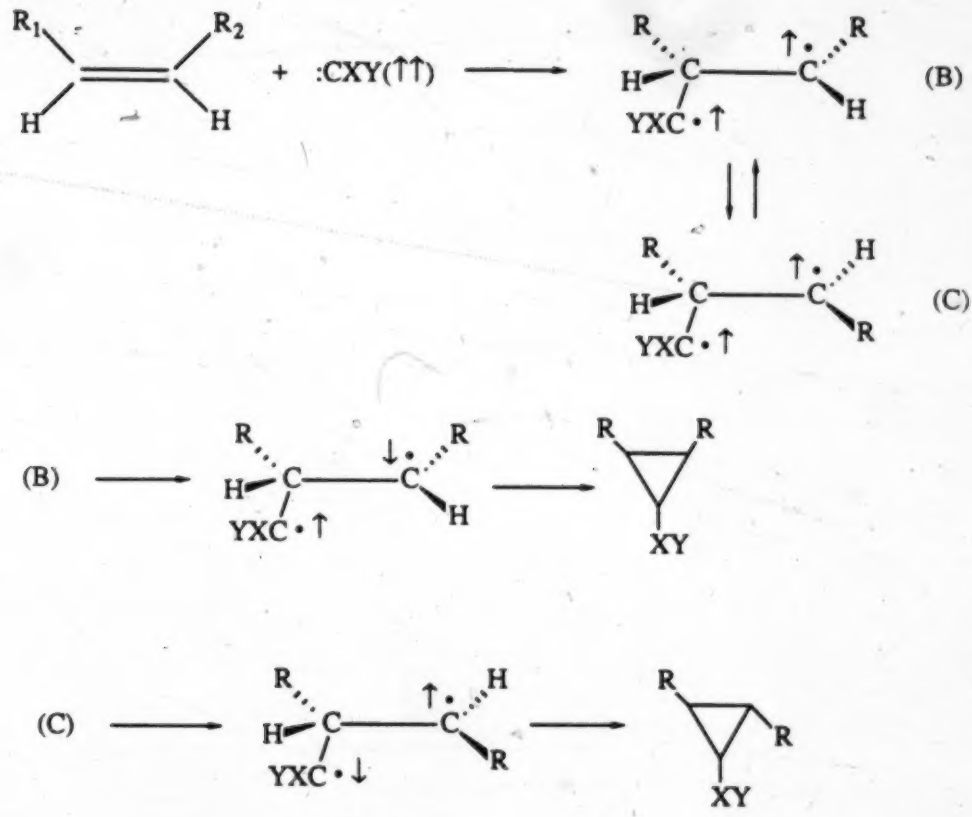

Additional examples of qualitative studies of insertion and addition reactions of carbenes are described in Reference 1.

Very limited data have been reported on the absolute rate constants of carbene reactions with unsaturated hydrocarbons, however, relative reactivities of various carbenes toward different sets of olefins have been studied extensively [1]. Based on these relative reactivities, a selectivity scale for carbenes has been constructed and a carbenic phílicity has been formulated [15]. According to this carbenic philicity formulation, CX_2 (X = F, Cl, Br) act as an electrophile in its reactions with unsaturated bonds whereas carbenes such as $C(OMe)_2$ and $MeOCNMe_2$ act as nucleophiles. The selectivity of the reactions of methylene and dihalocarbenes, CX_2, follows the order

$CH_2 < CBr_2 < CCl_2 < CF_2$ *i.e.* CF_2 is the most selective and thus the least reactive in its reactions with olefins, whereas CH_2 is the least selective and thus the most reactive. The increase in the relative selectivity and the decrease in reactivity of dihalocarbenes CX_2 in the order Br < Cl < F has been suggested [16] to be due to the ability of halogen atoms to supply electrons to the electron-deficient carbene carbon and thus to stabilize the singlet carbenes through canonical forms such as:

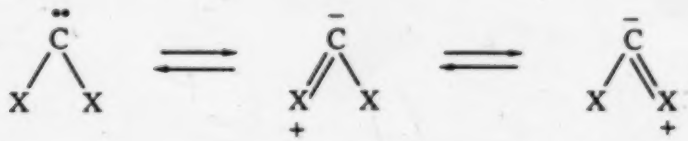

Hack *et al.* [17] have measured absolute rate constants for the reactions of $^1CH_2$ with a series of olefins using the laser pulse photolysis/laser induced fluorescence technique. They observed that the reactions of $^1CH_2$ with various olefins are very fast, of the order of 10^{11} $M^{-1}s^{-1}$, and are independent of alkyl substituents on the olefinic double bond. This observation is in accordance with the selectivity scale which characterizes CH_2 as the least selective. Their values are in good agreement with the previously reported values of Langford *et al.* [18].

No data on absolute rate constants for the reactions of CX_2 (X = F, Cl, Br) with unsaturated hydrocarbons are available to compare their reactivity towards a common substrate. However, some direct kinetic data on the reactions of PhCX (X = F, Cl, Br) with a set of olefins ($Me_2C{=}CMe_2$, $Me_2C{=}CHMe$, trans-$MeCH{=}CHEt$, n-$BuCH{=}CH_2$) in solution at 23°C have been recently reported [19]. For every olefin used, the rate constants were in the order BrCPh > ClCPh > FCPh and the spread in the numerical values of the absolute rate constants, *i.e.* their selectivity, followed the reverse order which is in accordance with the inverse type correlation between reactivity and selectivity.

Quantitative studies of the reactions of methylene and dihalocarbenes with inorganic species are of main interest here, since the present study concerns the quantitative investigations of reactions of dichloro- and dibromosilylenes, the silicon analogs of carbenes, with inorganic substrates.

For the $^3CH_2$ + NO reaction, absolute rate constant values have been measured by five independent research groups [20 – 24]. These values are in good agreement, within a factor of ~4.5, and range from 6.02 x 10^9 $M^{-1}s^{-1}$ [21] to (2.2 ± 0.5) x 10^{10} $M^{-1}s^{-1}$ [24]. Similarly, the absolute rate constant of the $^3CH_2$ + O_2 reaction has also been measured by five different research groups [20 – 23, 25]. These values are within a factor of 3.5, ranging from 7.2 x 10^8 $M^{-1}s^{-1}$ [21] to (2.0 ± 0.5) x 10^9 $M^{-1}s^{-1}$ [25]. The values reported by Pilling and Robertson [21] are the lowest in both cases and were obtained from the analysis of the effect of added substrate on the product yields from the flash-photolyzed $^3CH_2$ precursor. On the other hand, the upper limit values of Seidler *et al.* [24] for reaction with NO, and of Bohland *et al.* [25] for that with O_2, were obtained by directly monitoring $^3CH_2$ using laser magnetic resonance spectroscopy. Since $^3CH_2$ was directly monitored in these studies [24, 25], their values should be more accurate. These values, k_{NO} = (2.2 ±0.5) x 10^{10} $M^{-1}s^{-1}$ [24] and k_{O_2} = (2.0 ± 0.5) x 10^9 $M^{-1}s^{-1}$ [25], are also in excellent agreement with those of other recently reported direct measurements [23], k_{NO} = 1.7 x 10^{10} $M^{-1}s^{-1}$ and k_{O_2} = (1.95 ± 0.2) x 10^9 $M^{-1}s^{-1}$.

Seidler *et al.* [24] have proposed that the $^3CH_2$ + NO reaction proceeds through initial formation of an adduct which could be either cyclic (D) or linear (E) with subsequent chemical decay *via* different channels. The end products of this reaction are not known.

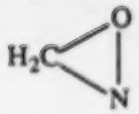

(D)

H_2CNO

(E)

The formation of ^{14}CO and $^{14}CO_2$ was observed following the photolysis of $^{14}CH_2CO$ in the presence of O_2 and these products were proposed to be due to the reaction of $^3CH_2$ with O_2 [26]. However, formation of ^{14}CO from photolysis of $^{14}CH_2CO$ even in the absence of O_2 has been reported [27], so the above argument is somewhat illogical. A mechanism involving initial formation of an excited intermediate HCOOH, which can either decompose *via* various routes or be stabilized, has been proposed [28]:

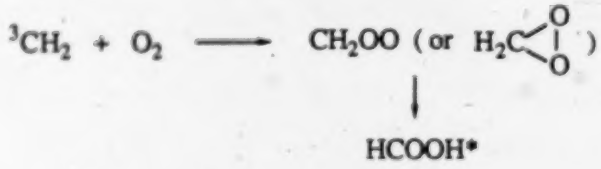

The $^3CH_2$ + CO reaction has been found to be very slow and only an upper limit of $k \leq 6 \times 10^5 M^{-1}s^{-1}$ has been reported [20, 21].

A few independent measurements of the reactions of singlet methylene ($^1CH_2$) have also been reported. Laufer and Bass [20] have reported the upper limits of $k < 1.8 \times 10^{10} M^{-1}s^{-1}$, $< 2.4 \times 10^{10} M^{-1}s^{-1}$ and $< 5.4 \times 10^9 M^{-1}s^{-1}$ for the reactions of $^1CH_2$ with O_2, NO and CO, respectively, using the vacuum UV-flash photolysis-GC analysis technique in which the $^1CH_2$ concentration was deduced from product analysis. Later on, Ashfold *et al.* [29] and Langford *et al.* [18] also measured the absolute rate constants of these reactions by following the $^1CH_2$ concentration directly. Ashfold *et*

al. used time-resolved laser induced fluorescence, while Langford *et al.* used laser absorption spectrometry to monitor $^1CH_2$. The values of absolute rate constants reported by these two groups are in very good agreement and are more reliable than the upper limits reported by Laufer and Bass [20]. These values are:

$k_{O_2} = (4.5 \pm 0.3) \times 10^{10}\ M^{-1}s^{-1}$ [18], $1.8 \pm 0.2 \times 10^{10}\ M^{-1}s^{-1}$ [28].

$k_{NO} = (9.6 \pm 0.9) \times 10^{9}\ M^{-1}s^{-1}$ [18].

$k_{CO} = (2.9 \pm 0.2) \times 10^{10}\ M^{-1}s^{-1}$ [18], $(3.4 \pm 0.3) \times 10^{10}\ M^{-1}s^{-1}$ [28].

Rowland *et al.* [30] observed that the products of the $^1CH_2 + O_2$ reaction were the same as those of the $^3CH_2 + O_2$ reaction, *i.e.* CO, CO_2 and H_2O. They proposed that in the former case these products were formed *via* initial quenching of $^1CH_2$ to $^3CH_2$.

Neither the products nor the mechanism of the $^1CH_2 + NO$ reaction have yet been reported.

From the $^{14}CH_2$ ($^1A_1$) + CO reaction , Montague and Rowland [27] observed the formation of ^{14}CO and proposed that this reaction proceeds through an oxirene intermediate (F), although there was no evidence of a stabilized adduct other than the [^{14}C] ketene. They observed that 840 Torr CO was needed to stabilize 50% of the $^{14}CCH_2O$ complexes.

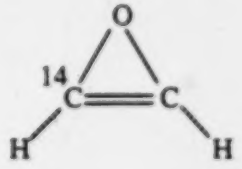

(F)

Very little quantitative data have been reported on the reactions of dihalocarbenes.

Modica [31] studied the reaction of CF_2 with NO by heating a mixture of C_2F_4 and NO in excess argon in a shock tube and the disappearence of CF_2 was analysed by time-resolved UV absorption at 260 nm. The products were analysed mass spectrometrically. He proposed that below 2500K the major reaction is

$$CF_2 + NO \rightleftharpoons CF_2NO$$

and that above 2500K additional reactions occurred, yielding N_2O, CF_2O and N_2 :

$$CF_2NO + NO \longrightarrow CF_2O + N_2O$$

$$2\ CF_2NO \longrightarrow 2\ CF_2O + N_2$$

Burks and Lin [32], however, using chemical laser emission spectroscopy and mass spectrometric analysis of the products, proposed a different path for this reaction in order to account for the presence of F atoms in their reaction system:

$$CF_2 + NO \longrightarrow CF_2O + N$$

$$CF_2 + N \longrightarrow FCN + F$$

They also suggested that in Modica's experiment [31] at high temperature, N_2O may form from the reaction

$$NO + NO \longrightarrow N_2O + O$$

No other data on this reaction are yet available to support either of the above reaction mechanisms.

Dalby [33] studied the reactions of CF_2 with O_2, C_2F_4 and C_2H_4 quantitatively and concluded that at 25°C CF_2 is unreactive towards these substrates. The main reaction observed was dimerization, for which he measured an absolute rate constant of $k = 1.7 \times 10^7\ M^{-1}s^{-1}$. For the reaction with O_2

$$CF_2 + O_2 \longrightarrow CF_2O_2$$

an upper limit of $k < 10^4\ M^{-1}s^{-1}$ was proposed.

Recently, Tiee *et al.* [34] have studied the kinetics of the reactions of CCl_2 and CClF with O_2, NO and CO using the laser-induced fluorescence technique. They reported the following values for the rate constants of the reactions of CCl_2 and CClF with NO, CO and O_2 respectively.

CCl_2 : $1.8 \times 10^8\ M^{-1}s^{-1}$ (NO); $3.0 \times 10^7\ M^{-1}s^{-1}$ (CO); $\leq 1.8 \times 10^6\ M^{-1}s^{-1}$ (O_2).

CClF : $6.0 \times 10^6\ M^{-1}s^{-1}$ (NO); $9.0 \times 10^5\ M^{-1}s^{-1}$ (CO); $\leq 1.8 \times 10^5\ M^{-1}s^{-1}$ (O_2).

No other data on the absolute rate constants of the reactions of dihalocarbenes have yet been reported. However, it can be seen from the above results [34] that as the electronegativity of the substituent on the carbene carbon increases, the rate constant decreases in direct proporiton to the increased stability of the carbene CX_2 in the order X = Cl < F, as mentioned above.

I.3. Carbenes *vs* Silylenes.

Although silylenes and other group IV A analogs of carbenes have been studied extensively, it was not until 1970, after the insertion reaction of silylene into the Si—H bond was firmly established, that silylenes were recognised as an important class of

reactive intermediates. Since then many excellent reviews have been written concerning the chemistry of various silylenes [35 – 39].

As one moves on from carbon to silicon chemistry, the following changes in the atomic properties should be noted:

(i) Si is larger and heavier than C (the atomic radius of Si is 0.117 nm and that of C is 0.077 nm).

(ii) Si is less electronegative than C (the electronegativity of Si is 1.8 and that of C, 2.5).

(iii) Both Si and C have an ns^2 np^2 valence shell electronic configuration. Si has 3d orbitals in its valence shell which allows Si to expand its valence beyond 4 whereas C is limited to a valence of 4 due to the unavailability of d-orbitals in its valence shell.

All these factors may contribute to some dissimilarities in the physical and chemical properties of silylenes and carbenes.

Consider, for instance, the simplest silylene, SiH_2, the silicon analog of the simplest carbene, methylene (CH_2). The spectrum of SiH_2 in the 480 – 650 nm region resembles the red bands of methylene [40]. In contrast to CH_2 which is triplet ($^3B_1$) in the ground state, SiH_2 has a singlet ground state ($^1A_1$) as was first predicted by Jordan [11] and experimentally confirmed by Zeck *et al.* [41]. An explanation for this difference in the ground state spin multiplicity between CH_2 and SiH_2 has been provided by the electronegativity theory of Harrison *et al.* [9] as mentioned above. Although both CH_2 and SiH_2 are bent in their ground states, their molecular structures are different, and therefore the chemistry involved in the reactions of ground state

silylene may be expected to be different from that of the reactions of ground state methylene. However, the structures of SiH_2 and CH_2 in their lowest singlet states ($^1A_1$) are quite similar:

SiH_2 ($^1A_1$): r(Si–H) = 1.52 Å; θ(HSiH) = 92.1° [40]

CH_2 ($^1A_1$): r(C–H) = 1.11 Å; θ(HCH) = 102.4° [42]

thus SiH_2 ($^1A_1$) and CH_2 ($^1A_1$) could be expected to undergo similar reactions, as will now be discussed.

Both CH_2 and SiH_2 insert into the H_2 molecule to give CH_4 and SiH_4, respectively. The energy barrier for insertion of SiH_2 has been calculated to be 8.6 kcal mol^{-1} whereas the same calculations predict no energy barrier for the insertion of CH_2 [39].

SiH_2 inserts into the O—H bond of water to form SiH_3OH, for which the following mechanism has been proposed [39]:

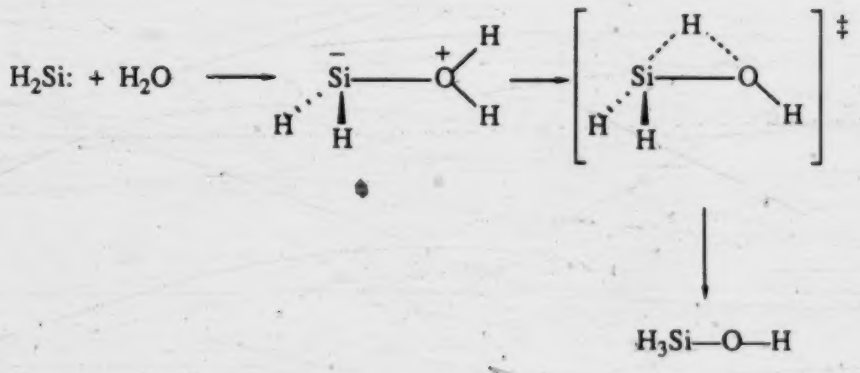

$^1CH_2$ has also been reported to react with H_2O to give CH_3 and OH radicals. Initial insertion into the O—H bond yielding CH_3OH^*, which could decompose to CH_3 and OH or be stabilized, has been proposed [43]:

$$CH_2 + H_2O \rightleftharpoons CH_3OH^* \longrightarrow CH_3 + OH$$

SiH_2 inserts into the Si—H bond of silane and disilane, similarly to CH_2 insertion into the C—H bond of alkenes [35]:

$$SiH_2 + SiH_4 \longrightarrow Si_2H_6$$

$$SiH_2 + Si_2H_6 \longrightarrow Si_3H_8$$

$$CH_2 + CH_4 \longrightarrow C_2H_6$$

$$CH_2 + C_2H_6 \longrightarrow C_3H_8$$

SiH_2 adds to olefinc bonds in a similar way as $^1CH_2$ to give silacyclopropanes which, unlike cyclopropanes, are not stable and thus undergo rearrangement.

$$H_2Si + H_2C{=}CH_2 \longrightarrow \left[\begin{array}{c} H_2C\text{—}CH_2 \\ \diagdown\ \diagup \\ Si \\ H_2 \end{array}\right] \longrightarrow H_2C{=}CH\text{-}SiH_3$$

Like CH_2, SiH_2 is also known to add to acetylenes and conjugated dienes. More examples of qualitative investigations of such reactions are given in the reviews listed in References 35 – 39. Since a detailed comparison between the chemistry of carbenes and silylenes is beyond the scope of this chapter and moreover, since the primary interest of the present work is in quantitative data, therefore the rest of this section will be focused on comparing the quantitative results available for carbenes and silylenes.

Absolute rate constants for the reactions of CH_2 and SiH_2 in their lowest singlet state, ($^1A_1$), with hydrocarbons and some inorganic substrates such as H_2, O_2, NO and N_2 are compiled in Table I.2. Insertion of SiH_2 into C—H bond of CH_4 and into H—H bond of H_2 is slower than that of $^1CH_2$. Stronger C—H bond than Si—H bond {D(C—H) = 98 kcal mol^{-1} *vs* D(Si—H) = ~89.6 $kcalmol^{-1}$ [48]} could be the driving force for faster insertion of $^1CH_2$. For both species, insertion into H—H and C—H bonds is slower than addition to unsaturated bonds which is very fast. $^1CH_2$ shows almost no discrimination among olefins whereas SiH_2 shows a little selectivity. In general, the reactions of CH_2 with hydrocarbons as well as with inorganic molecules are faster than those of SiH_2. This could be due to the fact that the reacting $^1CH_2$ is in its first excited state and thus these rate constant values include physical quenching of the ($^1A_1$) to the ($^3B_1$) ground state, whereas SiH_2 ($^1A_1$) is already in its ground state. Both $^1CH_2$ and SiH_2 show a similar reactivity trend towards the radical scavengers O_2 and NO *i.e.* $k_{NO} > k_{O_2}$. With CO, $^1CH_2$ reacts much faster than SiH_2. The formation of stable ground state ketene (CH_2=C=O) from the $^1CH_2$ + CO reaction is in accordance with the spin conservation rule and therefore this could be the driving force behind this fast reaction. The reaction with ground state methylene, $^3CH_2$, which would yield a triplet ketene, *i .e.* an excited state ketene, is very slow ($k \leq 6 \times 10^5 M^{-1}s^{-1}$ [20,21]). Yamabe and Morokuma [49], from their MO and state correlation calculations on the photodecomposition of ketene which, as they pointed out, follows a bent out of plane (C_s symmetry) route, have reported that $^1(CH_2 + CO)$ correlates with ground ($^1A'$) state ketene whereas $^3(CH_2 + CO)$ correlates with a higher-lying triplet ($^3A'$) state instead of the lowest triplet ($^3A''$) state of ketene. Even though their state correlations predict a faster reaction with $^1CH_2$ than that with $^3CH_2$, as has been reported form quantitative studies [18, 20, 21], they were unable to resolve the energies of the singlet and triplet

Table I.2. Absolute rate constants of the reactions of CH_2 ($^1A_1$) and SiH_2 ($^1A_1$).

Substrate	k, $M^{-1}s^{-1}$	
	SiH_2	CH_2
H_2	2.7×10^8 [44]	6.3×10^{10} [18]
CH_4	1.5×10^7 [45]	4.4×10^{10} [47]
C_2H_6	7.2×10^6 [45]	
C_2H_2	5.9×10^{10} [45]	2.2×10^{11} [17]
C_2H_4	3.2×10^{10} [45]	1.4×10^{11} [17]
C_3H_6	7.2×10^{10} [45]	2.0×10^{11} [17]
i-C_4H_8		2.0×10^{11} [17]
1,3-C_4H_6	1.1×10^{11} [45]	2.1×10^{11} [17]
N_2	$< 6 \times 10^7$ [46]	6.6×10^9 [18]
NO	1.0×10^{10} [46]	9.6×10^{10} [18]
O_2	4.6×10^9 [46]	4.5×10^{10} [18]
CO	$< 6 \times 10^7$ [46]	2.9×10^{10} [18]

states at the minimal level of theory (STO-3G basis set) used in their calculations, and thus these results are not too reliable.

The existence of a stable silaketene has not yet been proven. A recent *ab initio* study predicts the formation of a Lewis acid-base type adduct (G) rather than a silaketene (H) from the SiH_2 + CO reaction [50].

(G)

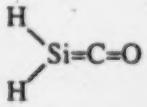

(H)

The slow reaction between SiH_2 and CO may be in part due to the formation of such a weak acid-base type adduct.

Halogen substituents on both methylene and silylene have similar effects on the relative energies of their lowest singlet and triplet electronic states. For comparison, the known values of ΔE_{ST} (= $E_{Singlet} - E_{Triplet}$) of substituted carbenes and silylenes are given in Table I.3.

Two trends in ΔE_{ST} values can be seen from these data, *i.e.* ΔE_{ST} becomes more negative as:

(i) the electronegativity of the substituent increases in both the CX_2 and SiX_2 series; and

(ii) as one goes from a carbene to the corresponding silylene.

Table I.3. Singlet–triplet energy separation (ΔE_{ST})[a] of carbenes, CX_2, and silylenes, SiX_2.

X	ΔE_{ST} (CX_2), kcal mol^{-1}		ΔE_{ST} (SiX_2), kcal mol^{-1}	
	Experimental	Calculated	Experimental	Calculated
H	9.09 [7]	9.09 [8]	≤ – 14.0 [52]	–20.0 [54]
Br		– 8.0 [10]		– 33.4 [55]
Cl		– 25.9 [8]		– 38.5 [55]
F	– 56.6 [51]	– 57.5 [8]	– 75.2 [53]	– 73.5 [54]

[a] Negative values indicates that the singlet ($^1A_1$) state is lower in energy than the triplet ($^3B_1$) state.

Both these observations are consistent with Harrison.*et al.*'s theory [9] as mentioned earlier, according to which the stability of the lowest singlet state relative to the lowest triplet state of species MX_2 increases as the substituent X becomes more electronegative or as the central atom M becomes more electropostive while keeping the substituents, X, unchanged.

The dihalosilylenes, SiX_2 (X = F, Cl, Br), have a singlet ($^1A_1$) ground state like their carbene analogs and the stability of their ground state relative to that of their lowest triplet state (Table I.3) varies in the same way as that of dihalocarbenes, with the electronegativity of the substituents. One would therefore expect trends in the reactivities of dihalosilylenes similar to those of dihalocarbenes.

Among the dihalosilylenes, difluorosilylene (SiF_2) has been most widely investigated although most of the work reported is qualitative in nature. In the gas phase SiF_2 has been reported to be quite long lived with a half life of ~150 sec and to decay exclusively *via* a wall reaction to form polymer [56]. Because it was initially believed to be inert in the gas phase, most of its reactions were studied under co-condensation conditions in which thermally-generated SiF_2 is mixed with the substrate and the mixture is then condensed at – 196°C. Under these conditions, Margrave and coworkers observed that the reactions of SiF_2 with BF_3, C_2H_4 and C_2H_2 generated the following products [56, 57]:

$$BF_3 + SiF_2 \xrightarrow{-196°C} BF_2(SiF_2)_nF \qquad n = 1\text{–}3$$

$$H_2C{=}CH_2 + SiF_2 \xrightarrow{-196°C} \begin{array}{c} SiF_2 \\ | \\ SiF_2 \end{array} + \begin{array}{c} SiF_2 \\ | \\ SiF_2 \end{array}$$

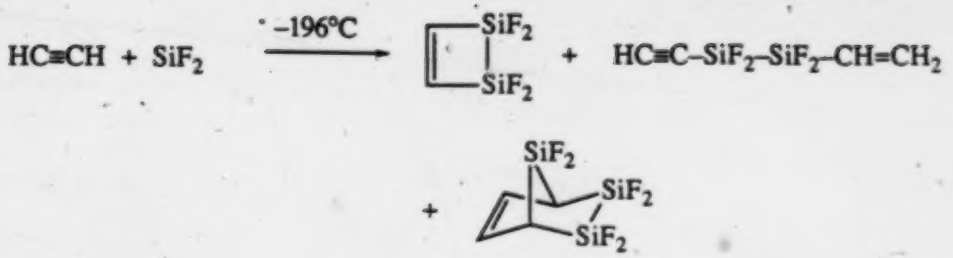

Based on the observation that all the major products of these reactions contained the $(SiF_2)_2$ moiety, the authors suggested that the initial step was dimerization of SiF_2 and that the resulting $\cdot F_2SiSiF_2\cdot$ radical was the reactive species [56, 57]. The proposed mechanism of the reaction with C_2H_2 is illustrated in scheme I [57]. Reactions with other substrates such as aromatic compounds, alkyl substituted acetylenes, BF_3, O_2 were also believed to involve diradical intermediates of the type $\cdot(SiF_2)_n\cdot$ (n = 1, 2, 3 etc.) [56, 58 – 60].

Scheme I:

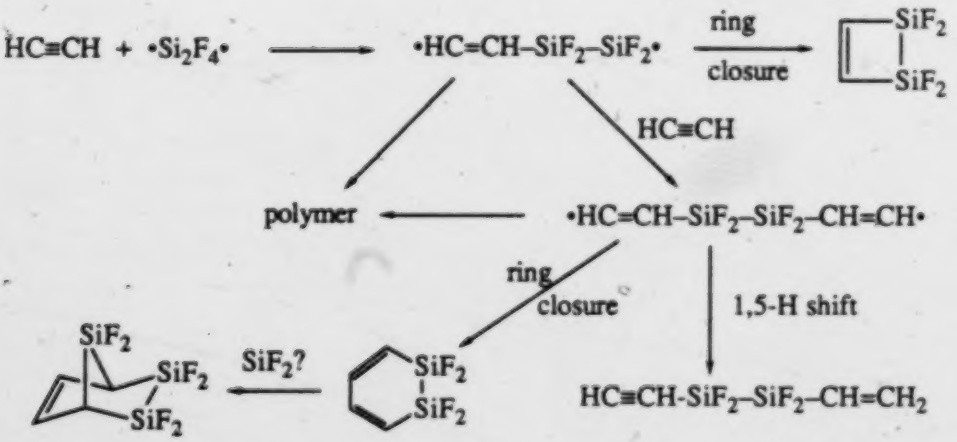

In 1978, however, Seyferth and Duncan [61] suggested that a more plausible reaction mechanism would involve addition of SiF_2 across an unsaturated bond,

followed by secondary reaction of the silirane or silirene adduct such as ring expansion, dimerization or reaction with another SiF_2, as illustrated in scheme II for the case of acetylene. Such a mechanism fully explains all the products detected by Margrave and coworkers. While initial dimerization of SiF_2 cannot be excluded *a priori* , the rate of this reaction would be expected to be slow, compared to addition across a C=C or C≡C bond.

Scheme II:

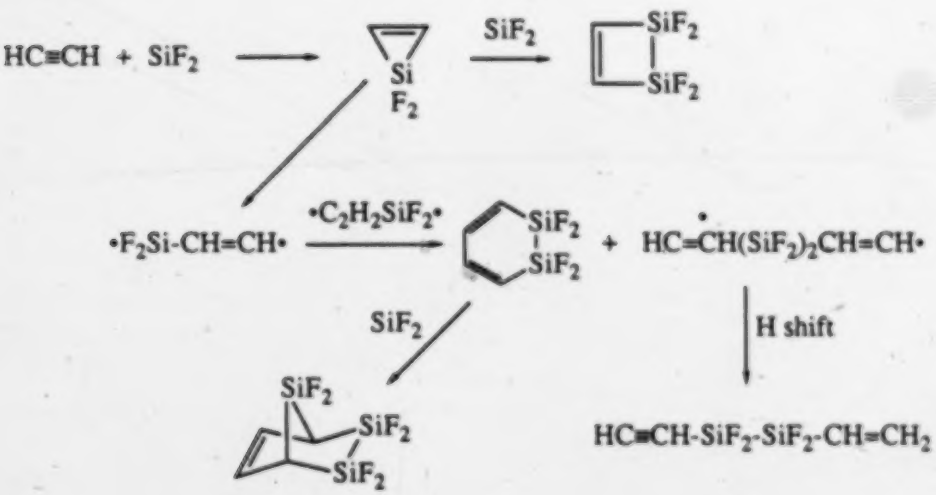

In later developements, Thompson *et al.* 's [62] ^{29}Si NMR spectroscopic evidence for the participation of monomeric SiF_2 in the reaction of SiF_2 with propene under co-condensation conditions, and the observation that SiF_2 reacts with halogenated olefins to generate SiF_2 + olefin adducts as stable products (see below) lend extra support to Seyferth and Duncan's mechanism.

Following this proposal the gas-phase reactions of SiF_2 were reinvestigated by Hwang and Liu [63, 64]. They observed that under the proper conditions, SiF_2 does

react in the gas phase with 1,3-butadiene, *cis*- and *trans*-difluoroethylene, vinyl chloride, vinyl fluoride and propene giving products containing only one SiF_2 unit, in agreement with Seyferth and Duncan's mechanism. It should be noted that the reaction of SiF_2 with haloolefins generates products that are entirely different from those formed in the reactions with unsubstituted olefins [56], *e.g.*

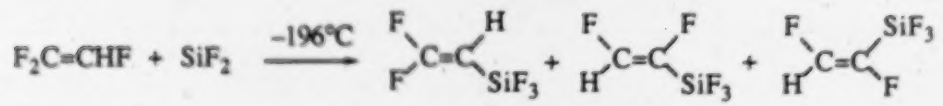

Margrave and Wilson [56] proposed that this type of reaction may proceed *via* initial formation of a silirane-type intermediate (I) which would then rearrange rapidly to give the final products; however, details of the mechanism were not given.

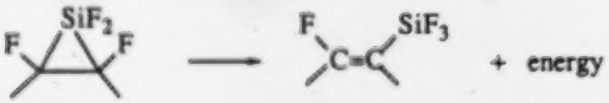

(I)

From a comparison of the products formed in the reaction of SiF_2 with vinyl fluoride in the gas phase and those formed under co-condensation conditions Liu and Hwang [64] concluded that the reaction at –196°C also involves monomeric SiF_2, although in addition to CH_2=$CHSiF_3$, which is the only product in the gas phase, some products contained two SiF_2 units, such as CH_2=$CHSiF_2SiF_3$ and 4,5-difluoro-1,1,2,2-tetrafluoro-1,2-disilacyclohexane. They further concluded that the mechanism for the gas-phase reaction is simple and involves initial attack of SiF_2 on an unsaturated bond followed by rearrangement when possible or polymerization, whereas the mechanism for the reaction under co-condensation conditions is quite complex.

Nucleogenic difluorosilylene, $^{31}SiF_2$, has also been shown to react in the gas phase with butadiene as a monomer yielding 1,1-difluorosilacyclopent-3-ene [65]

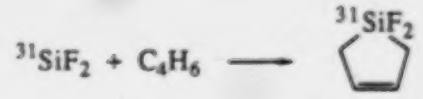

and with ethylene to yield 1,1-difluorosilacyclopentane *via* initial silirane formation [66].

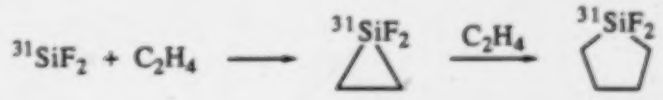

By competitive trapping experiments Tang and coworkers [66] observed that ethylene is 10 times less reactive than butadiene towards $^{31}SiF_2$, showing that SiF_2 is more selective than SiH_2, for which the reaction with ethylene is ~ 3 times slower than that with butadiene.

More examples of the reactions of monomeric SiF_2 with various hydrocarbons have been summarized in two recent reviews [38, 64]. It is now well accepted that the reactions of SiF_2 with unsaturated hydrocarbons follow a mechanism similar to that with singlet carbenes *i.e. via* initial silirane- or silirene-type intermediate formation, however, such intermediates have yet to be isolated.

The reactions of SiF_2 with inorganic molecules NO and CO in low-temperature matrices have also been reported to involve monomeric SiF_2. Bassler *et al.* [67], who carried out IR spectroscopic investigations of these reactions in Kr matrices at 20K proposed that SiF_2 reacts with the *cis* dimeric form of NO to yield an adduct which decomposes violently to N_2O and siliconoxyfluoride polymer upon warming the matrix to –150°. This adduct was proposed to have the cyclic structure (J).

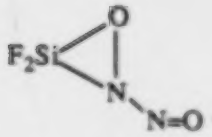

(J)

For the SiF_2 + CO reaction they proposed the initial adduct to be SiF_2CO which decomposed to volatile silicon oxyfluorides and a carbon-rich polymer upon warming the matrix. They failed to observe any reaction between SiF_2 and O_2 under the same conditions.

Quantitative data on the reactions of SiF_2 are very limited and the only rate constants reported for its reactions are listed in Table I.4 along with similar data on SiH_2, $^1CH_2$ and CF_2 for comparison. From these data it can be seen that the rate constant values of SiF_2 *vs* SiH_2 follow a trend similar to that of CF_2 *vs* $^1CH_2$ *i.e.* they decrease upon fluorine substitution in CH_2 and SiH_2. The lower reactivity of SiF_2 compared to that of SiH_2 towards O_2, H_2 and C_4H_6 could be due to the stabilization effect of the halogen substituents similar to the one that has been proposed for carbenes [16].

For insertion into H_2, Sosa and Schlegel's [69] *ab initio* calculations predict that fluorine substitution on both CH_2 and SiH_2 increases the energy barrier height of the reaction. They reported values of 2.0, 15.0 and 47.0 kcal mol^{-1}, and 12.0, 31.0 and 65.0 kcal mol^{-1} for insertion of CH_2, CHF and CF_2, and SiH_2, SiHF and SiF_2, respectively. This large difference in barrier height for MH_2 *vs* MF_2 (M = C, Si) insertion is consistent with the lower rate constant values associated with the MF_2 + H_2, as compared to the MH_2 + H_2, reaction (*cf.* Table I.4). It should be noted that for CH_2 and SiH_2 insertion, Sosa and Schlegel's values are slightly higher (2.0 and 3.4 kcal mol^{-1} respectively) than the previously reported theoretical values [39].

Table I.4. Absolute rate constants for the gas-phase reactions of SiX_2 and CX_2 (X = H, F).

X	k, $M^{-1}s^{-1}$ [a]			
	SiF_2	SiH_2	CF_2	$^1CH_2$
H_2	$< 6 \times 10^3$ [68]	2.7×10^8 [44]	$< 6 \times 10^4$ [68]	6.3×10^{10} [18]
O_2	$< 1.2 \times 10^4$ [68]	4.6×10^9 [46]	1.2×10^1 [68]	4.5×10^{10} [18]
1,3-C_4H_6	$> 10^6$ at 700°C [68]	1.1×10^{11} [45]		2.1×10^{11} [17]
Cl_2	3.1×10^8 [68]		2.1×10^6 [68]	
F_2	2.8×10^8 [68]		$< 1.2 \times 10^6$ [68]	

[a] At 25°C, unless otherwise noted.

Both SiF_2 and CF_2 are unselective towards halogens, *i.e.* their rate constants are about the same for reaction with Cl_2 and F_2. The higher reactivity of SiF_2 as compared to that of CF_2 was suggested [68] to be related to the higher exothermicities of the SiF_2 reactions.

From the above discussion one can conclude that the fluorine (the most electronegative of halogens) substituent stabilizes both methylene and silylene, *i.e.* reduces their reactivity significantly. With unsaturated hydrocarbons SiF_2 reacts by a mechanism similar to that of singlet carbene addition. Although the data on relative or absolute rate constants of SiF_2 reactions do not allow the demonstration of broad selectivity trends, it is a fact that SiF_2 is more selective than SiH_2 between ethylene and butadiene and this parallels the selectivity of CF_2 *vs* CH_2.

It is quite reasonable for one to expect the other dihalosilylenes ($SiCl_2$ and $SiBr_2$) to behave similarly, *i.e.* to exhibit more selectivity than SiH_2. One could expect dihalosilylenes to follow a similar selectivity trend as that of dihalocarbenes *i.e.* increasing in the order: $MBr_2 < MCl_2 < MF_2$ (M = C, Si), and their reactivities to follow the reverse order.

Since the present work comprises quantitative studies of the gas-phase reactions of dichloro- and dibromosilylene with various substrates and since several excellent reviews have been written on the chemistry of other silylenes [35 – 39], the remaining part of this chapter will focus on the chemistry of $SiCl_2$ and $SiBr_2$ only.

I.4. Generation of Dichloro- and Dibromosilylene.

The two most widely-used methods of generating dihalosilylenes ($SiCl_2$ and $SiBr_2$) are thermal and photochemical in nature.

I.4.1. Thermochemical Generation.

Two decades ago thermal methods were the most general ways of generating silylenes. For example, the reduction of tetrahalosilanes or of metal halides over a silicon surface has been reported to yield dihalosilylenes at temperatures above 800°C [70]:

$$SiX_{4\,(g)} + Si_{(s)} \rightleftharpoons 2\,SiX_{2\,(g)} \qquad (X = Br, Cl, F)$$

$$2\,CuCl + Si \longrightarrow 2\,Cu + SiCl_2$$

High-temperature reduction of $SiCl_4$ by H_2 has also been used to produce $SiCl_2$ [70]:

$$SiCl_4 + H_2 \longrightarrow 2\,HCl + SiCl_2$$

Atwell and Weyenberg [71] have used the thermolysis of unsymmetrical disilanes to produce various silylenes, including dihalosilylenes. The general reaction yielding silylenes is

$$ZYXSiSiXYZ \longrightarrow SiXY + SiXYZ_2$$

(Z = H, halogen, alkoxy)

(X, Y = H, halogen, alkoxy, alkyl or aryl)

Chernyshev *et al.* [72] have reported that the one-stage thermal decomposition of perchloropolysilane is an efficient method for producing dichlorosilylene *via* α-elimination:

$$Cl_3Si(SiCl_2)_nSiCl_3 \xrightarrow{500-600°C} (n+1)\,SiCl_2 + SiCl_4 \qquad n \geq 0$$

Doncaster and Walsh [73] studied the kinetics and mechanism of the gas-phase decomposition of Si_2Cl_6 in the presence of I_2 and suggested the following mechanism, involving the formation of $SiCl_2$ by unimolecular elimination as the initial step:

$$Si_2Cl_6 \xrightarrow{596-655K} SiCl_2 + SiCl_4 \qquad \text{slow}$$

$$SiCl_2 + I_2 \longrightarrow Cl_2SiI_2 \qquad \text{fast}$$

For the slow $SiCl_2$ extrusion, they reported the following parameters: $\log(A/s^{-1}) = 13.49 \pm 0.12$ and $E_a = 49.2$ kcal mol^{-1}.

Kagramanov *et al.* [74] have reported the mass spectrometric detection of $SiCl_2$ in a yield of 90% from the reduction of CCl_4 with Si at 1000°C, and of $SiBr_2$ in 95% yield from the reduction of $SiBr_4$ by Si at 1100°C:

$$CCl_4 + Si \xrightarrow{1000°C} SiCl_{2\,(g)} + C$$

$$SiBr_{4\,(g)} + Si \xrightarrow{1100°C} SiBr_{2\,(g)}$$

Hargittai *et al.* [75] observed that the reduction of Si_2Cl_6 by Si gives higher yields of $SiCl_2$ than the analogous reduction of $SiCl_4$:

$$Si_{(s)} + Si_2Cl_{6\,(g)} \longrightarrow SiCl_{2\,(g)}$$

The formation of dichlorosilylene from the pyrolysis of cyclic silaalkanes, silaalkenes and siladienes has been reported by Chernyshev and coworkers [76 – 78]. $SiCl_2$ was detected by trapping experiments. A few examples are:

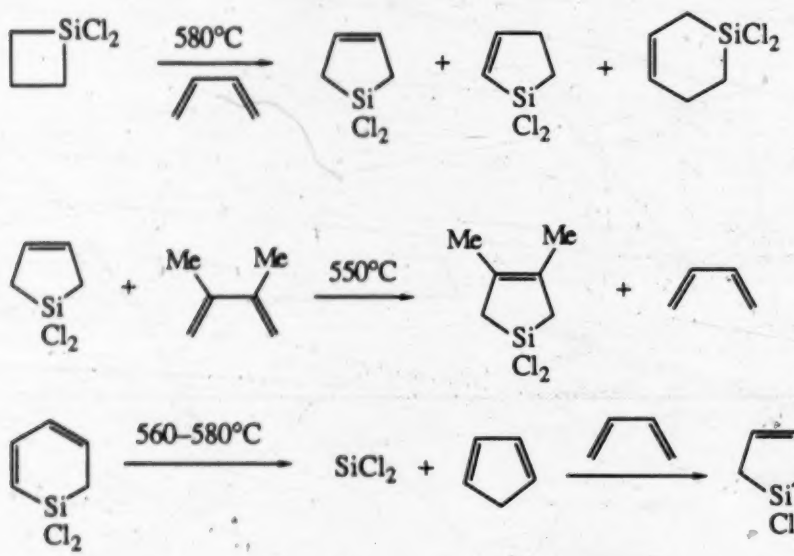

I.4.2. Photochemical Generation.

Flash photolysis of hexachlorodisilane or 1,1-dichlorosilacyclobutane in a Suprasil system, with a single flash of 2900J, was used by Ruzsicska *et al.* [79] to produce $SiCl_2$ in order to record its absorption spectrum in the UV region.

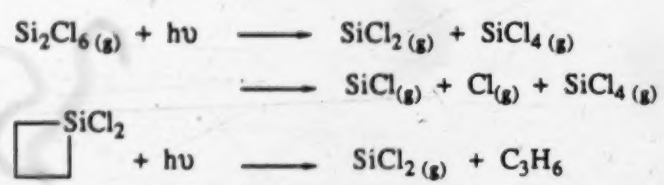

Washida *et al.* [80] have demonstrated the generation of $SiCl_2$ from the vacuum UV photolysis of the chlorinated silanes SiH_2Cl_2 and $SiHCl_3$, but they did not observe any silylene formation from the photolysis of $SiCl_4$ under similar conditions.

$$SiH_2Cl_2 + h\upsilon \longrightarrow SiCl_2 + H_2 \qquad \Delta H = 34.6 \text{ kcal mol}^{-1}$$

$$SiHCl_3 + h\upsilon \longrightarrow SiCl_2 + HCl \qquad \Delta H = 57.6 \text{ kcal mol}^{-1}$$

Kr and Xe lamps were used as photolysis light sources and $SiCl_2$ was identified by its emission spectrum.

Sausa and Ronn [81] used the IR multiphoton excitation of SiH_2Cl_2 to produce electronically excited $SiCl_2$ and recorded its emission spectrum.

Suzuki *et al.* [82] reported the formation of $SiCl_2$ from the photolysis of dichloro- and trichlorophenylsilane, $PhSiHCl_2$ and $PhSiCl_3$, in conventional flow and supersonic free jet experiments. Excimer lasers (KrF, 248 nm and ArF, 193 nm) were used as photolysis light sources.

The only report on the photochemical generation of $SiBr_2$ is that of Ruzsicska *et al.* [83] who photolysed $SiBr_4$ in a Suprasil system with a single flash of 2900J and recorded its absorption spectrum in the UV region.

$$SiBr_4 + h\upsilon \longrightarrow SiBr_2 + Br_2 \qquad \Delta H = 89 \text{ kcal mol}^{-1}$$

$$\longrightarrow SiBr_2 + Br + Br \qquad \Delta H = 142 \text{ kcal mol}^{-1}$$

I.4.3. Other Modes of Generation.

Madix and Schwarz [84] used the molecular beam method to produce $SiCl_2$ *via* the abstraction of Si from a silicon single crystal using a low pressure (10^{-6} – 10^{-5} Torr) molecular beam of chlorine at temperatures 770 to 1500K.

$$Si\ (single\ crystal) + Cl_2\ (beam) \longrightarrow SiCl_2$$

Bochkarev *et al.* [85] investigated the $SiCl_2$ extrusion reaction from a series of dichlorosilanes under the impact of 30 eV electrons by measuring the intensity of the $(P\text{-}SiCl_2)^+$ ions mass spectrometrically.

$$RR_1SiCl_2 + e^- \longrightarrow [RR_1SiCl_2]^{+\bullet} + 2e^-$$

$$[RR_1SiCl_2]^{+\bullet} \longrightarrow RR_1^{+\bullet} + SiCl_2$$

They observed the formation of $SiCl_2$ for R, $R_1 = C_6H_5$, α-C_4H_3S, or $R = C_6H_5$, α-$C_{10}H_7$ and $R_1 = H$. Elimination of $SiCl_2$ from some unsaturated cyclic dichlorosilanes was observed as well. Some examples of these compounds are:

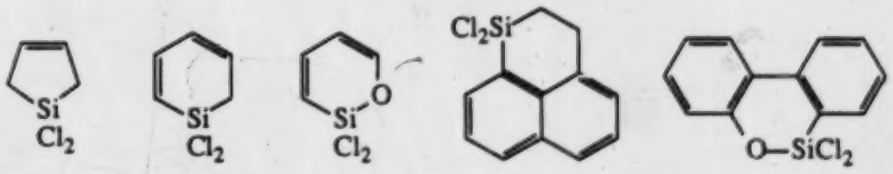

Radiofrequency-excited low-pressure discharge in a parallel plate reactor with a rapid gas flow was used to generate $SiCl_2$ from $SiCl_n(CH_3)_{4-n}$ (n = 1 – 4) by Sameith *et al.* [86]. A radiofrequency power density of 0.5 W cm^{-2} at a frequency of 2.6 MHz was used and $SiCl_2$ was identified by its emission spectrum.

Bock *et al.* [87] have generated $SiCl_2$ from the photoelectron spectroscopically optimized thermal decomposition of various precursors and have recorded the photoelectron spectrum of $SiCl_2$. The reactions were carried out in an electron-impact-heated system.

$$Si_2Cl_6 \xrightarrow{1450K/Si_{ex}} 3\ SiCl_2$$

$$Si_2Cl_6 \xrightarrow{>1250K/Si_{ex}} SiCl_4 \xrightarrow{1450K/Si_{ex}} SiCl_2$$

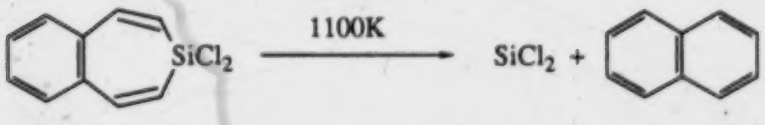

I.5. Spectroscopy and Molecular Geometry of Dichloro- and Dibromosilylene.

I.5.1. Spectrum of $SiCl_2$.

The assignment of the electronic spectrum of $SiCl_2$ has been a controversial subject under investigation for about half a century. The first report of the observation of the electronic spectrum of $SiCl_2$ was made in 1938 by Asundi *et al.* [88] who, from a discharge through flowing $SiCl_4$ vapor, observed a broad structured emission spectrum consisting of two well-known band systems of the SiCl radical and two sets of unknown bands. They attributed these two new band systems to two electronically excited states of the $SiCl_2$ radical, lying at 29952 and 28295 cm^{-1} above the ground state. For the ground state they determined the fundamental frequencies ϑ_1'' and ϑ_2'' to be 540 and 248 cm^{-1}, respectively. For the upper state at 29952 cm^{-1} they estimated the vibrational frequencies ϑ_1' and ϑ_2' to be 445.3 and 201.1 cm^{-1}, respectively. Later

on, Burger and Eujen [89] suggested that the electronic state at 29952 cm^{-1} was the $^1B_1$ state. They also suggested that the vibrational structure of the spectrum observed by Asundi *et al.* should be re-analysed.

In 1951, Weiland and Heise [90] reported the observation of a continuous absorption spectrum with an intensity maximum near 315 nm from the reaction of Si with $SiCl_4$ at 800 – 900°C. They assigned this absorption spectrum to $SiCl_2$ which would be formed according to the reaction

$$Si + SiCl_4 \longrightarrow 2\ SiCl_2$$

however, neither the experimental details nor the spectrum itself were described. They also observed the well-known band systems of SiCl in the UV region upon heating the system to 1150°C.

Milligan and Jacox [91], in 1968, studied the vacuum UV photolysis of SiH_2Cl_2 and SiD_2Cl_2 in an argon matrix at 14K using IR and UV spectroscopy to detect the intermediates. A microwave discharge (2450 MHz, 125W) through 1 Torr of H_2 : He = 1 : 9 mixture was used as the photolysis light source. In the IR spectrum of the photolyzate, two new strong absorptions at 502 and 513 cm^{-1} were observed, and assigned to the stretching fundamentals ($\bar{\vartheta}_1$ and $\bar{\vartheta}_3$) of $SiCl_2$. However, the authors could not decide which one of these two frquencies is due to symmetric stretch ($\bar{\vartheta}_1$). They also estimated the frequency of the bending mode ($\bar{\vartheta}_2$) to be around 200 cm^{-1}. In the UV spectra of the photolyzed Ar:SiH_2Cl_2 and Ar:SiD_2Cl_2 samples they observed a broad (~5 nm half-width) unstructured absorption near 315 nm.

In 1972 Maass *et al.* [92] studied the IR spectrum of matrix-isolated $SiCl_2$, produced by the reaction of $SiCl_4$ with Si at ~1150°C and trapped in a matrix (Ar, Ne or

N_2) at 15K. From chlorine isotopic spilitting measurements, they assigned the observed bands at 512.5 and 501.4 cm^{-1} to the symmetric ($\bar{\upsilon}_1$) and asymmetric ($\bar{\upsilon}_3$) stretching modes of $SiCl_2$, respectively. They were also able to observe a weak band at 202.2 cm^{-1} due to a bending mode ($\bar{\upsilon}_2$) of $SiCl_2$. Their frequency measurements were in excellent agreement with those of Milligan and Jacox. The ∠ ClSiCl bond angle in $SiCl_2$ was calculated to be 105 ± 3°.

Also from the IR spectrum of matrix-isolated $SiCl_2$ at 15 – 20K, Svyatkin *et al.* [13] reported the following values for the vibrational frequencies of $SiCl_2$, which are in good agreeement with Maass *et al.*'s values; $\bar{\upsilon}_1$ = 512 cm^{-1}, $\bar{\upsilon}_2$ = 202.2 cm^{-1} (calculated), $\bar{\upsilon}_3$ = 501.2 cm^{-1}.

In 1977 Cornet and Dubois [93] cast doubt on Asundi *et al.*'s [88] assignment of the emission spectrum of $SiCl_2$. They proposed that the two band systems discovered by Asundi *et al.* in the emission spectrum of the condensed discharge through $SiCl_4$ vapors and assigned by them to the $SiCl_2$ radical, are, in fact, emitted by some other species. In Asundi *et al.*'s experiment $SiCl_4$ vapor, before reaching the discharge tube, was passed through P_2O_5 for the removal of water vapor, and then through an NaOH bulb for CO_2 removal. However, in 1956 Remey [94] showed that $SiCl_4$ reacts with P_2O_5 to give $POCl_3$ which was later shown to produce PO and P_2 radicals in a condensed discharge [95]. Cornet and Dubois claimed that in Asundi *et al.*'s experiment PO and P_2 radicals were produced instead of $SiCl_2$ and excited by the discharge. Cornet and Dubois were able to match each of the several bands, observed and attributed by Asundi *et al.* to $SiCl_2$, with the two well-known systems of PO: the $\tilde{B}\ ^2\Sigma^+ — \tilde{X}\ ^2\Pi_r$ (β) [96, 97] and the $\tilde{B}'\ ^2\Pi_i — \tilde{X}\ ^2\Pi_r$ [97 – 99] transitions, and the well-known $\tilde{C}\ ^1\Sigma_u^+ — \tilde{X}\ ^1\Sigma_g^+$ transition of P_2 [96]. Cornet and Dubois thus concluded that all the bands claimed to be due to $SiCl_2$ [88] were in fact

emitted by PO and P_2 radicals while the electronic spectrum of $SiCl_2$ was yet to be discovered.

The discovery of the absorption spectrum of gas-phase $SiCl_2$ in the UV region was reported in 1985 by Ruzsicska *et al.* [79]. The spectrum was obtained employing the flash photolysis-kinetic absorption spectroscopy technique and Si_2Cl_6 was used as the silylene precursor. Upon photolysing 0.2 – 2 Torr Si_2Cl_6 in the presence of 50 Torr argon with a single flash of 2900J, Ruzsicska *et al.*, in addition to 19 known absorption peaks of SiCl ($\tilde{B}\ ^2\Sigma^+ \leftarrow \tilde{X}\ ^2\Pi_r$ and $\tilde{B}\ ^2\Delta \leftarrow \tilde{X}\ ^2\Pi_r$) in the 297.00 – 274.58 nm region and 15 known emission peaks of SiCl ($\tilde{B}\ ^2\Sigma^+ \rightarrow \tilde{X}\ ^2\Pi_r$) in the 306.70 – 292.20 nm region, observed a new structured absorption band in the 308.70 – 328.22 nm region with the most intense peak at 317.4 nm. From GC and mass spectrometric analyses of the photolyzate in the presence of up to 5 Torr of added butene, the authors assigned this spectrum (*c.f.* Figure I.2) to $SiCl_2$ and not to the $SiCl_3$ radical which could also have been formed in the photolysis of Si_2Cl_6. In order to obtain an independent confirmation of their assignment they flash photolysed 1,1-dichlorosilacyclobutane, which could produce $SiCl_2$ but not $SiCl_3$, under similar conditions and the spectrum obtained was identical to the one obtained from the Si_2Cl_6 photolysis.

Based on the reported absorption bands of the analogous group IV A dihalides, Ruzsicska *et al.* assigned this newly-discovered absorption band of $SiCl_2$ to the $\tilde{A}\ ^1B_1 \leftarrow \tilde{X}\ ^1A_1$ transition and the measured interval between the absorption peaks, 148 ± 11 cm^{-1}, to the bending frequency, ϑ_2', of the $^1B_1$ state. By analogy, the most intense peak at 317.4 nm was assigned to the $\tilde{A}\ ^1B_1(0,8,0) \leftarrow \tilde{X}\ ^1A_1(0,0,0)$ transition and tentative assignments of other vibrational levels in the $^1B_1$ state were made. The authors

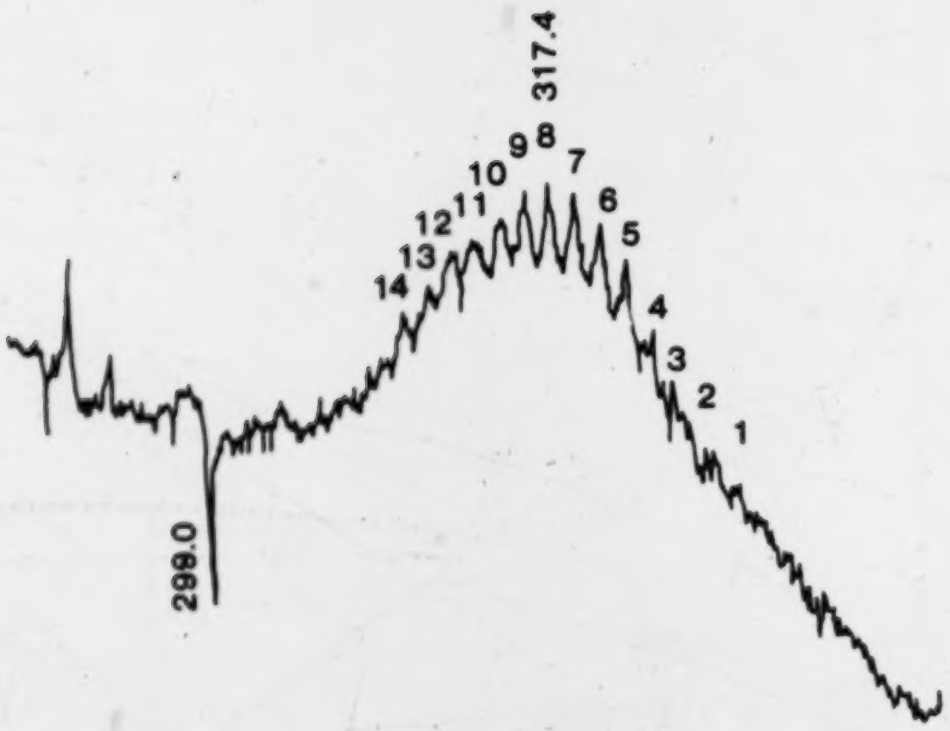

Figure I.2. Absorption spectrum of $SiCl_2$ [79].

reported the observed electronic energy of the upper state ($^1B_1$) to be $T_{00} \leq 30{,}000$ cm^{-1}.

Shortly afterwards, Sausa and Ronn [81] reported that the IR multiphoton (CO_2 TEA laser) decomposition of SiH_2Cl_2 under collision-free conditions is accompanied by an electronic emission which they attributed to an electronically excited $SiCl_2$ radical. The emission spectrum consisted of a broad band with an intensity maximum at 330 nm. Based on product analysis and photodecomposition reaction energetics, they concluded that this emission is due to a spontaneous one-photon radiative decay from electronically excited $SiCl_2$ ($^1B_1 \rightarrow {}^1A_1$) and measured the lifetime of this transition to be 4.5 μs. However, they could not determine whether $SiCl_2$ was formed *via* one-step photodetachment of a H_2 molecule or a stepwise loss of H atoms *i.e.*

$$SiH_2Cl_2 \longrightarrow SiCl_2 + H_2$$

or

$$SiH_2Cl_2 \longrightarrow SiHCl_2 + H$$

$$SiHCl_2 \longrightarrow SiCl_2 + H$$

Later on, Washida *et al.* [80] recorded emission spectra following the vacuum UV photolysis of chlorinated silanes SiH_2Cl_2 and $SiHCl_3$ using rare gas (Ar, Kr, Xe) resonance lamps as photolysis sources. In both cases the common emission band in the 300 – 400 nm region was broad and unstructured with an intensity maximum at about 340 nm. The fluorescence excitation spectrum of $SiHCl_3$ was also recorded by these workers using synchrotron orbital radiation. Based on the energetics of the various possible photodecomposition paths for chlorinated silanes and the appearence energy of

the emission, this broad emission band with maximum at ~340 nm was attributed to the $\tilde{A}\ ^1B_1 \rightarrow \tilde{X}\ ^1A_1$ electronic transition of $SiCl_2$. The general features of the emission band are in good agreement with those of the absorption spectrum [79], considering the difference in equilibrium geometry between the upper electronic state and the ground state.

Following Ruzsicska *et al.*'s discovery of the absorption spectrum of $SiCl_2$, Gosavi and Strausz [100], using *ab initio* molecular orbital methods, calculated the excitation energy for the $\tilde{A}\ ^1B_1(0,0,0) \leftarrow \tilde{X}\ ^1A_1(0,0,0)$ transition of $SiCl_2$ to be 30677.1 cm^{-1}, in good agreement with the experimental value ~30300 cm^{-1} * obtained from the absorption spectrum. They reported the following values for the harmonic vibrational frequencies of $SiCl_2$ in the ground electronic state ($^1A_1$): $\vartheta_1^{''}$ = 530.89 cm^{-1}, $\vartheta_2^{''}$ = 212.78 cm^{-1} and $\vartheta_3^{''}$ = 521.08 cm^{-1}. These values are 3.6 – 5.2% higher than those obtained experimentally [13, 91, 92] and this could be due to the anharmonicity correction which was not taken into account in the calculations.

Another theoretical investigation of the low-lying electronic states of $SiCl_2$ was carried out by Ha *et al.* [101] using *ab initio* methods at different levels of accuracy. For the $\tilde{A}\ ^1B_1 \leftarrow \tilde{X}\ ^1A_1$ transition their value of 32423 cm^{-1} for the vertical excitation energy {$^1B_1(0,n,0) \leftarrow {}^1A_1(0,0,0)$} is in good agreement with that calculated by Gosavi and Strausz [100] (32507.9 cm^{-1}) and also with the experimental value of 31505 cm^{-1} for the most intense absorption peak {$^1B_1(0,8,0) \leftarrow {}^1A_1(0,0,0)$} [79].

Sameith *et al.* [86] have carried out a vibrational analysis of 52 individual bands of the $\tilde{A}\ ^1B_1 \rightarrow \tilde{X}\ ^1A_1$ transition of $SiCl_2$. They recorded the emission spectrum of

* The originally reported value of ≤ 30,000 cm–1 [79] was an estimate.

$SiCl_2$ following an *rf* discharge in the flowing $SiCl_4$ vapor, in the 300 – 450 nm region. Their spectrum was dominated by two broad and intense emissions with maxima at 330 and 390 nm, the former being assigned to the $\tilde{A}\ ^1B_1 \rightarrow \tilde{X}\ ^1A_1$ transition of $SiCl_2$ [80]. The broad emission recorded following the plasma-chemical production of $SiCl_2$

$$Si + SiCl_4 \overset{\text{plasma}}{\rightleftharpoons} 2\ SiCl_2$$

consisted of a large number of individual vibrational bands.

From the analysis of the emission centered at 330 nm, Sameith *et al.* concluded that the spectrum was dominated by a ϑ_2' progression with $\vartheta_2'' = 0$, similar to the absorption spectrum [79]. Their numerical assignment of each v_2' level of the $^1B_1$ state is in excellent agreement with the one made tentatively by Ruzsicska *et al.* [79]. From their analysis, the following values for the bending modes of $SiCl_2$ in the ground state ($^1A_1$) and the upper electronic state ($^1B_1$) have been reported: $\vartheta_2'' = 198.5 \pm 3.7\ cm^{-1}$ and $\vartheta_2' = 148.9 \pm 3.4\ cm^{-1}$. These agree very well with previously reported values [79, 91, 92]. Their derived electronic energy, $T_{00} = 30336\ cm^{-1}$, for the $\tilde{A}\ ^1B_1(0,0,0) \leftarrow \tilde{X}\ ^1A_1(0,0,0)$ transition is also in good agreement with that reported by Ruzsicska *et al.* [79] and calculated by Gosavi and Strausz [100].

In 1986 Suzuki *et al.* [82] reported the laser excitation fluorescence spectrum and dispersed fluorescence spectra of the $\tilde{A}\ ^1B_1 \rightarrow \tilde{X}\ ^1A_1$ transition of the gas-phase $SiCl_2$. $PhSiHCl_2$, $PhSiCl_3$ and Si_2Cl_6 were used as silylene precursors, excimer lasers (KrF,248 nm and ArF =, 193 nm) as photolysis light sources, and a frequency doubled Nd:YAG pumped dye laser was used as a probe laser. From all three precursors identical spectra were obtained in a conventional flow system. The spectral features were similar to those of the absorption spectrum of $SiCl_2$ [79] and thus the spectrum was assigned to $SiCl_2$. From the dispersed fluorescence spectrum they were able to

make vibrational assignment for most of the bands in the excitation spectrum. They assigned the most intense peak (321.9 nm) to the $v_2' = 7$ vibrational level in the upper electronic state ($^1B_1$). By least square fitting they estimated the energy of the $\tilde{A}\ ^1B_1(0,0,0) \rightarrow \tilde{X}\ ^1A_1(0,0,0)$ transition to be $T_{00} = 30003.6 \pm 5\ cm^{-1}$, which is in good agreement with the value ~30300 cm^{-1} observed from the absorption spectrum [79] and the calculated value of Gosavi and Strausz [100]. Their vibrational frequency for the bending mode of $SiCl_2$ in the $^1B_1$ state, $\vartheta_2' = 149.9 \pm 0.5\ cm^{-1}$, is also in agreement with Ruzsicska *et al.*'s value of $148 \pm 11\ cm^{-1}$. Other frequency values reported by them, $\vartheta_1' = 526.5\ cm^{-1}$ and $\vartheta_2'' = 201.2\ cm^{-1}$, also agree with previously reported values from matrix experiments: $\vartheta_1'' = 512.5\ cm^{-1}$ and $\vartheta_2'' = 202.2\ cm^{-1}$ [92]. Except for the vibrational level assignment of the upper electronic state, the absorption spectrum [79] and the laser excitation spectrum of $SiCl_2$ are in good agreement. According to Suzuki *et al.*'s assignment, the most intense peak (317.4 nm) in the absorption spectrum should be assigned to $v_2' = 10$ instead of the $v_2' = 8$ level of the upper electronic state as assigned by Ruzsicska *et al.* [79].

Wavelength and vibrational level assignments of the various peaks of the absorption spectrum of $SiCl_2$ as made tentatively by Ruzsicska *et al.* [79] are given in Table I.5.

The vibrational frequencies of $SiCl_2$ in its ground electronic state, $^1A_1$, and first excited singlet state, $^1B_1$, as reported by different workers, are compiled in Table I.6. Energy values of the electronic transition $\tilde{A}\ ^1B_1(0,0,0) \text{ — } \tilde{X}\ ^1A_1(0,0,0)$ of $SiCl_2$ obtained from different studies are presented in Table I.7.

Table I.5. Assignment of the absorption spectrum of $SiCl_2$ [79].

v_2'	λ, nm	υ, cm^{-1}	Δυ, cm^{-1}
0[a]	~ 330	~ 30300	
1	328.22	30467	146
2	326.66	30613	150
3	325.07	30763	154
4	323.45	30917	139
5	322.00	31056	151
6	320.44	31207	157
7	318.84	31364	141
8	317.41	31505	137
9	316.04	31642	146
10	314.58	31788	152
11	313.09	31940	138
12	311.74	32078	159
13	310.20	32237	157
14	308.70	32394	
			Mean Δυ = 148 ± 11

[a] Since the origin of the absorption spectrum was not very well resolved, λ and υ for $v_2' = 0$ are estimated values using either $\upsilon_0 = \upsilon_1 - \Delta\upsilon_{avg.}$, or, $= \upsilon_n - n\Delta\upsilon_{avg.}$, (n = 1,2,...)

Table I.6. Fundamental vibrational frequencies of $SiCl_2$ in the $\tilde{X}\ ^1A_1$ and $\tilde{A}\ ^1B_1$ electronic states.

Electronic State	υ_1, cm^{-1}		υ_2, cm^{-1}		υ_3, cm^{-1}	
	Experimental	Calculated	Experimental	Calculated	Experimental	Calculated
$\tilde{X}\ ^1A_1$	513 [91]	530.9 [100]	~ 200[a] [91]	202.2 [13]	502 [91]	521.1 [99]
	512.5 [92]	505.5 [55]	202.2 [92]	212.8 [100]	501.4 [92]	501.0 [55]
	512 [13]		201.2 [82]	204.1 [55]	501.2 [13]	
	526 [82]		198.5 ± 3.7 [86]			
$\tilde{A}\ ^1B_1$	435 ± 5 [82]		148 ± 11 [79]			
			148.9 ± 3.4 [86]			
			149.9 [82]			

[a]Estimated value.

Table I.7. Electronic transition energy, T_{00} {$\tilde{A}\ ^1B_1(0,0,0) \leftarrow \tilde{X}\ ^1A_1(0,0,0)$}, of $SiCl_2$.

	T_{00}, cm^{-1}	Reference.
Experimental	~ 30300	[79]
	30336	[86]
	30003.6 ± 5	[82]
Calculated	30677.1	[100]

All the experimental values of the frequencies of $SiCl_2$ are in excellent agreement and also in fairly good agreement with the calculated values (*c.f.* Table I.6). Therefore, the following values for the vibrational frequencies of $SiCl_2$ in its ground state and first excited singlet ($^1B_1$) state are recommended:

	υ_1, cm^{-1}	υ_2, cm^{-1}	υ_3, cm^{-1}
$^1A_1$:	512.5	202.2	501.4
$^1B_1$:	435 ± 5	148.9 ± 3.4	—

(υ_3 for the $^1B_1$ state has not yet been reported.)

The calculated values of the vibrational frequencies of Gosavi and Strausz [100] (*cf.* Table I.6) are slightly higher than the experimental values due to the anharmonicity correction, as mentioned earlier. The other set of calculated values in Table I.6 is the one reported by Coffin *et al.* [55] which seems to be in better agreement with the experimental values than those of Gosavi and Strausz. It should be noted that Coffin *et al.*'s values actually represent the corrected calculated vibrational frequencies obtained by applying the scale factors of 0.870 for υ_1 and υ_3, and 0.918 for υ_2 in order to fit the calculated data to the observed ones.

The data on T_{00} values in Table I.7 exhibit a good agreement among various experimental values and also between the experimental and the calculated values. The value of 30336 cm^{-1} [86] for T_{00} $\{\tilde{A}\ ^1B_1(0,0,0) \leftarrow \tilde{X}\ ^1A_1(0,0,0)\}$ is recommended.

I.5.2. Spectrum of $SiBr_2$.

There has not been as much controversy about the electronic spectrum of $SiBr_2$ as for that of $SiCl_2$. In 1969 Kuznetsova and Kuzyakov [102] recorded the emission spectrum from a glow discharge in $SiBr_4$ vapor. In addition to the known bands of SiBr and $SiBr^+$ they also observed two new systems in the 415 – 435 nm and 425 – 595 nm regions. The first of these two new systems was clearly assigned to the $^2\Delta - \tilde{X}\ ^2\Pi$ transition of SiBr. The second band showed very complex rotational structure and did not allow an unequivocal assignment to SiBr or $SiBr_2$. Therefore, vibrational assignments were made assuming that it may belong to either SiBr or $SiBr_2$ although the authors favored $SiBr_2$ as the carrier of the spectrum. From the $SiBr_2$ assignments they deduced the values 425 and 240 cm^{-1} for the stretching frequencies of $SiBr_2$ in the ground and excited states, respectively, and for the bending modes, 170 and 120 cm^{-1}, respectively.

Later, Babu Rao and Haranath [103] assigned the band system in the 433 – 657 nm region, obtained from a discharge through $SiBr_4$ vapor, to the $^2\Sigma^+ - \tilde{X}\ ^2\Pi_r$ transition of the SiBr radical. More recently, Bosser *et al.* [104] also discovered 30 new bands in 430 – 520 nm region and assigned them to the $\tilde{A}\ ^2\Sigma - \tilde{X}\ ^2\Pi_{1/2}$ system of the SiBr radical.

Maass *et al.* [92] studied the IR spectrum of $SiBr_2$ produced from the reaction of Si with $SiBr_4$ at elevated temperature,

$$SiBr_4 + Si \xrightarrow{950°C} 2\ SiBr_2$$

and isolated in an Ar or N_2 matrix at 15K. From silicon isotopic studies they assigned the peaks at 402.6 and 399.5 cm^{-1} to the $\tilde{\upsilon}_1$ and $\tilde{\upsilon}_3$ stretching modes of $SiBr_2$.

respectively. They failed to observe any peaks due to the bending mode, ϑ_2'', of $SiBr_2$ but estimated its value to be around 120 cm^{-1}.

The first electronic absorption spectrum of $SiBr_2$ in the gas phase has been reported very recently by Ruzsicska *et al.* [83], using the flash photolysis-kinetic absorption spectroscopic technique. They photolyzed 1.0 Torr $SiBr_4$ in 30 Torr argon in a Suprasil system with a single flash of 2900J and observed a broad absorption in the 340 – 400 nm region with a maximum at 362 nm (Figure I.3). This absorption spectrum was assigned to the $\tilde{A}\ ^1B_1 \leftarrow \tilde{X}\ ^1A_1$ transition of $SiBr_2$ partly by analogy with the known spectra of other group IV A dihalides, and partly on the basis of the chemistry involved in its generation. For the $\tilde{A}\ ^1B_1 \leftarrow \tilde{X}\ ^1A_1$ electronic transition of $SiBr_2$ they reported the vertical excitation energy to be 27600 cm^{-1}.

More recently Coffin *et al.* [55] have calculated the fundamental vibrational frequencies of ground state $SiBr_2$, and, after correcting these calculated values employing scale factors of 0.870 for υ_1 and υ_3, and 0.918 for υ_2, reported the following values: $\vartheta_1'' = 395.9\ cm^{-1}$, $\vartheta_2'' = 128.2\ cm^{-1}$ and $\vartheta_3'' = 394.6\ cm^{-1}$. The calculated values of the fundamental stretching and bending frequencies are in good agreement with the values reported by Maass *et al.* [92].

The vibrational frequencies of $SiBr_2$ in its ground state ($^1A_1$), as reported by different workers are listed in Table I.8 along with the vertical excitation energy of its electronic transition $\tilde{A}\ ^1B_1 \leftarrow \tilde{X}\ ^1A_1$.

Energies of the $\tilde{A}\ ^1B_1 — \tilde{X}\ ^1A_1$ electronic transitions of group IV A dihalides are compiled in Table I.9. Dihalosilylenes show a similar trend as the other group IV A dihalides *i.e.* the electronic energy of any MX_2 dihalide series (M = C, Si, Ge, Sn, Pb) decreases in the order X = F > Cl > Br. The electronic transition energy increases on

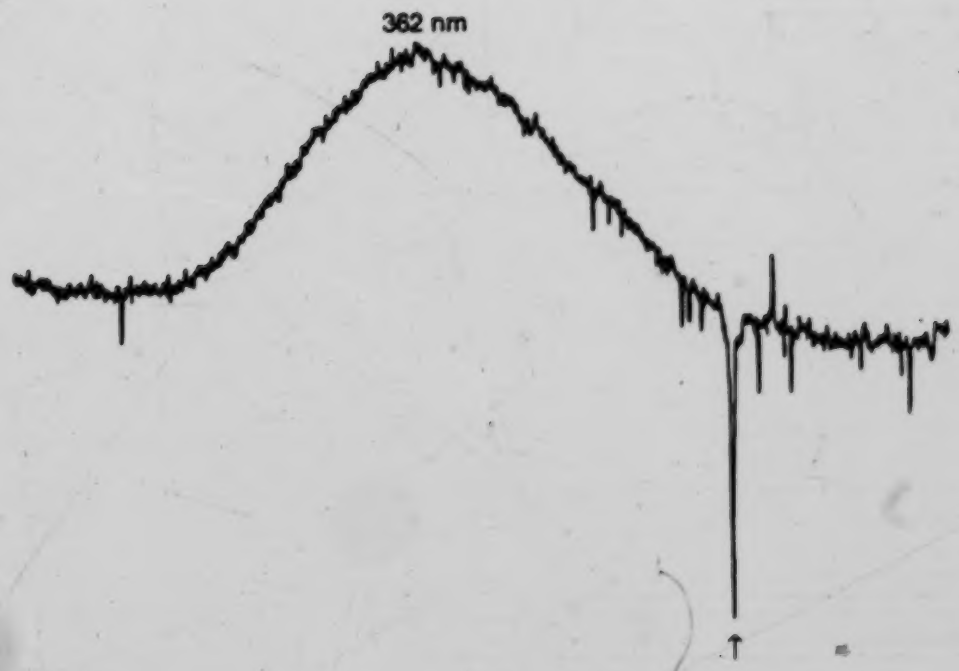

Figure I.3. Absorption spectrum of $SiBr_2$ [83].

(very sharp emission line indicated by an arrow, ↑, is the charcteristic atomic emission from the spectroscopic lamp.)

Table.I.8. Vibrational frequencies of $SiBr_2$ ($^1A_1$) and the vertical excitation energy, T_e (cm^{-1}), of its $\tilde{A}\ ^1B_1 \leftarrow \tilde{X}\ ^1A_1$ transition.

Fundamental	Frequency, cm^{-1}	Reference.
υ_1	402.6 (experimental)	[92]
	395.9 (calculated)	[55]
υ_2	120 (estimated)	[92]
	128.2 (calculated)	[55]
υ_3	399.5 (experimental)	[92]
	394.6 (calculated)	[55]
T_e	27600 (experimental)	[83]

Table I.9. $\tilde{A}\ ^1B_1 \leftarrow \tilde{X}\ ^1A_1$ electronic energies of group IV A dihalides MX_2 (M = C, Si, Ge, Sn and Pb).

X	$T(\tilde{A}\ ^1B_1 \leftarrow \tilde{X}\ ^1A_1)$, cm^{-1}				
	C	Si	Ge	Sn	Pb
F	36878 [105]	44109 [89]	43843 [106]	40741 [108]	40560 [108]
Cl	17093 [105]	30336 [86]	30969 [107]	31055[a] [107]	31000[a] [107]
Br	14962 [105]	27600[a] [83]		27400[a] [109]	

[a] Values obtained at band maximum, not band origin.

going from carbenes to the corresponding silylenes. Both these trends could be explained by Harrison *et al.*'s [9] electronegativity theory as explained above. The similarities in the electronic energies of MX_2 (M = Si, Ge, Sn, Pb) species are also in accordance with the electronegativity theory since Si, Ge, Sn and Pb all have similar electronegativities.

I.5.3. Molecular Geometries of $SiCl_2$ and $SiBr_2$.

According to Walsh's rule both $SiCl_2$ and $SiBr_2$, with 18 valence electrons, are bent in their ground ($^1A_1$) electronic state and have C_{2v} symmetry, like dihalocarbenes, SiH_2 and SiF_2:

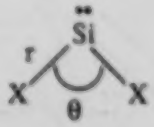

X = H, Br, Cl, F

The predicted bent geometries of $SiCl_2$ and $SiBr_2$ have been supported by various reports on their molecular parameters, which are in good agreement. For example, Hargittai *et al.* [75] reported r(Si – Cl) = 2.083Å and ∠ ClSiCl = 102.8° from electron diffraction combined with mass spectrometry, and Ha *et al.* [101], using *ab initio* methods, obtained r(Si – Cl) = 2.083Å and ∠ClSiCl = 101.49°. All the reported values are presented in Table I.10. The molecular parameters of $SiCl_2$ in its first excited singlet ($^1B_1$) state have also been reported and are presented in Table I.10. On going from the ($^1A_1$) to the ($^1B_1$) state of $SiCl_2$, the Si—Cl bond distance decreases while the Cl–Si–Cl bond angle increases. A similar change in the molecular parameters of CCl_2 ($^1A_1$) was observed in its ($^1B_1$) state. The molecular parameters for the ($^1B_1$) state of $SiBr_2$ are not yet available.

Table I.10. Molecular parameters of $SiCl_2$ ($^1A_1$ and $^1B_1$) and $SiBr_2$ ($^1A_1$).

Electronic State	r(Si–X), Å		θ(XSiX)°	
	$SiCl_2$	$SiBr_2$	$SiCl_2$	$SiBr_2$
$^1A_1$	2.083 ± 0.004[a] [75]	2.243 ± 0.005[a] [75]	102.8 ± 0.6[a] [75]	102.7 ± 0.3[a] [75]
	2.096 [100]	2.257 [55]	105 ± 3[a] [92]	109 ± 3[a] [92]
	2.083 [101]		102 ± 5[a] [13]	102.16 [55]
	2.066 [110]		101.19 [100]	
	2.102 [55]		101.40 [55, 101]	
			101.47 [110]	
$^1B_1$	2.03 ± 0.17 [82]		120.8 ± 0.9 [82]	
	2.14 ± 0.17 [82]		116.9 ± 0.9 [82]	
	2.070 [101]		118.2 [101]	
	2.074 [100]		119.9 [100]	

[a] Experimental values. All other values are calculated ones.

During the $\tilde{A}\ ^1B_1 \leftarrow \tilde{X}\ ^1A_1$ transition of $SiCl_2$, the small change in the Si—Cl bond distance is in accordance with the Frank-Condon principle and the large change in the Cl–Si–Cl bond angle corresponds to the progression in ϑ_2 as has been observed in the absorption spectrum [79].

I.6. Heats of Formation of $SiCl_2$ and $SiBr_2$.

Heats of formation values for dichloro- and dibromosilylene as reported by various workers are in good agreement and are compiled in Table I.11. JANAF tables [111] recommend a value of -40.3 ± 0.8 kcal mol^{-1} for $\Delta H_f^\circ(SiCl_2)$, based on the six independent studies of the equilibrium

$$Si_{(c)} + SiCl_{4\,(g)} \rightleftharpoons 2\,SiCl_{2\,(g)}$$

For $\Delta H_f^\circ(SiBr_2)$, JANAF tables[111] recommend a value of -12.5 ± 4 kcal mol^{-1} whereas CATCH tables [114] recommend -11.1 ± 0.8 kcal mol^{-1} based on the same two flow studies reported by Schaefer *et al.* [112], and Wolf and Herbst [116] of the equilibrium

$$Si_{(c)} + SiBr_{4\,(g)} \rightleftharpoons 2\,SiBr_{2\,(g)}$$

Subsequently, Farber and Srivastava [117] pointed out that in both cases the workers ignored the possible formation of $SiBr_3$ along with that of $SiBr_2$ and thus there must be a small error in their values. Farber and Srivastava, from their high-temperature mass spectrometric measurements, reported $\Delta H_f^\circ(SiBr_2) = -10.5 \pm 2.0$ kcal mol^{-1}. Walsh [118] however, doubted that $SiBr_3$ would be formed and recommended the weighted average of -11 ± 2 kcal mol^{-1} for $\Delta H_f^\circ(SiBr_2)$. Presently, this is the most commonly-accepted value.

Table I.11. Heats of formation of $^1SiCl_2$ (g) and $^1SiBr_2$ (g), ΔH_f°, kcal mol^{-1}.

$SiCl_2$	Reference	$SiBr_2$	Reference
-40.3 ± 0.8[a]	[111]	-12.5 ± 4.0	[111]
-38.2	[112]	-12.2	[112]
-40.6 ± 0.6	[113]	-10 ± 2	[116]
-39.9 ± 0.2	[114]	-11.1 ± 0.8	[114]
-37.6	[115]	-10.5 ± 2.0	[117]
		-11 ± 2[a]	[118]

[a] Recomended values to date.

I.7. Reactivities of Ground State Dichloro- and Dibromosilylene.

Like their carbon analogs, silylenes undergo both insertion and addition reactions. Until the 1980s, the reactions of dichlorosilylene had only been studied qualitatively but more recently, after the discovery of its absorption spectrum, some quantitative data on its reactivity have been reported. On the other hand, the reactivity of dibromosilylene has scarcely been investigated either qualitatively or quantitatively.

I.7.1. Qualitative Investigations.

A number of qualitative investigations on both the insertion and addition reactions of $SiCl_2$ have been reported. A few qualitative studies on the reactions of $SiBr_2$ are also reported. In all these studies both $SiCl_2$ and $SiBr_2$ were generated thermally. It has been shown that when these dihalosilylenes are generated in the absence of any reactive substrate, they undergo polymerization to give polysilanes [70]:

$$Si + SiX_4 \xrightarrow{\sim 800°C} SiX_2 \xrightarrow{> 900°C} (SiX_2)_n$$

X = Cl, Br

I.7.1a. Insertion Reactions.

Timms [119], in 1968, showed that $SiCl_2$, produced from the reduction of $SiCl_4$ with Si at 1350°, when co-condensed with BCl_3, PCl_3 or CCl_4 at – 196°C, inserts into B—Cl, P—Cl and C—Cl bonds, however, from his experimental description it is not clear whether the insertion occurs in the solid phase upon co-condensation, or in the gas phase prior to condensation. He isolated the insertion products by low-pressure, low-

temperature distillation and analysed them using IR, mass spectrometric and analytical techniques.

$$SiCl_2 + BCl_3 \longrightarrow Cl_3SiBCl_2$$

$$SiCl_2 + PCl_3 \longrightarrow Cl_3SiPCl_2$$

$$SiCl_2 + CCl_4 \longrightarrow Cl_3SiCCl_3$$

Later on, Chernyshev *et al.* [120] showed that $SiCl_2$ also inserts into the C—Cl bond of other chlorine-containing hydrocarbons. $SiCl_2$ was generated from the pyrolysis of Si_2Cl_6.

$$C_6H_5CH_2Cl \xrightarrow[450\text{–}500°C]{SiCl_2} C_6H_5CH_2SiCl_3$$

$$ClCH_2SiCl_3 \xrightarrow[580°C]{SiCl_2} Cl_3SiCH_2SiCl_3$$

$$Cl_2CH_2 \xrightarrow[620°C]{2\,SiCl_2} Cl_3SiCH_2SiCl_3$$

$SiCl_2$ also inserts into the C_{ar}—Cl bond, as shown by the formation of trichlorophenylsilane from the pyrolysis of benzyldichlorosilane in the presence of chlorobenzene [121]. An abstraction-recombination mechanism has been proposed for such insertion reactions [76]:

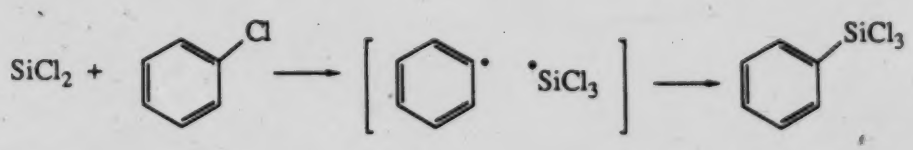

up to 70%

$SiCl_2$ also inserts into C_{ar}—X bonds (X = Br, F, I) [76]. although such reactions are complicated by halogen exchange:

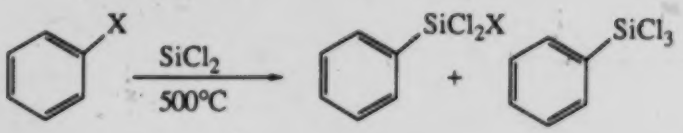

X = Br	22%	44%
F	15%	20%
I		40%

$SiCl_2$ has been reported [70] to react with chlorosubstituted polysilanes to give products arising from insertion into the Si—Cl bond:

$$SiCl_2 + Cl(SiCl_2)_nCl \longrightarrow Cl(SiCl_2)_{n+1}Cl$$

$$n \geq 2$$

$SiCl_2$ also inserts into the H—Cl bond [70, 122]:

$$SiCl_2 + HCl \longrightarrow HSiCl_3$$

Insertion into the C—H bond of methyl substituents in an aromatic ring [121] has also been observed

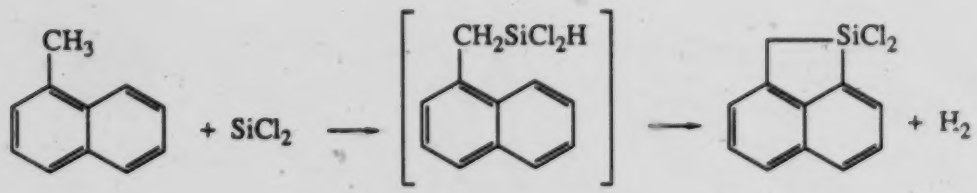

and also into the C_{ar}—H bond, as shown by the formation of 1,1,2,2-tetrachloro-1,2-disilaacenaphthene from the copyrolysis of trichlorosilane and trichloro-1-naphthylsilane [121]:

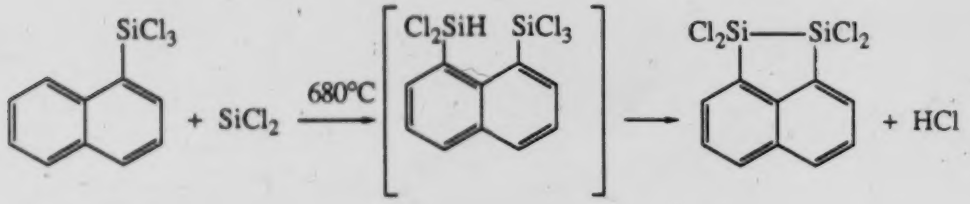

Insertion of $SiCl_2$ into the C_{ar}—C bond has been reported by Chernyshev *et al.* [121] on the basis of the observation of the following ring expansion reaction:

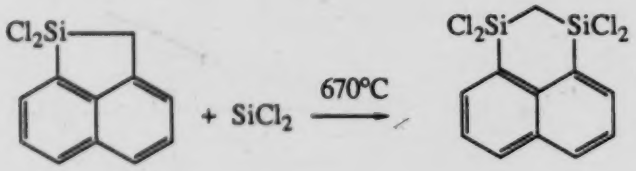

$SiCl_2$ inserts into both O—H and O—C bonds [121], as shown by the copyrolysis of phenol and Si_2Cl_6. The initial step is insertion into the O—H bond followed by insertion of another molecule of $SiCl_2$ into the O—C bond. However, different reaction routes have been proposed for different pyrolysis temperatures:

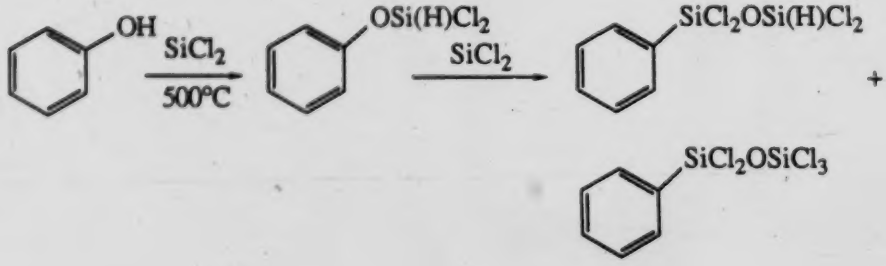

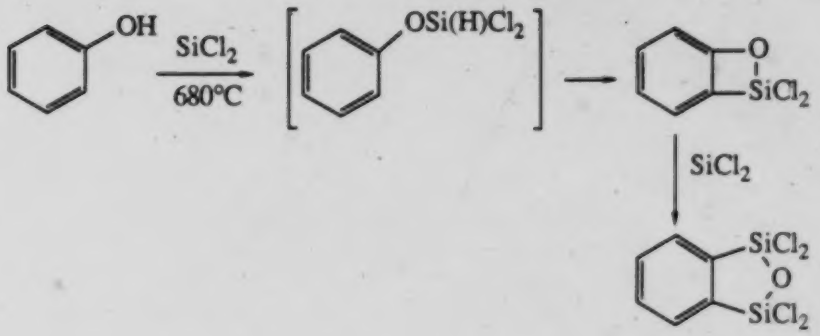

Insertion of $SiCl_2$ into the Si—H bond is also known [121] to occur, as shown by the following reaction:

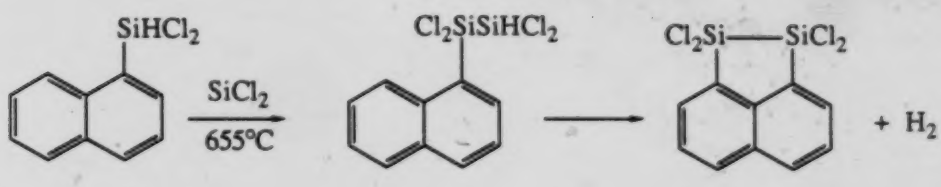

Data on the reactivity of $SiBr_2$ are very scarce. Other than its polymerization, it has been reported [70] to insert into the B—F bond of BF_3, followed by halogen exchange to give the final product:

$$SiBr_2 + BF_3 \longrightarrow FBr_2SiBF_2 \xrightarrow[\text{exchange}]{\text{halogen}} F_3SiBF_2$$

I.7.1b. Addition Reactions.

As for the case of the insertion reactions, a number of qualitative investigations concerning the addition of thermally-generated $SiCl_2$ to unsaturated bonds have been reported. However, no data are available on the addition reaction of $SiBr_2$.

Like singlet carbenes, $SiCl_2$ adds to olefinic and acetylenic bonds leading to the initial formation of silacyclopropanes and silacyclopropenes, respectively, which, unlike their carbon analogs, are unstable and thus undergo reactions such as dimerization, rearrangement etc. to give stable products as shown in the following examples.

Chernyshev *et al.* [72] observed the formation of 1,1,4,4-tetrachloro-1,4-disilacyclohexa-2,5-diene from the copyrolysis of Si_2Cl_6 with acetylene. They explained the formation of this product by initial addition of $SiCl_2$ across the acetylenic bond:

$$Si_2Cl_6 \xrightarrow{450-550°C} SiCl_2 + SiCl_4$$

$$SiCl_2 + HC{\equiv}CH \longrightarrow \left[\triangleright SiCl_2\right] \xrightarrow{\text{dimerization}} \begin{array}{c} Cl_2Si \\ \diagup\quad\diagdown \\ \diagdown\quad\diagup \\ Si Cl_2 \end{array}$$

During the copyrolysis of hexachlorodisilane and ethylene, Chernyshev *et al.* [123] did not observe any cyclic Si-containing products. However, from the 70% yield of Si-containing compounds formed they proposed initial silacyclopropane formation with subsequent isomerization to the silapropylene structure:

$$SiCl_2 + H_2C{=}CH_2 \xrightarrow{500-550°C} \left[\triangleright SiCl_2 = Cl_2\dot{S}iCH_2CH_2\cdot\right]$$

$$\downarrow$$

$$Cl_2Si(H)CH{=}CH_2$$

$SiCl_2$ also reacts with conjugated dienes to give silacyclopentenes [124]:

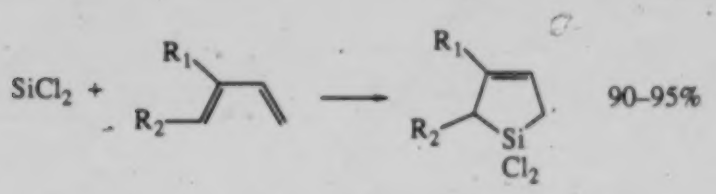

R_1 = H, CH_3, Cl; R_2 = H, CH_3

In 1978 Chernyshev and coworkers [123] suggested that although addition of $SiCl_2$ to conjugated dienes gives a 1,4-addition product, the possibility of initial 1,2-addition followed by rearrangement cannot be ruled out.

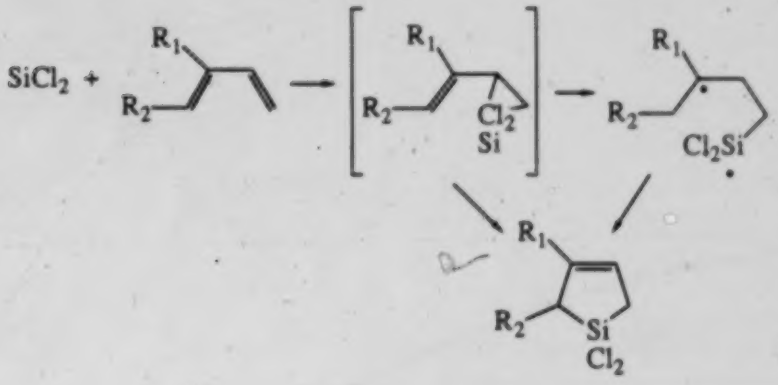

Later on [76] however, from the thermal decomposition of 1,1-dichloro-1-silacyclo-3-pentene in the presence of 2,3-dimethyl-1,3-butadiene, they concluded that $SiCl_2$ adds across conjugated double bonds in a concerted 1,4-addition.

$SiCl_2$ also reacts with cyclic conjugated dienes under similar conditions. Initial addition of $SiCl_2$ across a double bond with subsequent rearrangement of the bicyclic intermediate to a six-membered heterocyclic product has been proposed [124]:

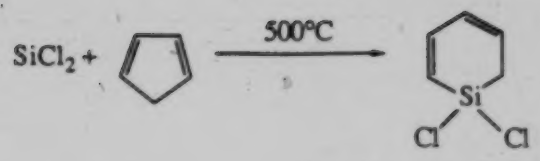

It also reacts with the double bonds of furan[124]:

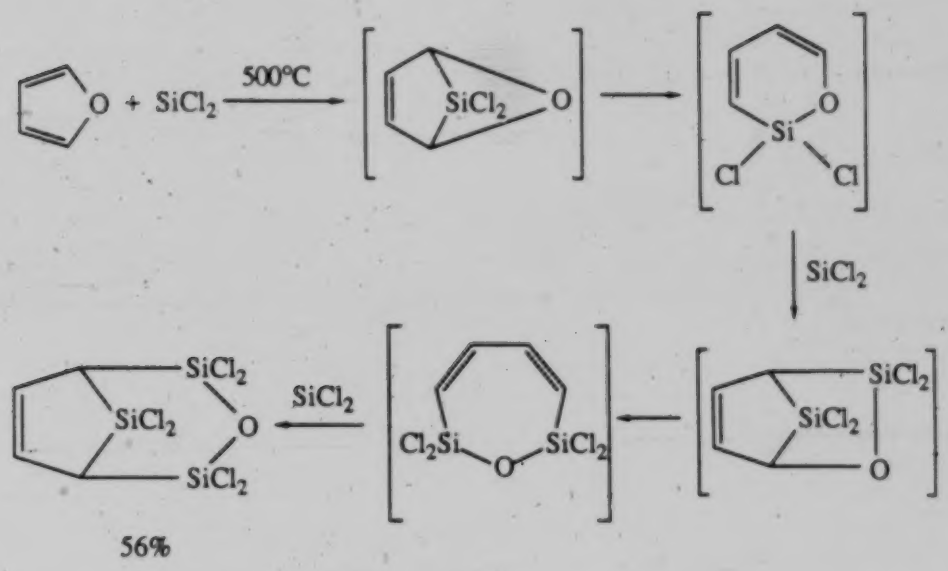

56%

I.7.2. Quantitative Investigations.

Following the discovery of the UV absorption spectrum of $SiCl_2$ in the gas phase [79] Safarik *et al.* [125] have reported the first absolute rate constant measurements for the gas-phase reactions of $SiCl_2$ with a series of unsaturated hydrocarbons using the flash photolysis-kinetic absorption spectroscopic technique in which the $SiCl_2$ absorption spectrum was used to monitor its concentration. These rate constant values, along with the known values for the similar reactions of SiH_2, are compiled in Table I.12.

Table I.12. Absolute rate constants for the gas-phase reactions $SiX_2 + R \rightarrow$ Products, (X = H, Cl).

R	k, $M^{-1}s^{-1}$	
	$SiCl_2$ [125]	SiH_2 [45]
C_2H_2	$(4.3 \pm 1.1) \times 10^7$	$(5.9 \pm 0.7) \times 10^{10}$
1-C_4H_6	$(7.9 \pm 1.9) \times 10^8$	—
C_2H_4	$(7.8 \pm 2.0) \times 10^7$	$(3.2 \pm 0.3) \times 10^{10}$
C_3H_6	$(2.3 \pm 0.6) \times 10^8$	$(7.2 \pm 0.6) \times 10^{10}$
t-C_4H_8	$(3.1 \pm 0.8) \times 10^8$	—
Si_2Cl_6	$< 5.3 \times 10^8$	—

No quantitative data on the reactions of $SiBr_2$ have been reported thus far.

For the reactions of $SiCl_2$, rate constant values increase with increasing alkyl substitution on the C—C double and triple bond, thus exhibiting the electrophilic nature of $SiCl_2$, like that of SiH_2. From the limited data given in Table I.12 it can be seen that SiH_2 reacts faster with unsaturated hydrocarbons than $SiCl_2$, and thus one can roughly conclude that the selectivity of $SiCl_2$ *vs* SiH_2 is parallel to that of CCl_2 *vs* CH_2 *i.e.* the dihalospecies MX_2 (M = C, Si) are less reactive than MH_2 species.

Measurements of absolute rate constants for the reactions of SiX_2 (X = H, halogen) with more substrates are needed in order to draw a more meaningful comparison of their reactivity.

I.8. Synthetic and Industrial Applications.

Qualitative investigations of the chemistry of $SiCl_2$ have led to the synthesis of several otherwise inaccessible novel organosilicon compounds. A few examples are [121, 124]:

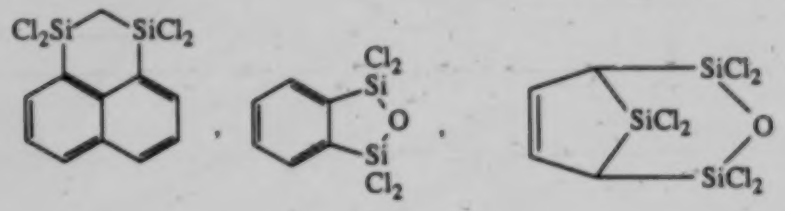

$SiCl_2$ has also been found to be an important intermediate in technologically-important processes, such as chemical vapor deposition of thin silicon films, and as one of the reaction products in the chemical etching of silicon wafers. Both these processes, *i.e.* chemical vapor deposition (CVD) and chemical etching, are two of the several

processes employed repeatedly in the production of integrated circuits for the microelectronics industry.

Chemical vapor deposition (CVD) can simply be defined as a process in which gaseous molecules undergo thermal decomposition or react with other gaseous species on a solid surface to leave behind solid materials of well-defined properties. CVD processes are used to deposit thin films of a variety of conducting, semiconducting and insulating materials essential for the fabrication of integrated circuits. Two most commonly employed CVD reactors are:

1. *Cold Wall Reactor:* The object of this type of reactor is to cause the desired reaction only on the surface of the hot wafer and keep all other surfaces free of deposits. A sketch of a cold wall reactor is shown in Figure I.4a. These reactors are used at pressures of several Torr to one atmosphere and thus this process is also called atmospheric pressure CVD (APCVD). The reactant gas or mixture of gases flow continuously down a quartz tube over a heated susceptor aligned parallel to the flow. The susceptor is heated by an rf source or optically, using UV lamps. The wafers to be coated are placed on the susceptor. The wafer, on which integrated circuits are built, is a single crystal of very pure silicon in flat circular shape. Cold-wall types of reactors are often used for the growth of thin films of polysilicon, SiO_2 and epitaxial silicon which is single-crystal silicon layer. A carefully-grown epitaxial Si film is much purer than the underlying Si wafer, in fact it is of such high quality that integrated circuits are actually built on the epitaxial film, whereas the single-crystal Si wafer serves as a mere holder for the epitaxial film.

2. *Hot Wall Reactor:* one of the problems with cold wall reactors is the difficulty in

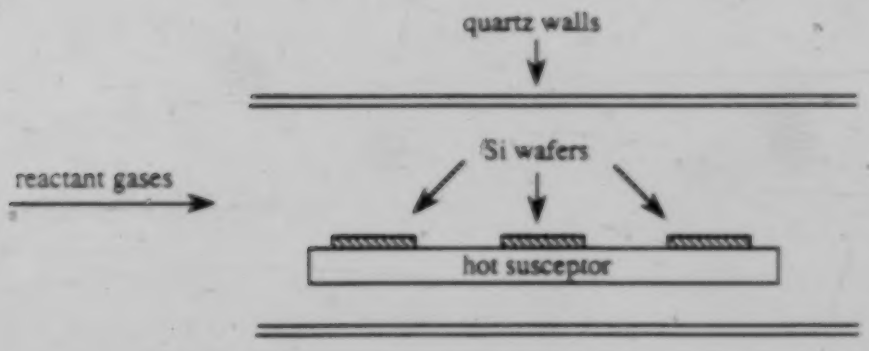

(a) Cold wall reactor

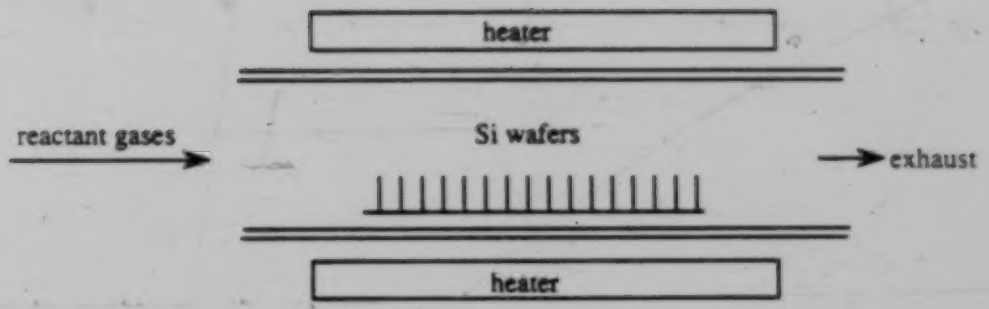

(b) Hot wall reactor

Figure I.4. Chemical vapor deposition reactors.

maintaining a uniform temperature on the wafers. Such problems can be solved by using a hot-wall reactor in which the entire reaction chamber is placed in a furnace. It is typically used at pressures below 1 Torr and thus this process is also known as low pressure CVD (LPCVD). A basic diagram of this reactor is shown in Figure I.4b. The reactant gases are introduced at one end of the furnace and pumped out the other end. Wafers are loaded vertically and thus several hundred wafers can be processed in a single run. The problem with this type of reactor is that film deposition also occurs on the reactor walls and thus the reactor must be cleaned frequently. Such systems are commonly used to deposit polysilicon, SiO_2 and Si_3N_4 films.

The intermediacy of $SiCl_2$ in the CVD of epitaxial Si from Si-Cl-H (*i.e.* $SiCl_2H_2$, $SiCl_3H$ or $SiCl_4$ in H_2) and Si-Cl-He ($SiCl_4$ in He) systems has been reported. Smith and Sedgwick [126] were the first to report the formation of $SiCl_2$ during CVD of epitaxial Si from Si-Cl-H systems using inelastic scattering spectroscopy as a reaction probe. $SiCl_2$ was found to be the dominant Si-containing species at high temperature. Sedgwick and coworkers [127, 128] then studied the formation of $SiCl_2$ as a function of deposition conditions such as temperature, flow rate of source gas and input reactants, using $SiCl_2$ fluorescence as a reactor probe. Sedgwick and coworkers reported that $SiCl_2$ fluoresces in 488 and 514.5 nm light. However, from Gosavi and Strausz's *ab initio* calculations $SiCl_2$ has no singlet state in this energy range, and the only excited state of $SiCl_2$ in this range is $^3A_1$ (445 nm, 22467 cm^{-1}). Radiative transition from this state would be phosphorescence and not fluorescence, as reported by Sedgwick and coworkers. They concluded that $SiCl_2$ forms homogeneously in the

gas phase during CVD of Si by the following reactions:

$$SiCl_4 + H_2 \xrightarrow{1200°C} SiCl_2 + 2\,HCl$$

$$SiCl_2H_2 \xrightarrow{1050°C} SiCl_2 + H_2$$

and as the wafer surface is approached, $SiCl_2$ diffuses to the surface and is reduced to Si by the reaction:

$$SiCl_2 + H_2 \xrightarrow{surface} Si_{(s)} + 2\,HCl$$

They also found that the $SiCl_2$ gradient at the surface is proportional to the growth rate.

Ban [129], who studied the epitaxial growth of Si using a mass spectrometer coupled to a CVD reactor, also observed the formation of $SiCl_2$ in the vapor phase at 1300K as well as several other Cl- and H-containing products during CVD of epitaxial Si from the Si-Cl-H system. The concentrations of $SiCl_2$ were, however, small, and $SiCl_2$ was proposed to be formed from the reaction:

$$SiCl_{4\,(g)} + H_{2\,(g)} \longrightarrow SiCl_{2\,(g)} + 2\,HCl$$

In contrast to Sedgwick and coworkers' [127, 128] proposal, Ban claimed that the major heterogeneous decomposition reaction is:

$$SiCl_{4\,(g)} + 2\,H_{2\,(g)} \longrightarrow Si_{(s)} + 4\,HCl$$

Subsequently, Nishizawa and Saito [130] studied the growth mechanism of the CVD of Si films from Si-Cl-H systems, using IR direct spectroscopic detection of the

reaction products. From their observations they proposed that the most probable mechanism of Si CVD involves $SiCl_2$ as an important intermediate:

$$SiCl_4 + H_2 \rightleftharpoons SiHCl_3 + HCl$$

$$SiHCl_3 + H_2 \rightleftharpoons SiH_2Cl_2 + HCl$$

$$SiH_2Cl_2 \rightleftharpoons SiCl_2 + H_2$$

$$SiHCl_3 \rightleftharpoons SiCl_2 + HCl$$

$$SiCl_2 + H_2 \overset{\text{surface?}}{\rightleftharpoons} Si_{(s)} + 2\,HCl$$

It is now generally accepted that $SiCl_2$ is the major depositing species during CVD of Si.

After the desired pattern is transfered onto the Si wafer and protected by a photoresist coating using a lithographic technique, the unprotected Si film is removed by chemical etching. Dry etching processes are most commonly used since highly anisotropic profiles, very critical in integrated circuits, can be obtained and very small amounts of reactant gases are required as compared to wet etching. Plasma chemical etching is one of the dry etching processes in which Si wafers to be etched are exposed to an etching gas atmosphere in a vacuum system. The etching gas molecules in the vicinity of the gas-solid interface are dissociated, *e.g.* by an rf excitation, to produce reactive species. These transient species then react with the surface atoms to produce volatile compounds which eventually escape from the surface, yielding the etched surface.

Sputter etching is another dry etching process which uses energetic noble gas ions such as Ar^+ to bombard the wafer surface and etching of the surface is accomplished by physically knocking atoms off the wafer surface.

Sedgwick and coworkers [127, 128] observed the formation of $SiCl_2$ during the dry etching of Si by HCl in H_2 or $SiCl_4$ in He and proposed that $SiCl_2$ is formed at the Si surface according to the following reactions:

$$SiCl_{4\,(g)} + Si_{(s)} \longrightarrow 2\,SiCl_2 \qquad \text{in He}$$

$$2\,HCl_{(g)} + Si_{(s)} \longrightarrow SiCl_2 + H_2 \qquad \text{in } H_2$$

Ban [129] also investigated the etching of Si by HCl and $SiCl_4$-He, and observed the formation of $SiCl_2$ generated in the above two heterogeneous reactions, in both cases.

More recently, Li *et al.* [131] studied the laser-induced etching of a Si surface by a chlorine molecular beam under 355 and 560 nm irradiation. The desorbed reaction products were detected mass spectrometrically and the formation of only $SiCl_2$ and $SiCl_3$ was observed under both irradiation conditions.

Industrial applications of $SiBr_2$ are not known yet, perhaps due to the unavailability of any data on its reactivity. It could be expected as one of the etching products if Br_2 gas is used as an etchant.

I.9. Aim of the Present Investigation.

In the previous sections it has been shown that silylenes, an important class of reactive intermediates, have molecular geometries and spectral features similar to those of their carbene analogs. Qualitative studies have shown that they undergo the same type of reactions as those of carbenes. Of the dihalosilylenes, dichlorosilylene has been shown to be a precursor for the synthesis of novel organosilicon compounds and has also been shown to play a siginificant role in such processes as chemical vapor deposition and chemical etching of Si which are employed to fabricate integrated circuits used in the fast-growing area of microelectronics.

Dihalocarbenes have been studied extensively and their relative reactivity towards unsaturated hydrocarbons as well as some inorganic compounds (O_2, NO, CO) is well established. The reactivity increases in the order $CF_2 < CCl_2 < CBr_2 < CH_2$. Some data on the absolute rate constants of the reactions of CF_2, CCl_2 and CH_2 with O_2, NO and CO have also been reported.

In contrast to carbenes, studies of dihalosilylene chemistry are limited. Although a number of qualitative investigations of $SiCl_2$ reactions have been reported, quantitative data are scarce. The reactions of $SiBr_2$ have never been investigated either qualitatively or quantitatively.

Quantitative information is essential in understanding the mechanistic details of any reaction. At the time this project was undertaken, the only quantitative data available on $SiCl_2$ were the absolute rate constants of its reactions with acetylenes and alkenes [125], which reflected its electrophilic nature towards addition to unsaturated bonds. No qualitative or quantitative information on its reactions with inorganic

compounds was known. A few absolute rate constant values of SiF_2 reactions are available and show that, like CF_2, SiF_2 reacts extremely slowly with both organic and inorganic compounds.

Thus the primary aims of this investigation were:

1. to measure the absolute rate constants of the reactions of gas-phase $SiCl_2$ with

   (a) inorganic molecules O_2, NO, CO and N_2O which have never been studied before, qualitatively or quantitatively;

   (b) 1,3-butadiene, since $SiCl_2$ is known to react with conjugated dienes but the rates of reactions have not yet been reported;

   (c) saturated hydrocarbons such as isobutane, in order to measure the rate of $SiCl_2$ insertion into C—H bonds, which has been shown to occur from qualitative studies.

2. to measure the absolute rate constants of the gas-phase reactions of $SiBr_2$ with inorganic molecules since the reactivity of $SiBr_2$ had not been investigated in any manner, and to compare its reactivity with that of $SiCl_2$;

3. and lastly, to shed some light on the mechanistic aspects of these reactions on the basis of previous work and these measurements, and to see whether the relative reactivity of dihalosilylenes follow a trend similar to that known for dihalocarbenes.

Chapter II

EXPERIMENTAL

In direct investigations of fast reactions it is very important that the reaction initiation is accomplished in a time period shorter than the overall reaction time in order to create a high initial concentration of the reactive species, and in such a way that the reaction is homogeneous throughout the volume of the reaction mixture.

Years ago Norrish and Porter [132] introduced the method of flash photolysis to study fast reactions. Since then it has undergone many technical refinements and to date the photochemical initiation of reaction by flash photolysis is the most convenient method of bringing about a large extent of primary reaction, in a short interval of time, in a homogeneous system. Since it is a very well-established technique and has been the subject of several excellent review articles, therefore only a brief description of the conventional system is considered necessary here.

In flash photolysis, the reaction system is irradiated with a short-duration, high-intensity light flash, thus creating a non-equilibrium situation in a small interval of time of the order of micro-seconds. This provides a general means of producing relatively large concentrations of transient species which undergo subsequent reactions. The rate of disappearance of these transients, due to their reactions, is monitored by recording their absorption profile which may be investigated in two ways, flash spectroscopy or kinetic spectrophotometry. In the present study, flash spectroscopy was used, in which the whole range of wavelengths is recorded at a single time. This is accomplished by monitoring a beam from the spectroscopic flash discharged at a pre-set delay time after the photolysis flash discharge, which essentially provides a background continuum.

This beam, after passing through the reaction system, is resolved by the spectrograph and is recorded photographically. The process is repeated at various time delays and a time profile of the chosen absorption band of the transient is thus obtained.

II.1. Apparatus

II.1.1. The Vacuum System.

A conventional high vacuum system made of Pyrex was used to purify the reagents. It was completely grease-free, using helium-tested Hoke valves, and consisted of a distillation train and storage units (Figure II.1).

The whole system was evacuated to a pressure of 10^{-6} Torr by means of a mercury diffusion pump backed by a rotary pump (Duo-seal vacuum pump). Pressures were monitored by Pirani Vacuum Gauges (type GP-140), Magnevac Vacuum Gauges (type GMA-140), MKS Baratron Pressure Meters (type 77, 315 BHS-100 and 170 M-6B) and mercury manometers which were capable of measuring pressures in the 10^{3} to 10^{-3} Torr range.

The distillation train, consisting of a series of three traps isolated by Hoke valves, was used to purify the reagents. The two storage units, one for the reagents and the other for the reaction mixtures, consisted of several one- or three-litre bulbs.

Argon was introduced into the main vacuum system after passage through a 30-cm long column of copper turnings (heated to 350°C for the removal of oxygen) and a 30-cm long column of molecular sieve (type 5A, for the removal of water vapor).

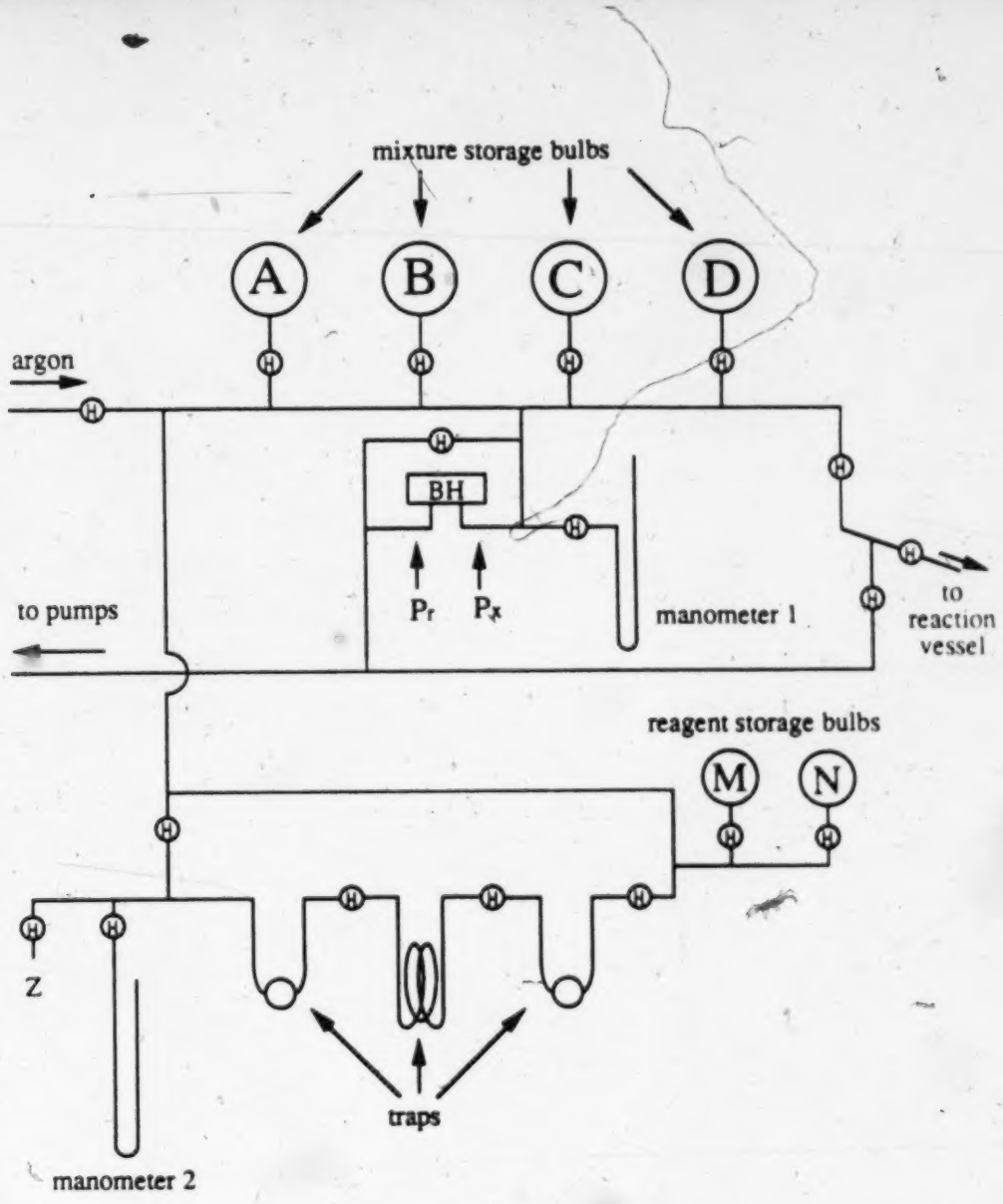

BH - Baratron Pressure Meter Head.

Z - Inlet for the introduction of reagents.

Ⓗ - Hoke Valve.

Figure II.1. The Main Vacuum System.

A separate mercury-free line was used to fill the flash lamps. Vacuum was achieved by a Duo-seal vacuum pump with a liquid nitrogen trap and the pressure was monitored by a Pirani Vacuum Gauge (type GP-140) and measured by Edwards CG3 gauges.

II.1.2. The Flash Photolysis-Absorption Spectroscopic System.

The four major components of the flash photolysis-absorption spectroscopic system are illustrated in Figure II.2.

II.1.2a. The Reaction Vessel and the Reflective Housing.

The reaction vessel used was a Suprasil (wavelength cutoff 165 – 170 nm) cylindrical tube 73 cm long and 25 mm in inner diameter. It was equipped with flat Suprasil windows on both ends and a side arm for the introduction and evacuation of the reaction mixture. The side arm was connected to the main vacuum system by a helium-tested Cajon valve, which facilitated the detachment of the reaction vessel from time to time for cleaning.

The reaction vessel, sitting on two end supports, was positioned at the centre of a reflective housing assembly lying horizontally along the optical path. Apertures on both ends allowed the passage of light in and out through the reaction vessel. Nitrogen gas was flushed through the reflective housing in order to prevent ozone formation from the photolysis flash.

The reflective housing (Figure II.3) was constructed of aluminum and was cylindrical in shape, 80 cm long and 15 cm in inner diameter. It consisted of two half cylinders joined together by hinges on one side, so that the upper half could be opened

for the removal of the reaction vessel and the photolysis lamp for cleaning. The lower half, upon which the ends of the reaction vessel and photolysis lamp rested, was mounted by two supports onto the optical bench. The inner surface of the housing was coated with $BaSO_4$ which is highly reflective in the UV region of the spectrum.

II.1.2b. The Photolysis Lamp.

The photolysis lamp (Figures II.2 and II.3) was a Suprasil tube 25 mm in diameter with a sidearm for filling and evacuation. Molybdenum alloy electrodes (Vitreosil Model T/E7/232) were sealed into each end by standard lead seals able to withstand high thermal and mechanical shock. The distance between the tips of the electrodes, 73 cm, was the same as the length of the reaction vessel. The side arm was connected to the lamp vacuum line through a high vacuum stopcock (Pyrex V-4) and a detachable ball joint. A stopcock isolated the lamp from the vacuum line, and the ball joint facilitated the removal of the lamp for cleaning.

The lamp was placed horizontally next to the reaction vessel with the electrodes resting on the ends of the reflector housing and protruding outside through the end apertures. When filled with ~19 Torr xenon gas, the light flash reached its maximum intensity in 10 μs and had a half life of about 20 μs with a long tail, as recorded by a photocell (Sylvania 90 CV) and displayed on an oscilloscope (Hitachi Denshi Ltd. LR 54541). The lamp circuit included an ignitron (National Electronics NL-7703) and a G.E. Energy Storage Capacitor (Capacitance 14.5 μF, 20 KV). The lamp circuit, when discharged at 20 KV, dissipated 2900 joules through the xenon atmosphere, creating a plasma which generated the high intensity light output. To condition a new lamp the following method was used: the lamp circuit was discharged initially at a low voltage and the discharges were then repeated with gradually increasing voltages until

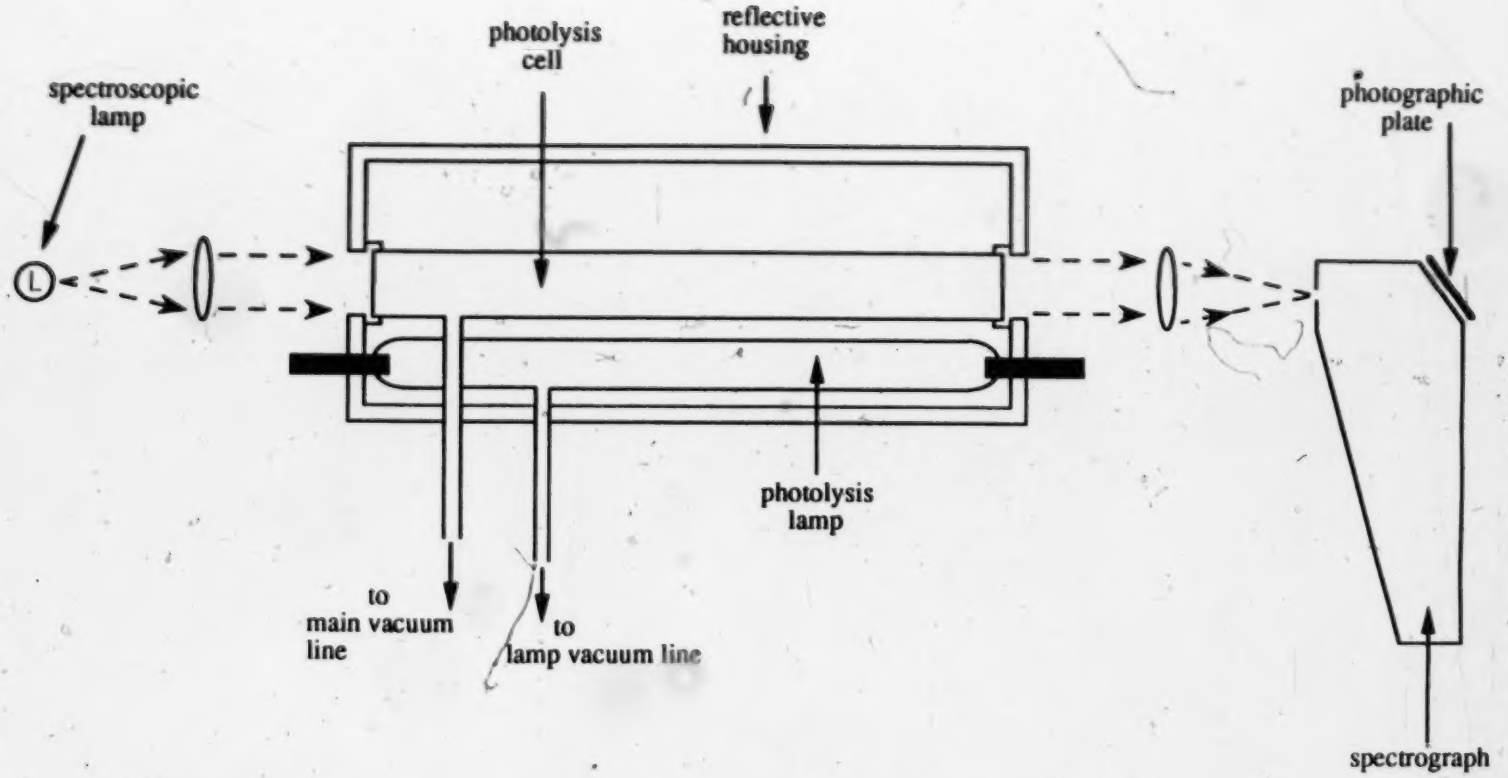

Figure II.2. The Flash Photolysis System.

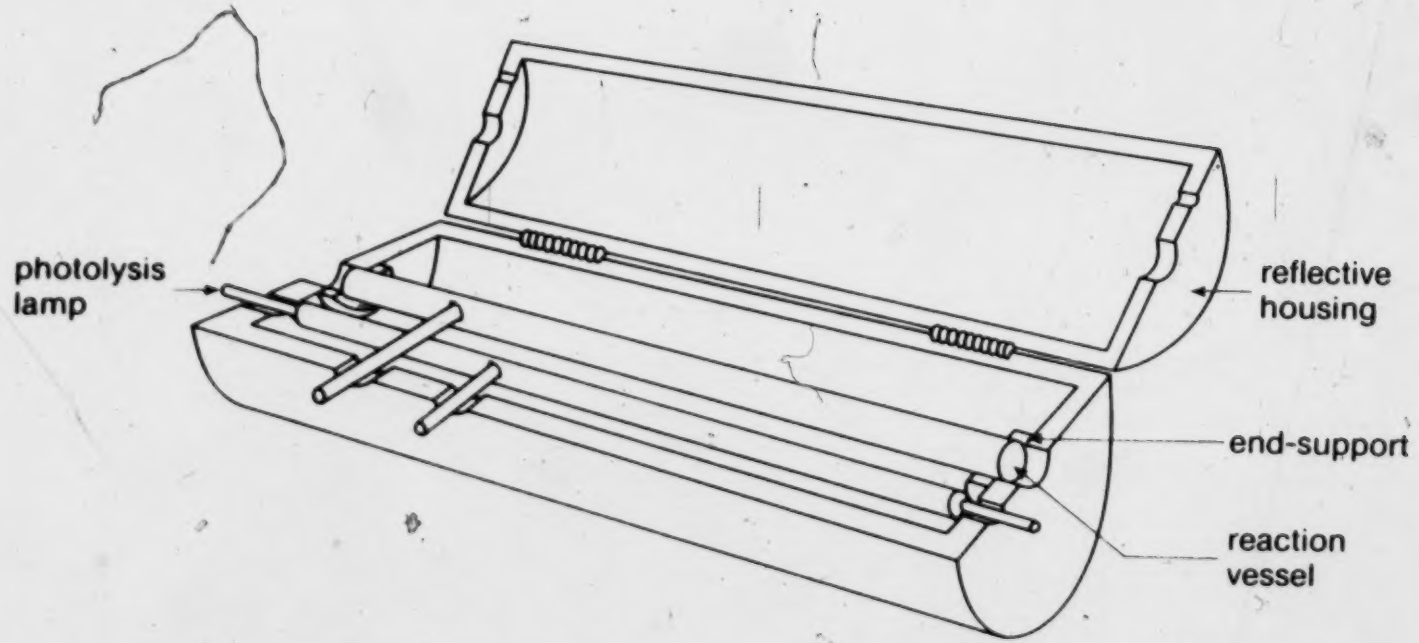

Figure II.3. The Reaction Vessel and the Reflective Housing.

the desired voltage was reached. The repeated discharges helped to condition the new lamp to the high thermal and mechanical shock of discharging at a high voltage.

II.1.2c. The Spectroscopic Lamp.

The spectroscopic lamp (Figure II.4) was also made of Suprasil with a flat Suprasil window at the end facing the reaction vessel. Molybdenum alloy electrodes (Vitreosil Model T/E7/232) were sealed into the sidearms by standard lead seals and were separated by a short capillary tube, 5 cm long and 3 mm in inner diameter, to ensure high current density and intense light output. An aperture close to the lamp window minimized the deposit of silica on the window and an expansion bulb was used to accomodate the shock which accompanied the discharge. The lamp parts were sealed together by Apiezon black wax to facilitate frequent cleaning and the lamp was connected to the lamp vacuum line through a high vacuum stopcock (Pyrex V-4) and a detachable ball joint. The spectroscopic lamp was filled with ~56 Torr xenon to provide a background continuum. The light flash reached its maximum intensity in 5 μs and had a half life of 10 μs. The spectroscopic lamp circuit included an ignitron (Westinghouse Size A, WL7703) and a CSI Energy Capacitor (Model 25 W067 TN, Capacitance 1.0 μF, 20 KV) which, when discharged at 20 KV, provided 200 joules per flash. The spectroscopic lamp was also conditioned by repeated discharges at lower voltages. Fused quartz lenses were used to collimate the light beam from the spectroscopic lamp through the reaction vessel and to focus it at the entrance slit of the spectrograph.

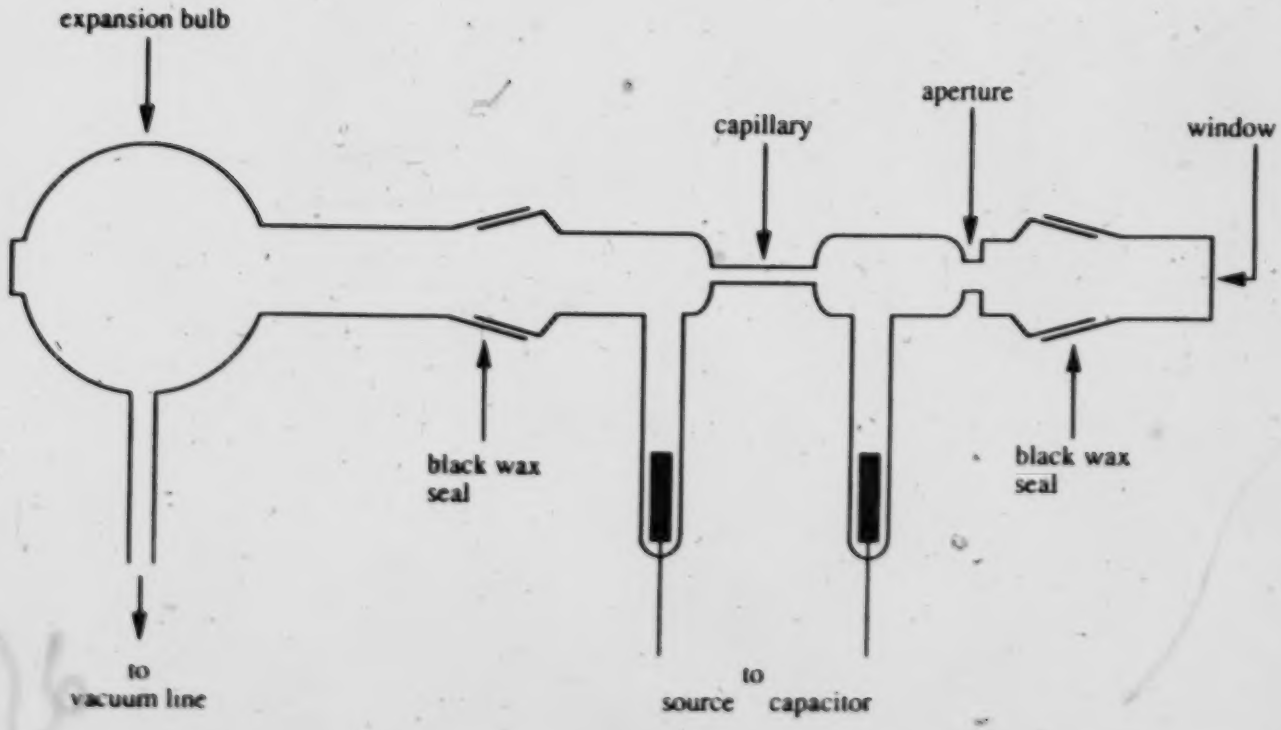

Figure II 4 The Spectroscopic Lamp

II.1.2d. The Spectrograph.

A Hilger-Watts spectrograph (Model E742.1/582) was used, which operates with a Littrow mounting system utilizing a quartz prism as a non-linear dispersion device (Figure II.5) and the resolved spectrum was focused on a light-sensitive photographic material. Kodak spectroscopic plates type 103a-o were used to record the absorption spectra. The absorption lines in the spectrum recorded by the photographic material were traced out as absorption peaks using a microdensitometer.

II.1.3. The Microdensitometer.

The microdensitometer (MK III C, Joyce, Loebl & Co. Ltd., Figure II.6) used in this study operates on the principle of a true double-beam light system in which two beams arise from a single light source and terminate in a single photoelectric receiver, making the instrument almost independent of its own parameters and thus achieving complete reproducibility of recording. The sample beam is scanned across the photographic material and the reference beam passes through an optical density wedge, and the two beams are alternately fed into a photomultiplier detector. Any difference in the intensities of the two beams produces a signal which, after amplification, activates a servo motor to drive the optical density wedge so as to nullify the intensity difference. A pen attached to the optical density wedge traces out the resulting spectrum.

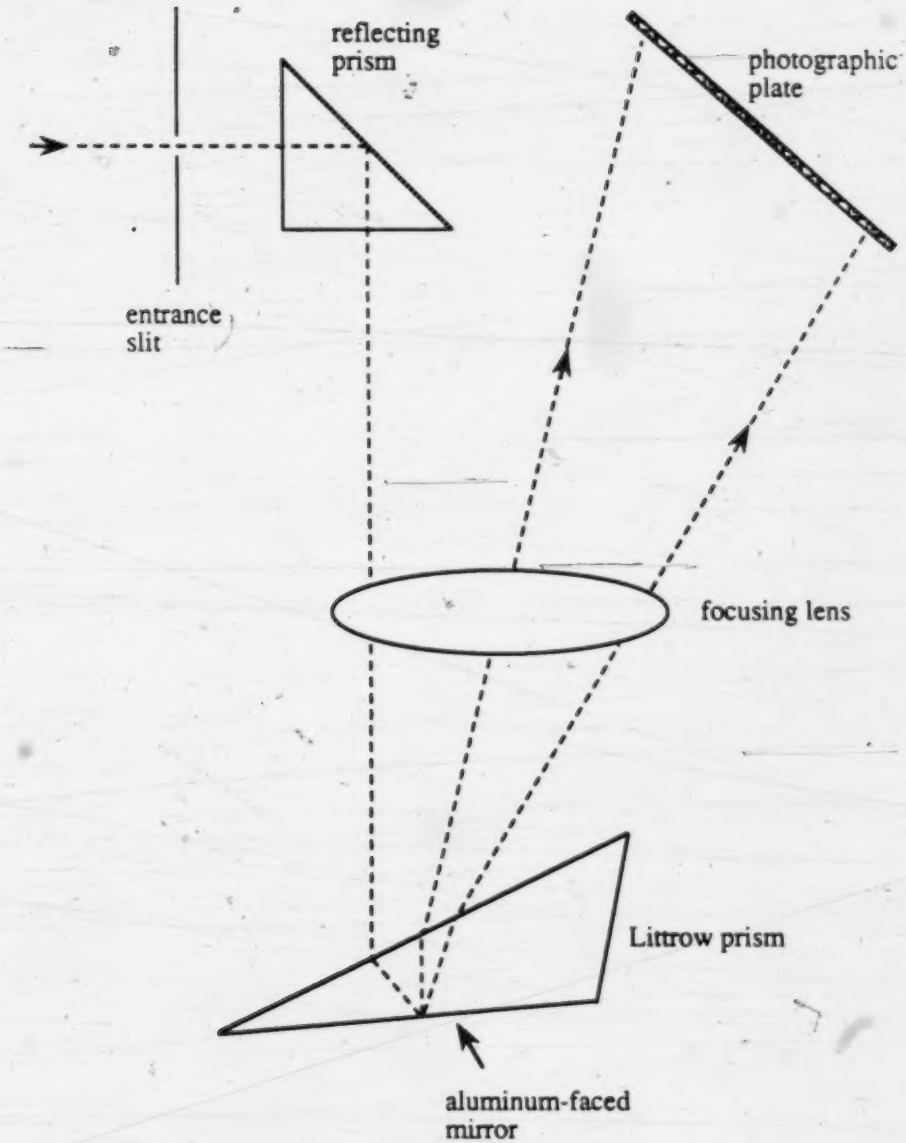

Figure II.5. The Littrow Prism and Mounting.

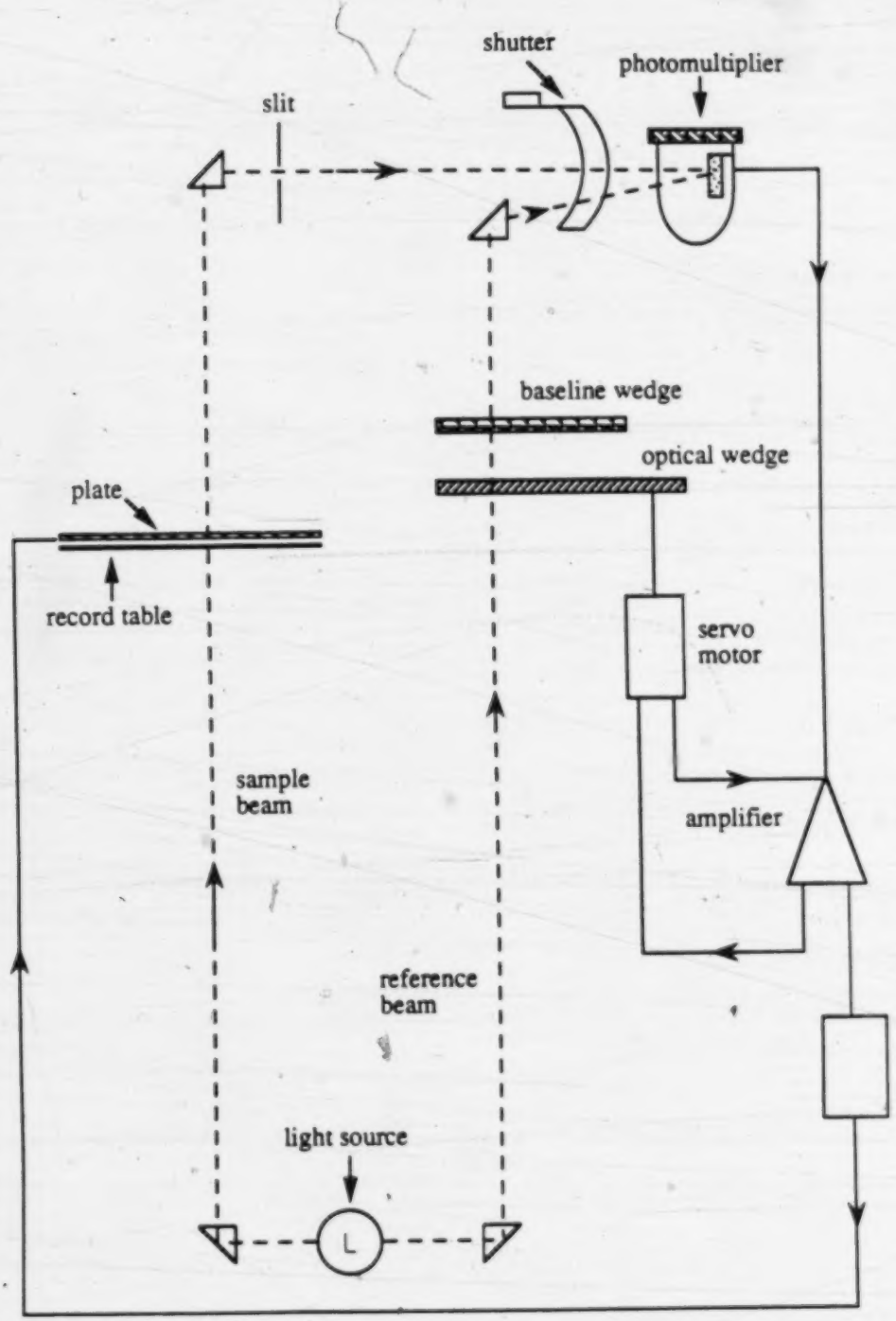

Figure II.6. Schematic Diagram of the Microdensitometer.

II.2. Operational Procedures.

II.2.1. Operation of the Flash Photolysis System.

The circuit diagram is illustrated in Figure II.7. The two lamp capacitors were first charged up to 20 KV voltage. Then a pulse delay generator was activated, which sent out two voltage pulses, one to the photolysis lamp ignition and the other to the spectroscopic lamp ignition. These pulses closed the lamp circuits and caused the capacitors to discharge through the lamps, producing the photolysis and spectroscopic light flashes. The delay between the two pulses could be adjusted from 1 to 9999 microseconds. The light pulses from the two discharges were picked up by a photocell (Sylvania 90 CV), amplified and displayed on an oscilloscope screen (Hitachi Denshi Ltd. LR 54541). The trace was photographed (Hewlett-Packard Oscilloscope Camera Model 197A using Polaroid film type 667) and the separation between the peak of the photolysis flash signal and that of the following spectroscopic flash signal was taken as the time delay. A typical oscilloscope trace is shown in Figure II.8.

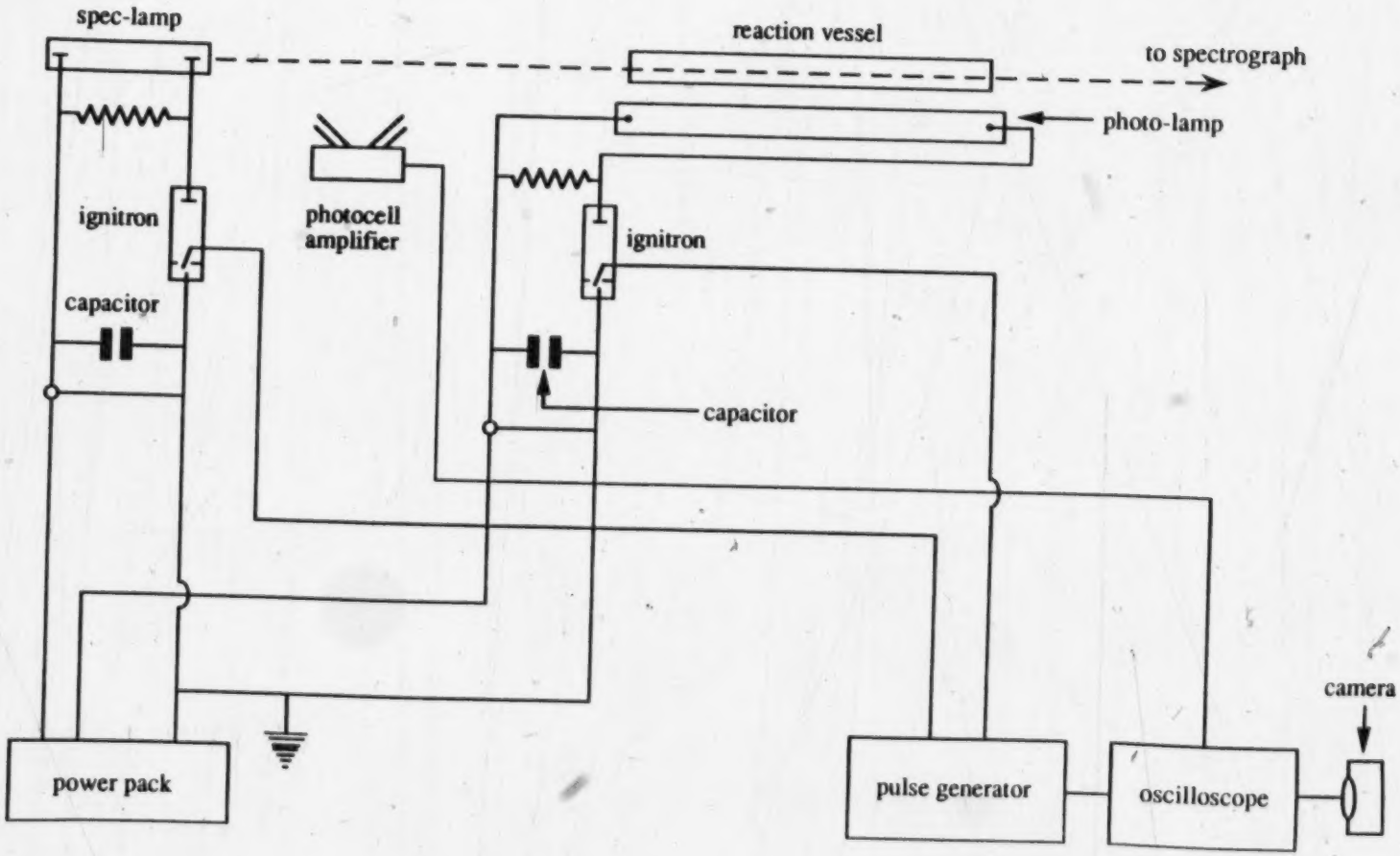

Figure II.7. Circuit Diagram of the Flash Photolysis System.

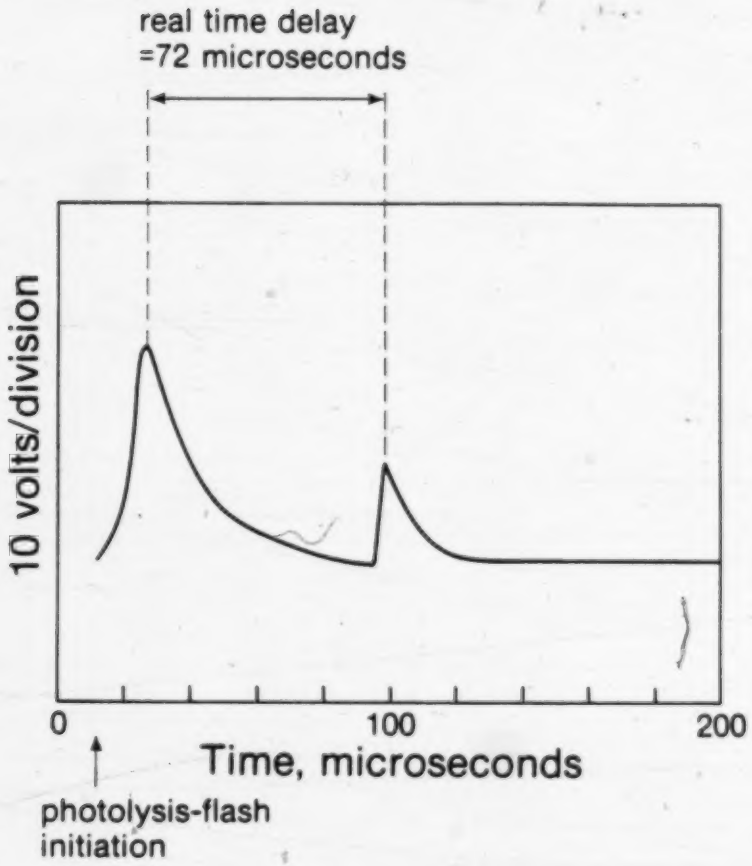

Figure II.8. Oscilloscope Trace.

II.2.2. Preparation of the Gas Mixtures.

For all the reaction systems investigated in this study, two gaseous mixtures were made for every experiment.

(a) the silylene precursor in a large excess of argon (hereon referred to as the blank).

(b) the silylene precursor and various amounts of a reactive substrate in a large excess of argon (hereon referred to as the mixture).

Both the blank and the mixture were made simultaneously. The following procedure was employed for preparing, as examples, a blank (consisting of 1.0 Torr Si_2Cl_6 in a total pressure of 500 Torr argon) and a mixture (consisting of 1.0 Torr Si_2Cl_6 and 0.30 Torr oxygen in a total pressure of 500 Torr argon) in storage bulbs A and B, respectively.

First, 1.0 Torr of purified Si_2Cl_6, from the reagent storage bulb, was introduced into the mixture storage bulbs A and B and the vacuum line. Pressure was monitored by the Baratron pressure meter. This pressure was allowed to stabilize for few minutes and the valve of bulb A was closed. 1.0 Torr Si_2Cl_6 in bulb B and the vacuum line was condensed in a trap, of negligibly small volume, on the vacuum line using liquid nitrogen as coolant. When the reading on the Baratron pressure meter reached 0.00, the valve of the trap was closed. 0.3 Torr of oxygen was then introduced into bulb B and the vacuum line. Si_2Cl_6 was slowly allowed to expand from the trap into bulb B and the vacuum line containing 0.3 Torr oxygen. The pressure was allowed to stabilize for a few minutes (until the Baratron Pressure Meter read 1.30 Torr), the valve connected to bulb B was closed and the vacuum line was evacuated. Then argon was introduced, first into bulb A and then into bulb B, the pressure being monitored by the mercury manometer. To introduce argon into bulbs A and B, argon was expanded in the vacuum

line and after the pressure was well past 2 Torr, the valve of one of the bulbs (A and B) was opened. 500 Torr argon was admitted into the bulb and excess argon was pumped away.

For all the $SiCl_2$ reactions, 1.0 Torr Si_2Cl_6 and differing amounts of a given substrate in a total pressure of 500 Torr argon was used in each experiment. For the $SiBr_2$ reactions, the initial gas mixture composition for each experiment was 5 Torr $SiBr_4$ and differing amounts of a given reactive substrate in a total pressure of 200 Torr argon.

The gas mixtures were stored overnight to achieve homogeneity. For the flash photolysis experiment, a mixture from one of the mixture storage bulbs was expanded into the reaction vessel until a pressure of 100 Torr (40 Torr in the case of $SiBr_2$ reactions) was achieved. After reaction the reaction vessel was evacuated, with pressure being monitored by the Pirani Vacuum Gauge. Each experiment was repeated after proper evacuation.

Due to deposition of solid materials from the photolysis of the mixtures, the reaction vessel had to be cleaned frequently by rinsing with 10% hydrofluoric acid, distilled water and finally with methanol, after which it was evacuated and treated with chlorotrimethylsilane to remove moisture and coat the glass surface with $^{\bullet}Si(CH_3)_3$. The two lamps were also cleaned frequently with 10% hydrofluoric acid to remove deposits of silica and metal from the glass.

II.2.3. Development of Photographic Plates.

The Kodak 103a-o spectroscopic plates were developed in Kodak D–19 developer for 3 min. at 24°C, 4 min. at 20°C or 5 min. at 16°C. They were then rinsed

successively in a stop bath (2–3% acetic acid) for 1 min., in Kodak rapid fixer for 4 min. and running water for 30 min. The photographic plates were then air-dried and placed on the microdensitometer for scanning.

II.3. Materials

Information on materials used in this study is compiled in Table II.1. Generally, the materials were introduced into the vacuum system, degassed several times to remove air contamination, distilled from trap to trap with retention of only the middle fraction and stored in vacuum-tight reagent storage bulbs.

Table II.1. Materials and Purification.

Material	Supplier	Minimum Purity (%)	Purification	
			Distilled @ (°C)	Degassed @ (°C)
Argon (Ar)	Matheson	99.95	Passed over Cu at 350°C and then molecular sieve 5A.	
Carbon monoxide (CO)	Matheson	99.9	Passed through liquid nitrogen trap.	
Chlorotrimethylsilane (Me_3SiCl)	Aldrich Chemicals	98	– 52	– 196
1,3-Butadiene (1,3-C_4H_6)	Matheson	99.87	– 104	– 130
Hexachlorodisilane (Si_2Cl_6)	PCR Chemicals	97	0	– 78
Isobutane (i-C_4H_{10})	Matheson	99.96	– 98	– 196
Nitric oxide (NO)	Matheson	99.0	– 186	– 196
Nitrous oxide (N_2O)	Matheson	99.99	– 130	– 196
Oxygen (O_2)	Matheson	99.98		
Tetrabromosilane ($SiBr_4$)	Alfa Chemicals	95+	0	– 78

Chapter III

RESULTS

The determination of absolute rate constants using the flash photolysis-kinetic absorption spectroscopy technique is based on measurements of the decay profiles of the reactive species in the absence and in the presence of an added substrate. The former is referred to as the background decay and the relationships between the concentrations of the transient species as a function of time and of pressure of the diluent gas must first be established since the observed decay rates in the presence of various amounts of added substrates have to be corrected for this background decay.

III.1. Background Decay of the Dihalosilylene Spectra as a Function of Time.

The $^1B_1 \leftarrow {}^1A_1$ transitions of the UV absorption spectra of $SiCl_2$ and $SiBr_2$ have been employed for the quantitative investigations of their reactions with various substrates.

The first- and second-order expressions for the disappearance of a dihalosilylene, SiX_2, in the absence of any reactive substrate are given by equations III.1 and III.2 respectively

$$-\frac{d[SiX_2]}{dt} = k_1 [SiX_2] \qquad \text{(III.1)}$$

$$-\frac{d[SiX_2]}{dt} = k_2 [SiX_2]^2 \qquad \text{(III.2)}$$

Upon integration these equations yield

$$\ln[SiX_2] = -k_1 t + \text{constant} \qquad \text{(III.3)}$$

$$\frac{1}{[SiX_2]} = k_2 t + \text{constant} \qquad \text{(III.4)}$$

where k_1 is the first-order rate constant and k_2 is the second-order rate constant for the decay of SiX_2 in the absence of any reactive substrate (background decay).

If the decay of SiX_2 in the absence of any reactive substrate follows first-order kinetics then according to equation III.3 the plot of $\ln[SiX_2]$ *vs* time, t, should be linear with a slope of $-k_1$. On the other hand if the decay of SiX_2 is second-order in SiX_2 concentration then the plot of $1/[SiX_2]$ *vs* time, t, should be linear with a slope of k_2 in accordance with equation III.4.

Concentrations of SiX_2 could be monitored using their absorption profiles (*cf.* Appendix A), and thus their reaction kinetics could be investigated.

The absorption spectra of $SiCl_2$ and $SiBr_2$ at different time delays were recorded in order to obtain a time profile of their concentrations, the concentrations being monitored by the peak heights of their absorption spectra. In the case of $SiCl_2$, the peak height of the most intense peak corresponding to the $^1B_1$ (0,8,0) $\leftarrow$ $^1A_1$ (0,0,0) transition at λ = 317.4 nm was measured and for the case of $SiBr_2$, the peak height of its absorption spectrum due to the $\tilde{A}\ ^1B_1 \leftarrow \tilde{X}\ ^1A_1$ transition was measured at λ_{max} = 362 nm. Peak height measurements for $SiCl_2$ and $SiBr_2$ as a function of time are listed in Tables III.1 and III.2 respectively, and the first- and second-order plots are shown in Figures III.1 and III.2 respectively. Both the $SiCl_2$ and $SiBr_2$ absorption spectra were found to decay according to first-order kinetics as shown by the linear relationships between ln(peak height) and time in Figures III.1 and III.2, respectively. The slopes of these first-order decay plots correspond to $-k_1$, *i.e.* the background decay rate constant for the corresponding dihalosilylene.

Table III.1. Peak heights as a function of time for the decay of $SiCl_2$ (Si_2Cl_6 = 0.2 Torr, Ar = 100 Torr).

Time, μs	Peak Height, mm	Ln(peak height)	(1/peak height) x 10^2,mm^{-1}
11	103	4.63	0.97
24	83	4.42	1.20
35	65	4.17	1.54
44	58	4.06	1.72
65	33	3.50	3.03
76	28	3.33	3.57
88	18	2.89	5.56
98	15	2.71	6.67

Table III.2. Peak heights as a function of time for the decay of $SiBr_2$ ($SiBr_4$ = 1.0 Torr, Ar = 40 Torr).

Time, μs	Peak Height, mm	Ln(peak height)	(1/peak height) x 10^2, mm^{-1}
13	58.1	4.06	1.72
21	50.5	3.92	1.98
28	47.4	3.86	2.11
39	40.8	3.71	2.45
47	38.0	3.64	2.63
55	35.8	3.58	2.79
63	28.8	3.36	3.47
71	25.2	3.23	3.96

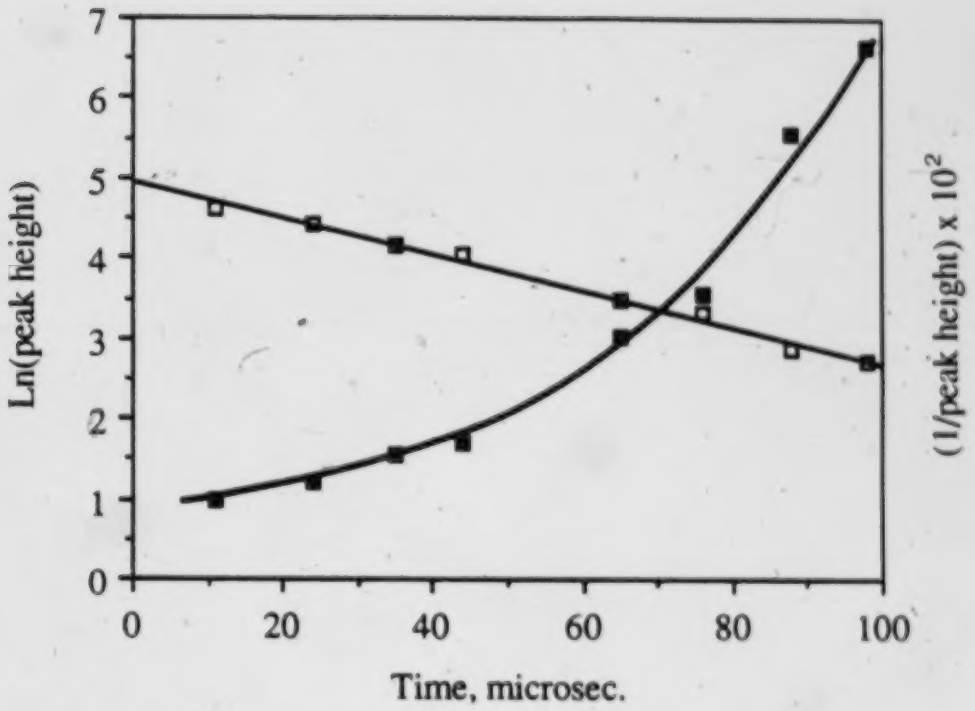

Figure III.1. Background decay curves of [$SiCl_2$]. (□): first-order decay; (■): second-order decay.

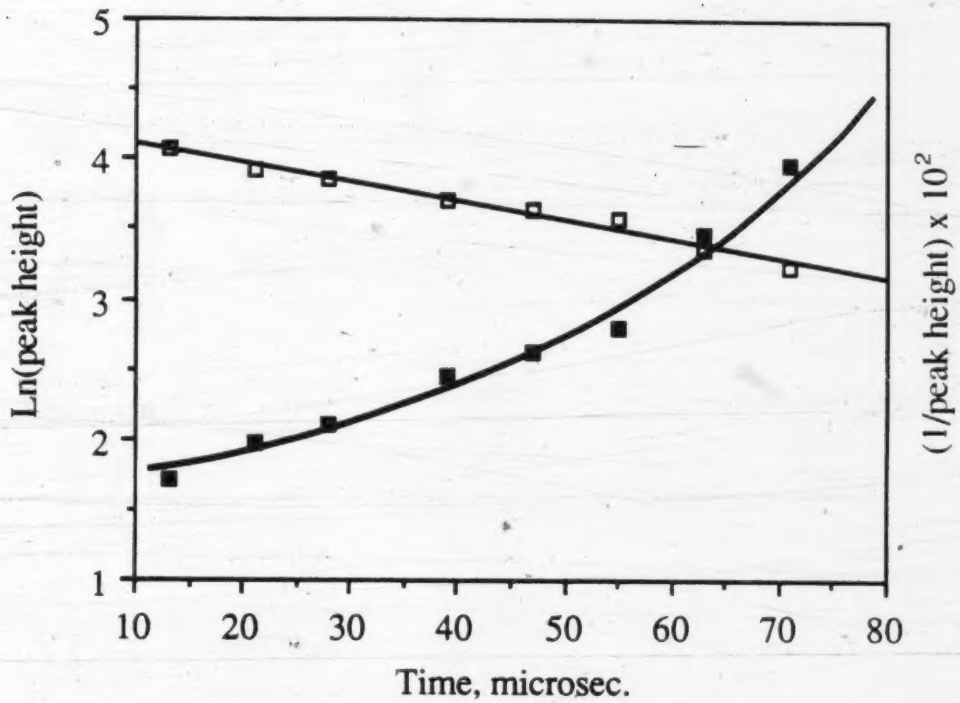

Figure III.2. Background decay curves of [$SiBr_2$]. (□): first-order decay; (■): second-order decay.

In the experiments on the decay of $SiCl_2$, both peak heights and peak areas were used to monitor its concentration and the results are summarized in Table III.3. Since the two procedures gave identical values, within experimental error, for the $SiCl_2$ background decay rate constant and since peak height measurement is less tedious as compared to peak area measurement, peak heights were subsequently used to monitor the dihalosilylene concentrations.

III.2. Background $SiCl_2$ Decay as a Function of Argon Pressure.

Rate constants for the decay of $SiCl_2$ in the presence of varying amounts of argon were measured. Data obtained from such measurements for the decay of $SiCl_2$ in the presence of total pressures of 50, 100 and 150 Torr of argon (at a fixed pressure of Si_2Cl_6 of 0.2 Torr) are given in Table III.4 and the decay plots are shown in Figure III.3. The background decay rate constants obtained from these plots are compiled in Table III.5. As the argon pressure was increased from 50 to 100 Torr, the decay rate increased, but on further increasing the argon pressure to 150 Torr, the decay rate remained almost the same. Therefore, for each reaction of $SiCl_2$ investigated in the present study, 100 Torr argon was used as diluent.

Table III.3. Decay rate constants for $SiCl_2$ as obtained from peak height and peak area measurements.

$[Si_2Cl_6]$, Torr	[Ar], Torr	$k(x10^4)$, s^{-1}	
		Peak Height	Peak Area
0.2	100	1.33	1.34
		1.66	1.65
		1.51	1.52

Table III.4. Decay of $SiCl_2$ in the presence of different amounts of Ar. $[Si_2Cl_6]$ = 0.2 Torr.

[Ar] = 50 Torr		[Ar] = 100 Torr		[Ar] = 150 Torr	
Time, μs	Ln(peak height)	Time, μs	Ln(peak height)	Time, μs	Ln(peak height)
15	4.08	13	4.49	14	4.33
20	4.08	19	4.41	20	4.28
26	4.08	25	4.34	26	4.14
32	4.03	38	4.19	32	3.99
38	3.97	43	4.01	43	3.89
49	3.89	48	3.95	48	3.95
54	3.83	53	3.91	54	3.66

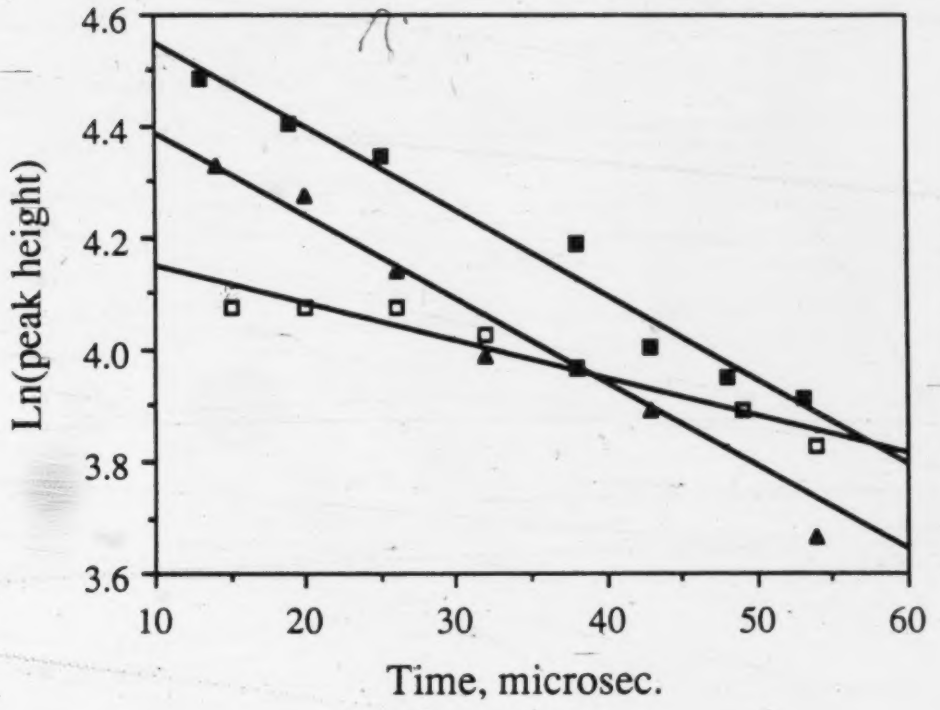

Figure III.3. Dependence of the decay of $SiCl_2$ on argon pressure. (□): 50 Torr; (■): 100 Torr; (▲): 150 Torr. $[Si_2Cl_6]$ = 0.2 Torr.

Table III.5. Dependence of $SiCl_2$ decay rate constants on Ar pressure.

$[Si_2Cl_6]$, Torr	[Ar], Torr	$k(x10^4)$, s^{-1}	Avg. $k(x10^4)$, s^{-1}
0.20	50	0.888	
		0.615	0.72
		0.667	
0.20	100	1.659	
		1.333	1.50
		1.511	
0.20	150	1.489	
		1.361	1.40
		1.344	

III.3. Reactions of Dihalosilylenes.

In the presence of an added reactive substrate, S, the rate of SiX_2 disappearance is given by

$$-\frac{d[SiX_2]}{dt} = k_1[SiX_2] + k[SiX_2][S] \quad \text{(III.5)}$$

$$= k_2[SiX_2] \quad \text{(III.6)}$$

which integrates to

$$\ln[SiX_2] = -k_2t + \text{constant} \quad \text{(III.7)}$$

or

$$\ln(\text{peak height})_{SiX_2} = -k_2t + \text{constant} \quad \text{(III.8)}$$

where

$k_2 = k_1 + k[S]$, the pseudo first-order rate constant for the decay of SiX_2 in the presence of a given amount of substrate, S;

k = second order rate constant for the reaction $SiX_2 + S \rightarrow$ Products;

and $(\text{peak height})_{SiX_2}$ = peak height of the absorption spectrum of the dihalosilylene SiX_2.

A plot of ln(peak height) *vs* time gives the pseudo first-order decay rate constant, k_2, of SiX_2 in the presence of a given substrate concentration.

These pseudo first-order rate constant values, k_2, obtained for the decay of SiX_2 in the presence of different amounts of a given substrate, must then be corrected for the

variable background decay rate constants, k_1, in order to obtain k[S]. These corrected data, when plotted against the substrate concentration, [S], yield the bimolecular rate constant, k, for the reaction

$$SiX_2 + S \xrightarrow{k} \text{Products}$$

The rate constant k thus obtained has units of $(\text{mm Hg})^{-1}\mu s^{-1}$ which can be converted to $M^{-1}s^{-1}$ units by multiplication by the conversion factor 62.36×10^6 T.

All measurements for the gas-phase reactions of SiX_2 with different substrates were conducted at room temperature ($25 \pm 3°C$).

In an attempt to detect any new absorbing species that might have been formed during the flash photolysis of Si_2Cl_6, and of $SiBr_4$ in the presence of different substrates, the spectrum of the photolyzate was scanned in the 200 – 700 nm region during each of the reactions studied. No new species were observed.

III.4. Reactions of $SiCl_2$.

The gas-phase reactions of $SiCl_2$ with O_2, NO, N_2O, CO, 1,3-C_4H_6 and *i*-C_4H_{10} were studied quantitatively. In all these reactions, 0.2 Torr Si_2Cl_6 in 100 Torr argon was used as $SiCl_2$ precursor in each experiment. Because of the complications arising from the solid polysilane buildup on the cell walls, the background decay of $SiCl_2$ was variable and thus had to be measured before and after each series of decay rate measurements in the presence of any of the substrates.

III.4.1. The $SiCl_2 + O_2$ Reaction.

The decay rate of $SiCl_2$ in the presence of O_2 at four different pressures was measured in the delay range 10 to 95 μs. The data obtained from such measurements are listed in Tables III.6 to III.9. The presence of oxygen had an accelerating effect on the decay rate of $SiCl_2$ as shown by ln(peak height) *vs* time plots in Figures III.4 to III.7, each of which is one representative plot for each oxygen pressure used. The variable background decay of $SiCl_2$ as measured in each case is also shown. The pseudo first-order rate constants obtained from the slopes of such plots as in Figures III.4 to III.7, after being corrected for the background decay of $SiCl_2$, by substracting the slope of the decay curve of $SiCl_2$ in the absence of oxygen from the slope of the decay curve of $SiCl_2$ in the presence of oxygen, are listed in Table III.10, and are plotted against oxygen concentration in Figure III.8, which shows a good linear relationship. The straight lines in this, and all the kinetic plots obtained in this work, represent the least mean square fits to the data, and the vertical error bars correspond to one standard deviation.

The gas-phase reaction

$$SiCl_2 + O_2 \rightarrow \text{Products}$$

is first order in both $SiCl_2$ and O_2 concentrations and the bimolecular rate constant as obtained (*cf.* Appendix B) from the slope of the linear plot in Figure III.8 is

$$k(SiCl_2 + O_2) = (3.4 \pm 0.2) \times 10^9\ M^{-1}s^{-1}.$$

Table III.6. Peak heights as a function of time for the reaction of $SiCl_2$ with 0.03 Torr oxygen.

$[O_2]$ = 0.00 Torr		$[O_2]$ = 0.03 Torr	
Time, μs	Ln(peak height)	Time, μs	Ln(peak height)
16	4.64	16	4.25
26	4.45	27	4.01
37	4.30	37	3.80
46	3.97	46	3.62
67	3.74	66	3.04
76	3.42	76	2.73
87	3.44	95	2.46

Table III.7. Peak heights as a function of time for the reaction of $SiCl_2$ with 0.05 Torr oxygen.

$[O_2]$ = 0.00 Torr		$[O_2]$ = 0.05 Torr	
Time, μs	Ln(peak height)	Time, μs	Ln(peak height)
15	5.15	14	4.44
24	5.02	24	4.23
33	4.94	34	3.92
42	4.66	41	3.81
51	4.69	51	3.40
58	4.52	59	3.28
68	4.28	67	3.38
		75	2.91

Table III.8. Peak heights as a function of time for the reaction of $SiCl_2$ with 0.06 Torr oxygen.

$[O_2]$ = 0.00 Torr		$[O_2]$ = 0.06 Torr	
Time, μs	Ln(peak height)	Time, μs	Ln(peak height)
09	4.91	10	4.58
20	4.84	19	4.19
30	4.61	29	4.19
39	4.49	35	4.03
47	4.34	42	3.79
54	4.30	50	3.39
60	4.15		
69	4.11		

Table III.9. Peak heights as a function of time for the reaction of $SiCl_2$ with 0.07 Torr oxygen.

$[O_2]$ = 0.00 Torr		$[O_2]$ = 0.07 Torr	
Time, μs	Ln(peak height)	Time, μs	Ln(peak height)
16	4.11	09	4.14
21	4.06	15	3.85
29	4.03	28	3.56
35	3.99	34	3.56
42	3.78	41	3.22
53	3.74	47	3.18
		53	3.04

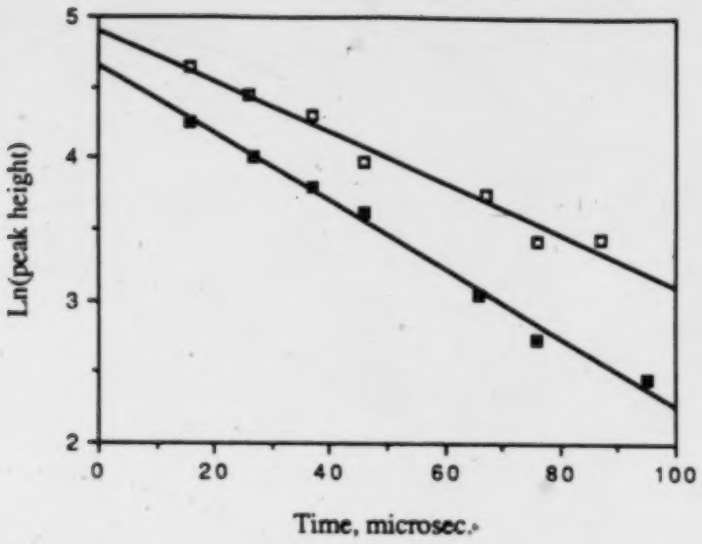

Figure III.4. Decay curves for [$SiCl_2$] in the absence (□) and presence (■) of 0.03 Torr oxygen.

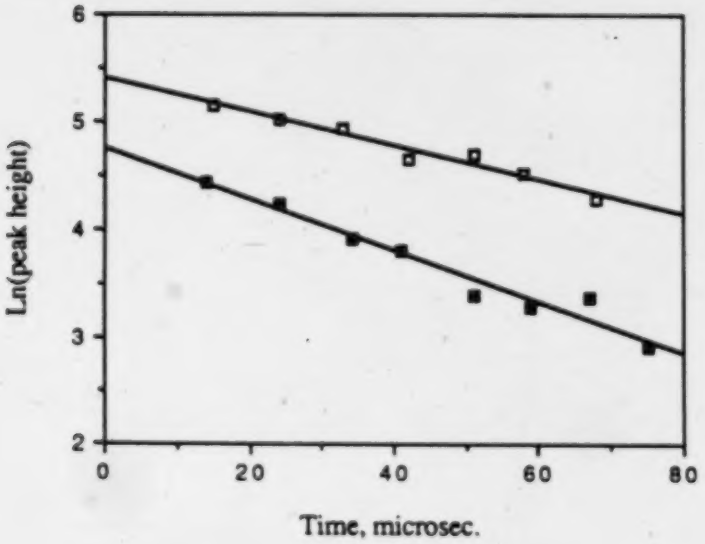

Figure III.5. Decay curves for [$SiCl_2$] in the absence (□) and presence (■) of 0.05 Torr oxygen.

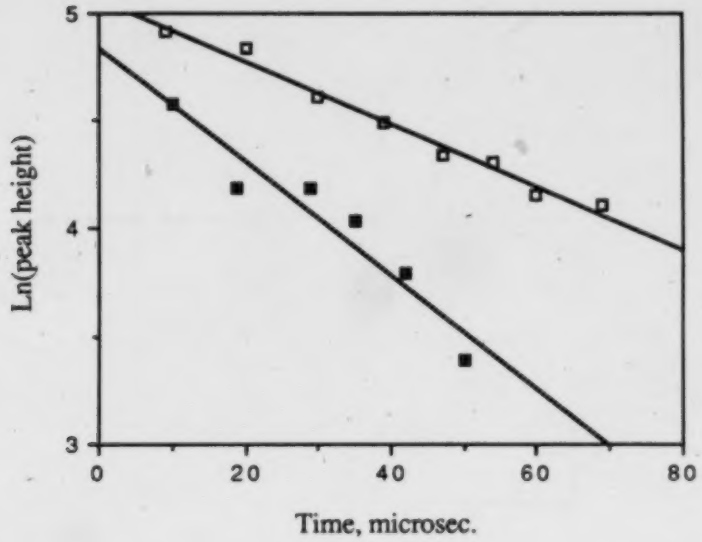

Figure III.6. Decay curves for [$SiCl_2$] in the absence (□) and presence (■) of 0.06 Torr oxygen.

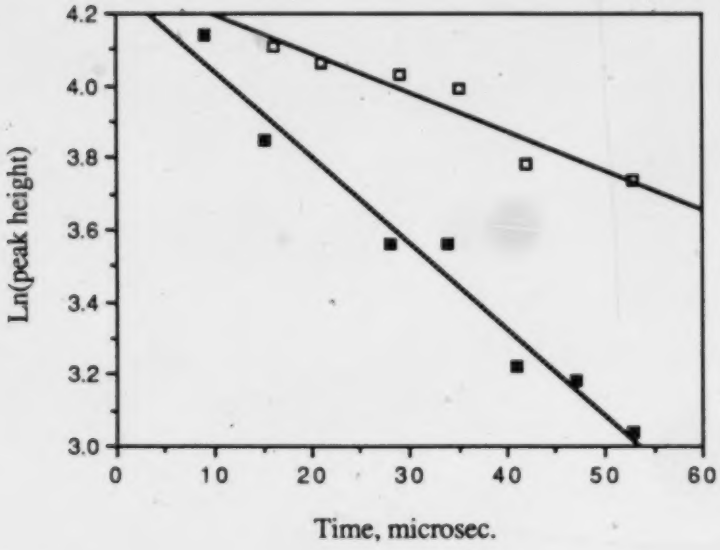

Figure III.7. Decay curves for [$SiCl_2$] in the absence (□) and presence (■) of 0.07 Torr oxygen.

Table III.10. Dependence of the pseudo first-order rate constants of the $SiCl_2 + O_2$ reaction on oxygen concentration.

$[O_2]$, Torr	$k[O_2] \times 10^3$, μs^{-1}	Avg. $k[O_2] \times 10^3$, μs^{-1} *
0.03	5.474	
	5.863	5.67 ± 0.39
0.05	8.122	
	7.062	
	9.086	
	9.171	
	9.348	8.56 ± 1.93
0.06	11.299	
	8.251	
	11.526	
	11.825	
	9.901	10.56 ± 2.97
0.07	12.699	
	15.163	
	13.190	13.68 ± 2.61

* Uncertainities reported in this as well as in Tables III.16, III.22, III.29, III.35, III.42 and III.48 correspond to 95% confidence limit.

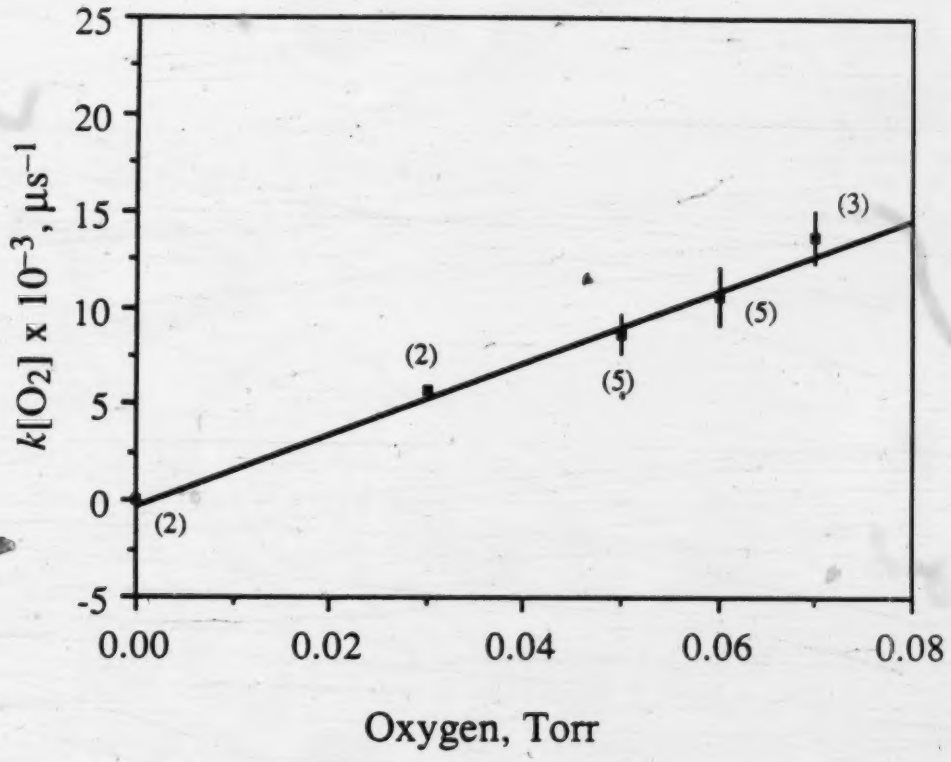

Figure III.8. Dependence of the pseudo first-order rate constants of $SiCl_2 + O_2$ reaction on the oxygen concentration. Numbers in the parentheses are the number of decay plots with 5 to 8 individual measurements.

III.4.2. The $SiCl_2$ + NO Reaction.

The $SiCl_2$ absorption peak height measurements as a function of time at four different nitric oxide pressures, in the 0.024 to 0.09 Torr range, are listed in Tables III.11 to III.15. Typical first-order plots for the decay of $SiCl_2$ in the absence and in the presence of nitric oxide are shown in Figures III.9 to III.13. The slopes of these plots yielded pseudo first-order rate constants for the decay of $SiCl_2$ in the presence of NO and, after being corrected for the background decay of $SiCl_2$, these are listed in Table III.16. The corrected pseudo first-order rate constants have a linear dependence on nitric oxide concentration as shown by the plot in Figure III.14, whose slope resulted (*cf.* Appendix B) in the following value for the bimolecular rate constant corresponding to the gas-phase reaction of $SiCl_2$ with NO:

$$k(SiCl_2 + NO) = (1.6 \pm 0.1) \times 10^9\ M^{-1}s^{-1}.$$

The formation of a volatile product from the photolysis of Si_2Cl_6–NO mixtures was observed upon pumping the photolyzate through a cold trap at –196°C. This product gave a purple ring around the trap mouth at the level of liquid nitrogen coolant. Upon gradual warmup, the purple color changed to orange, then to light yellow with a light blue outer ring, and finally the color completely disappeared. The same product was also formed simply by mixing Si_2Cl_6 with NO, but the color intensity was low.

Table III.11. Peak heights as a function of time for the reaction of $SiCl_2$ with 0.024 Torr nitric oxide.

[NO] = 0.00 Torr		[NO] = 0.024 Torr	
Time, μs	Ln(peak height)	Time, μs	Ln(peak height)
11	4.66	10	4.68
16	4.58	16	4.48
23	4.44	23	4.40
29	4.35	29	4.34
35	4.28	35	4.14
48	4.05	48	3.89
53	3.95		

Table III.12. Peak heights as a function of time for the reaction of $SiCl_2$ with 0.05 Torr nitric oxide.

[NO] = 0.00 Torr		[NO] = 0.05 Torr	
Time, μs	Ln(peak height)	Time, μs	Ln(peak height)
11	4.85	10	4.64
15	4.65	15	4.52
22	4.61	22	4.37
28	4.56	28	4.29
35	4.30	35	3.99
41	4.20	41	4.04
53	4.12	47	3.87

Table III.13. Peak heights as a function of time for the reaction of $SiCl_2$ with 0.066 Torr nitric oxide.

[NO] = 0.00 Torr		[NO] = 0.066 Torr	
Time, μs	Ln(peak height)	Time, μs	Ln(peak height)
09	4.71	09	4.36
15	4.58	15	4.25
22	4.53	22	3.99
28	4.40	28	3.82
35	4.14	35	3.72
41	4.22	41	3.53
47	3.95	47	3.54
54	3.84	54	3.21

Table III.14. Peak heights as a function of time for the reaction of $SiCl_2$ with 0.078 Torr nitric oxide.

[NO] = 0.00 Torr		[NO] = 0.078 Torr	
Time, μs	Ln(peak height)	Time, μs	Ln(peak height)
10	4.69	10	4.56
16	4.62	15	4.22
22	4.53	22	4.15
27	4.46	28	3.99
34	4.33	34	3.86
41	4.05	47	3.53
47	4.05	53	3.35
53	3.89		

Table III.15. Peak heights as a function of time for the reaction of $SiCl_2$ with 0.09 Torr nitric oxide.

[NO] = 0.00 Torr		[NO] = 0.09 Torr	
Time, μs	Ln(peak height)	Time, μs	Ln(peak height)
10	4.28	10	4.02
15	4.15	15	3.66
21	4.07	21	3.61
28	3.83	28	3.37
35	3.75	35	3.11
41	3.80	40	3.10
46	3.49	47	2.78
53	3.33	53	2.59

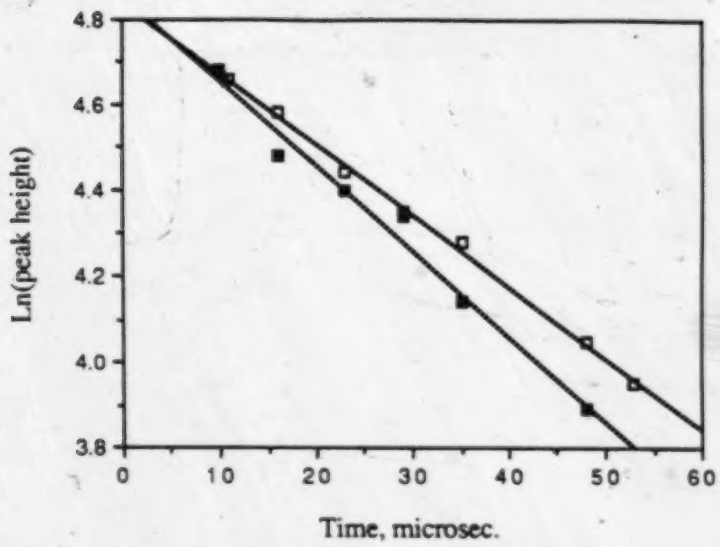

Figure III.9. Decay curves for [$SiCl_2$] in the absence (□) and presence (■) of 0.024 Torr nitric oxide.

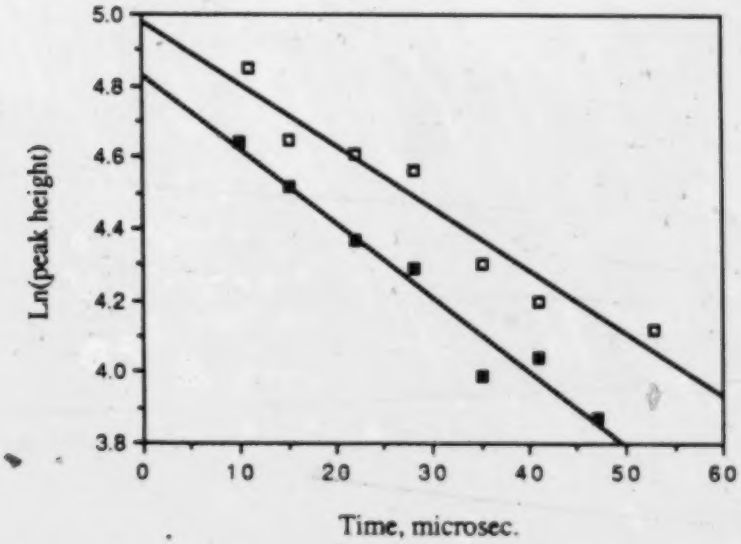

Figure III.10. Decay curves for [$SiCl_2$] in the absence (□) and presence (■) of 0.05 Torr nitric oxide.

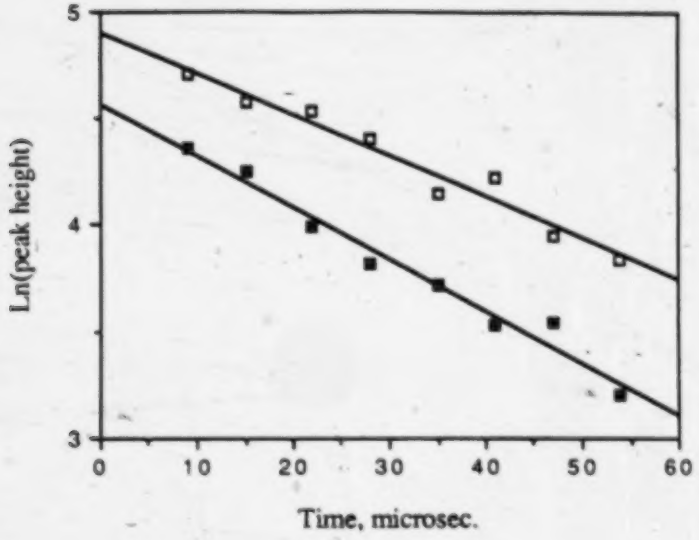

Figure III.11. Decay curves for [$SiCl_2$] in the absence (□) and presence (■) of 0.066 Torr nitric oxide.

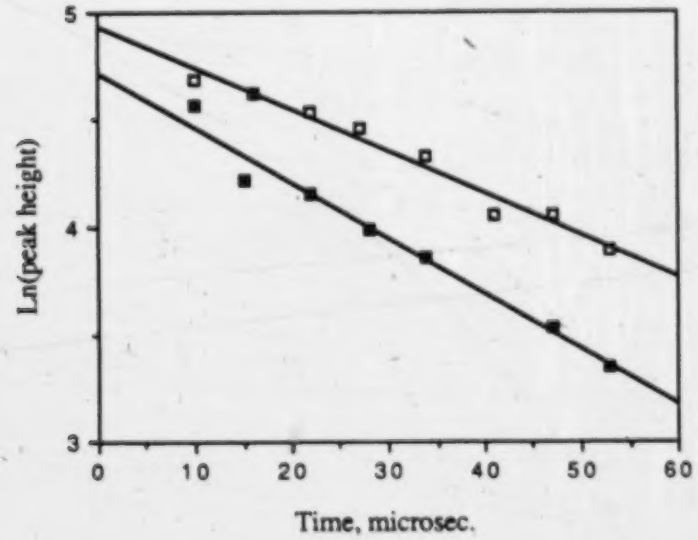

Figure III.12. Decay curves for [$SiCl_2$] in the absence (□) and presence (■) of 0.078 Torr nitric oxide.

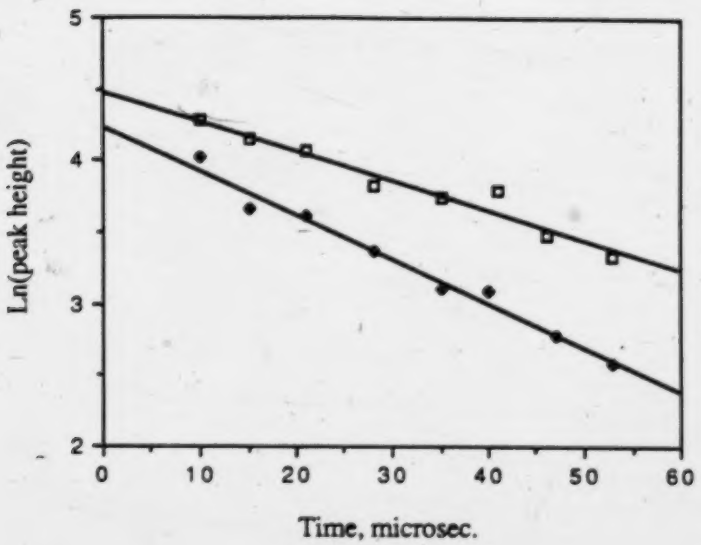

Figure III.13. Decay curves for [$SiCl_2$] in the absence (□) and presence (◆) of 0.09 Torr nitric oxide.

Table III.16. Dependence of the pseudo first-order rate constants of the $SiCl_2$ + NO reaction on nitric oxide concentration.

[NO], Torr	k[NO] x 10^3, μs^{-1}	Avg. k[NO] x 10^3, μs^{-1}
0.024	2.554	2.554
0.050	3.555	
	3.014	
	3.472	3.35 ± 0.62
0.066	4.614	
	5.983	5.30 ± 1.36
0.078	6.012	
	5.957	
	7.266	6.41 ± 1.99
0.090	8.166	
	7.838	
	7.016	7.67 ± 1.18

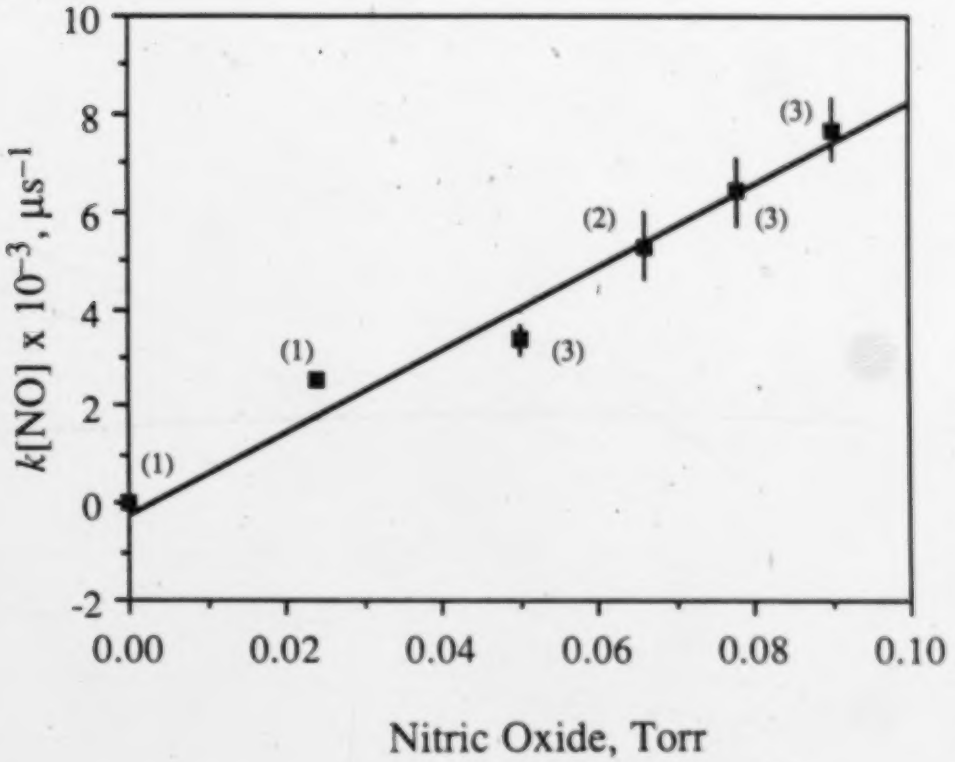

Figure III.14. Dependence of the pseudo first-order rate constants of $SiCl_2$ + NO reaction on the nitric oxide concentration. Numbers in the parentheses are the number of decay plots with 5 to 8 individual measurements.

III.4.3. The $SiCl_2$ + CO Reaction.

Five different pressures of carbon monoxide in the 0.10 to 0.16 Torr range were used to measure the rate constant for the gas-phase reaction between $SiCl_2$ and CO. The data on peak heights as a function of time, for such measurements, are listed in Tables III.17 to III.21. Figures III.15 to III.19 show the first-order decay plots of $SiCl_2$ in the absence and in the presence of CO. The corrected pseudo first-order decay rate constants, obtained from the slopes of such plots as in Figures III.15 to III.19, are compiled in Table III.22, and when plotted against carbon monoxide concentration, Figure III.20, a linear relationship was observed. The slope of the plot in Figure III.20 yielded (*cf.* Appendix B) the following value for the bimolecular rate constant for the $SiCl_2$ + CO reaction:

$$k(SiCl_2 + CO) = (6.3 \pm 0.7) \times 10^8\ M^{-1}s^{-1}.$$

Table III.17. Peak heights as a function of time for the reaction of $SiCl_2$ with 0.10 Torr carbon monoxide.

[CO] = 0.00 Torr		[CO] = 0.10 Torr	
Time, μs	Ln(peak height)	Time, μs	Ln(peak height)
11	4.53	11	4.43
17	4.23	17	4.25
24	4.19	24	4.19
29	4.10	29	4.06
36	4.20	36	3.91
42	3.83	43	3.69
49	3.69	49	3.59
55	3.53	55	3.35

Table III.18. Peak heights as a function of time for the reaction of $SiCl_2$ with 0.12 Torr carbon monoxide.

[CO] = 0.00 Torr		[CO] = 0.12 Torr	
Time, μs	Ln(peak height)	Time, μs	Ln(peak height)
10	4.75	07	4.73
16	4.67	11	4.66
22	4.56	16	4.55
30	4.41	23	4.45
34	4.33	28	4.28
40	4.22	34	4.08
47	4.10	42	3.91
53	4.04	48	3.86
		53	3.68

Table III.19. Peak heights as a function of time for the reaction of $SiCl_2$ with 0.14 Torr carbon monoxide.

[CO] = 0.00 Torr		[CO] = 0.14 Torr	
Time, μs	Ln(peak height)	Time, μs	Ln(peak height)
11	4.60	09	4.95
16	4.42	15	4.76
24	4.26	22	4.64
30	4.17	29	4.43
36	3.97	36	4.26
42	3.83	42	4.27
55	3.78	47	3.93

Table III.20. Peak heights as a function of time for the reaction of $SiCl_2$ with 0.15 Torr carbon monoxide.

[CO] = 0.00 Torr		[CO] = 0.15 Torr	
Time, μs	Ln(peak height)	Time, μs	Ln(peak height)
15	4.95	15	4.81
21	4.80	19	4.75
27	4.69	23	4.64
35	4.51	29	4.54
47	4.31	32	4.38
53	4.13	37	4.24
59	4.23	41	4.19
		45	4.14
		54	3.92

Table III.21. Peak heights as a function of time for the reaction of $SiCl_2$ with 0.16 Torr carbon monoxide.

[CO] = 0.00 Torr		[CO] = 0.16 Torr	
Time, μs	Ln(peak height)	Time, μs	Ln(peak height)
09	4.95	10	4.81
15	4.70	16	4.60
21	4.68	23	4.48
27	4.62	27	4.35
40	4.35	35	4.09
46	4.26	41	4.04
54	4.15	47	3.90
		53	3.78

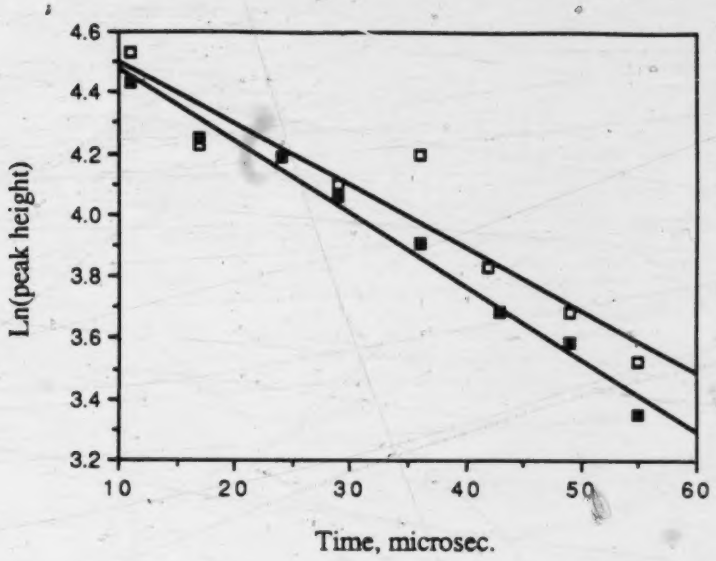

Figure III.15. Decay curves for [$SiCl_2$] in the absence (□) and presence (■) of 0.10 Torr carbon monoxide.

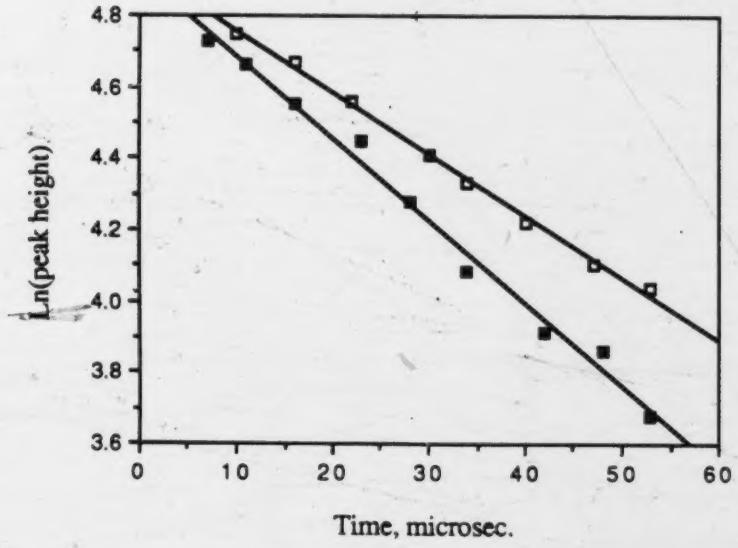

Figure III.16. Decay curves for [$SiCl_2$] in the absence (□) and presence (■) of 0.12 Torr carbon monoxide.

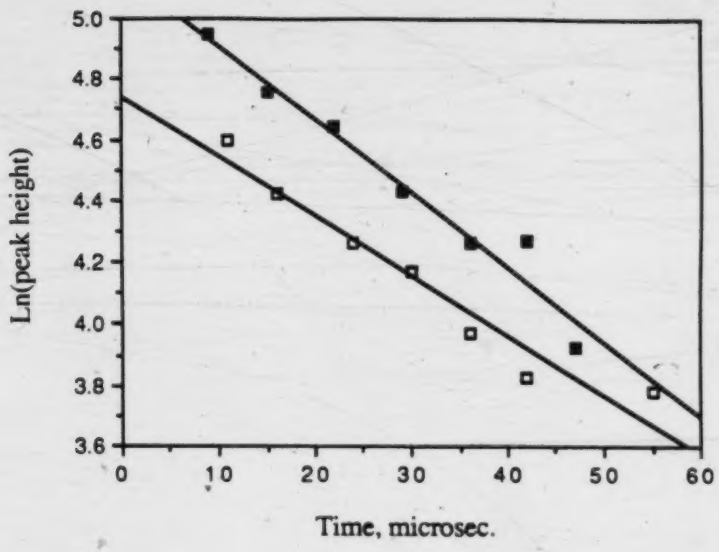

Figure III.17. Decay curves for [$SiCl_2$] in the absence (□) and presence (■) of 0.14 Torr carbon monoxide.

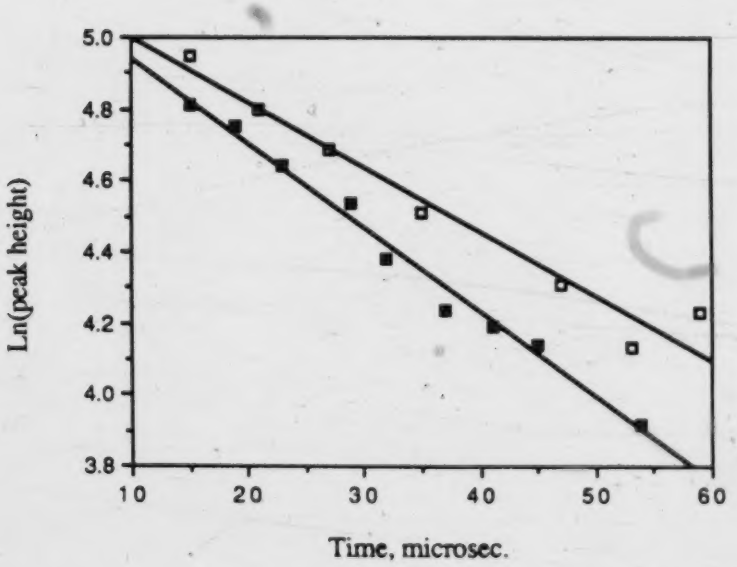

Figure III.18. Decay curves for [$SiCl_2$] in the absence (□) and presence (■) of 0.15 Torr carbon monoxide.

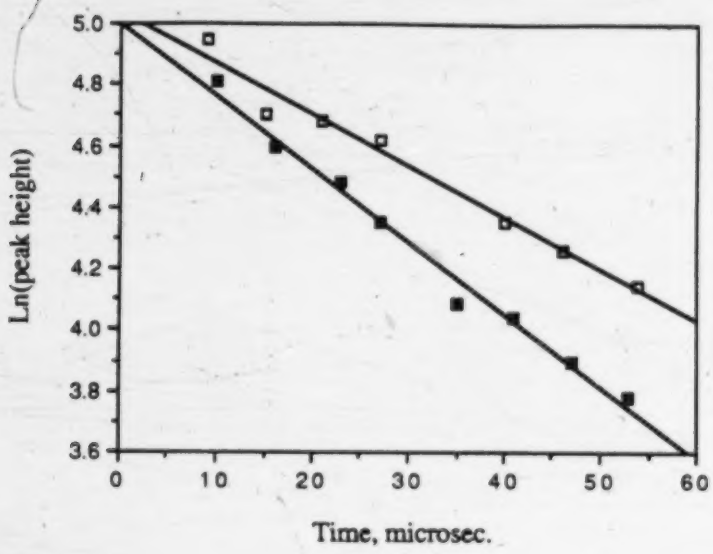

Figure III.19. Decay curves for [$SiCl_2$] in the absence (□) and presence (■) of 0.16 Torr carbon monoxide.

Table III.22. Dependence of the pseudo first-order rate constants of the $SiCl_2$ + CO reaction on carbon monoxide concentration.

[CO], Torr	k[CO] x 10^3, μs^{-1}	Avg. k[CO] x 10^3, μs^{-1}
0.10	2.885	
	2.928	
	1.832	
	3.880	
	3.236	
	2.938	2.95 ± 1.33
0.12	3.579	
	4.028	
	2.697	3.43 ± 1.34
0.14	3.514	
	2.448	
	6.005	
	3.410	
	4.716	4.02 ± 2.74
0.15	6.232	
	4.174	
	4.699	
	3.875	4.74 ± 2.10
0.16	6.963	
	5.327	
	5.725	
	5.684	5.92 ± 1.42

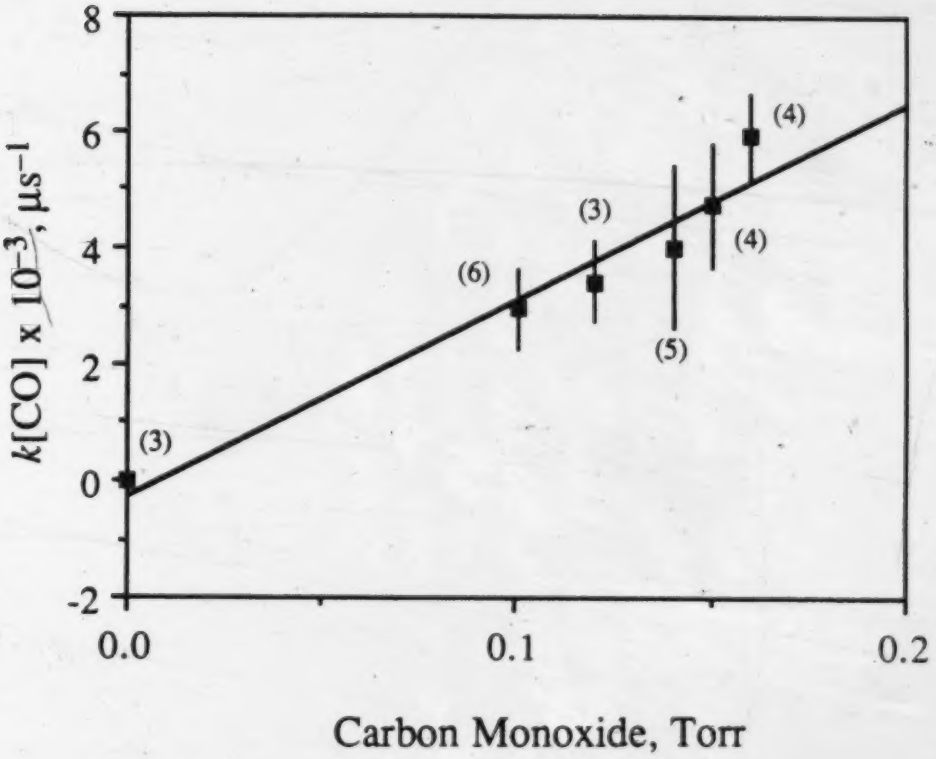

Figure III.20. Dependence of the pseudo first-order rate constants of $SiCl_2$ + CO reaction on the carbon monoxide concentration. Numbers in the parentheses are the number of decay plots with 5 to 8 individual measurements.

III.4.4. The $SiCl_2 + N_2O$ Reaction.

Peak heights of $SiCl_2$ measured as a function of time, in the absence and in the presence of 0.06 to 0.25 Torr of nitrous oxide, are listed in Tables III.23 to III.28 and the corresponding first-order decay plots are shown in Figures III.21 to III.26. The corrected pseudo first-order rate constants of $SiCl_2$ decay in the presence of N_2O, as obtained from these plots, are listed in Table III.29. The linear relationship of the corrected pseudo first-order rate constants with N_2O concentration is shown by the plot in Figure III.27. The slope of this plot resulted (*cf.* Appendix B) in the following value of the bimolecular rate constant for the gas-phase reaction of $SiCl_2$ with N_2O:

$$k(SiCl_2 + N_2O) = (5.7 \pm 0.3) \times 10^8\ M^{-1}s^{-1}.$$

Table III.23. Peak heights as a function of time for the reaction of $SiCl_2$ with 0.06 Torr nitrous oxide.

$[N_2O]$ = 0.00 Torr		$[N_2O]$ = 0.06 Torr	
Time, μs	Ln(peak height)	Time, μs	Ln(peak height)
13	5.14	13	4.92
21	5.02	17	4.78
21	4.99	26	4.69
31	4.70	31	4.54
39	4.59	34	4.37
49	4.37	44	4.30
55	4.36	49	4.08

Table III.24. Peak heights as a function of time for the reaction of $SiCl_2$ with 0.10 Torr nitrous oxide.

$[N_2O]$ = 0.00 Torr		$[N_2O]$ = 0.10 Torr	
Time, μs	Ln(peak height)	Time, μs	Ln(peak height)
19	4.68	15	4.61
25	4.62	20	4.50
30	4.44	27	4.39
39	4.27	33	4.19
43	4.14	38	4.02
49	4.05	45	3.92
57	4.00	49	3.87
		59	3.59

Table III.25. Peak heights as a function of time for the reaction of $SiCl_2$ with 0.12 Torr nitrous oxide.

$[N_2O]$ = 0.00 Torr		$[N_2O]$ = 0.12 Torr	
Time, μs	Ln(peak height)	Time, μs	Ln(peak height)
19	4.11	20	4.26
25	4.04	26	4.10
31	3.89	31	4.04
38	3.81	39	3.84
44	3.63	44	3.75
51	3.50	50	3.58
56	3.48	58	3.40

Table III.26. Peak heights as a function of time for the reaction of $SiCl_2$ with 0.16 Torr nitrous oxide.

$[N_2O]$ = 0.00 Torr		$[N_2O]$ = 0.16 Torr	
Time, μs	Ln(peak height)	Time, μs	Ln(peak height)
14	4.63	13	4.50
20	4.45	19	4.28
26	4.30	25	4.20
32	4.20	31	3.93
44	3.85	38	3.78
52	3.69	44	3.65
58	3.65	50	3.47

Table III.27. Peak heights as a function of time for the reaction of $SiCl_2$ with 0.20 Torr nitrous oxide.

$[N_2O]$ = 0.00 Torr		$[N_2O]$ = 0.20 Torr	
Time, μs	Ln(peak height)	Time, μs	Ln(peak height)
18	4.40	11	4.22
23	4.33	17	4.07
31	4.15	24	3.82
43	3.95	30	3.75
49	3.62	31	3.67
55	3.51	49	3.02

Table III.28. Peak heights as a function of time for the reaction of $SiCl_2$ with 0.25 Torr nitrous oxide.

$[N_2O]$ = 0.00 Torr		$[N_2O]$ = 0.25 Torr	
Time, μs	Ln(peak height)	Time, μs	Ln(peak height)
13	4.45	12	4.37
19	4.43	20	4.20
27	4.23	25	4.13
32	4.15	33	3.69
39	4.03	37	3.70
51	3.81	43	3.59
57	3.68	51	3.32
		58	3.24

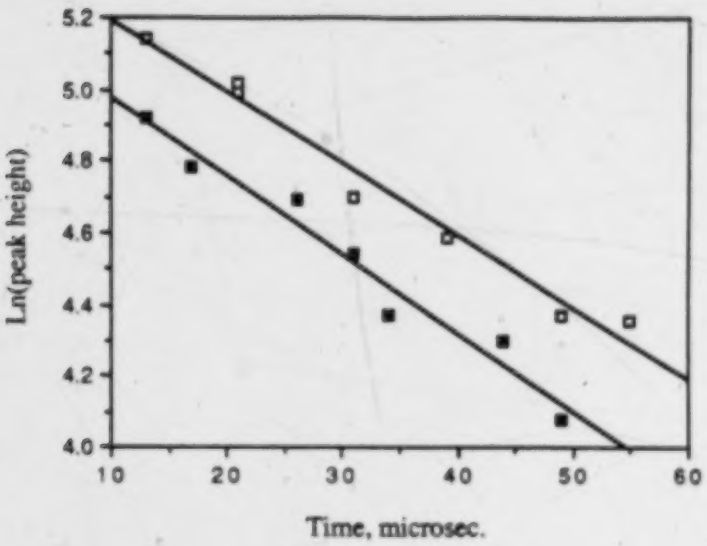

Figure III.21. Decay curves for [$SiCl_2$] in the absence (□) and presence (■) of 0.06 Torr nitrous oxide.

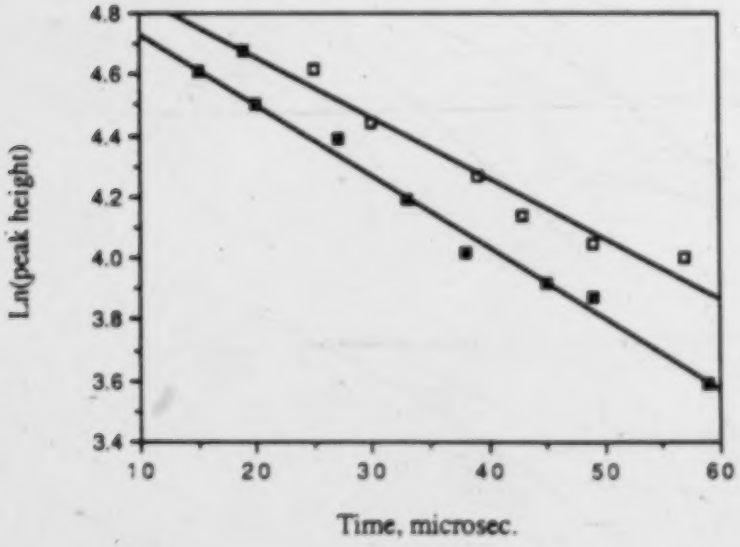

Figure III.22. Decay curves for [$SiCl_2$] in the absence (□) and presence (■) of 0.10 Torr nitrous oxide.

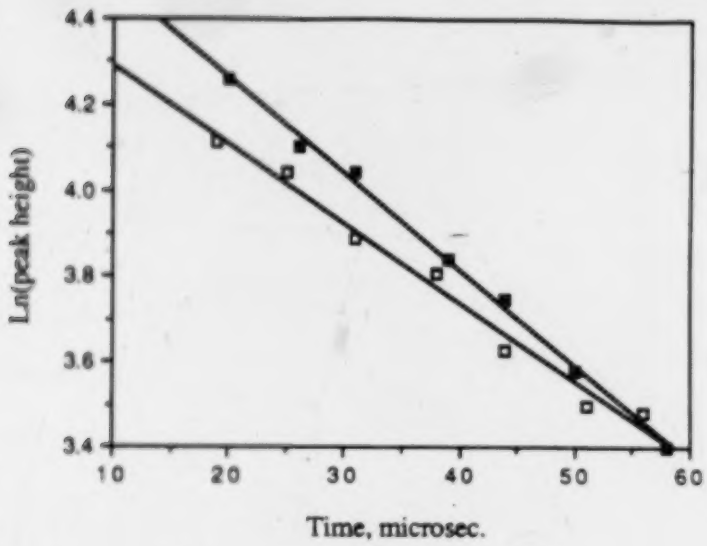

Figure III.23. Decay curves for [$SiCl_2$] in the absence (□) and presence (■) of 0.12 Torr nitrous oxide.

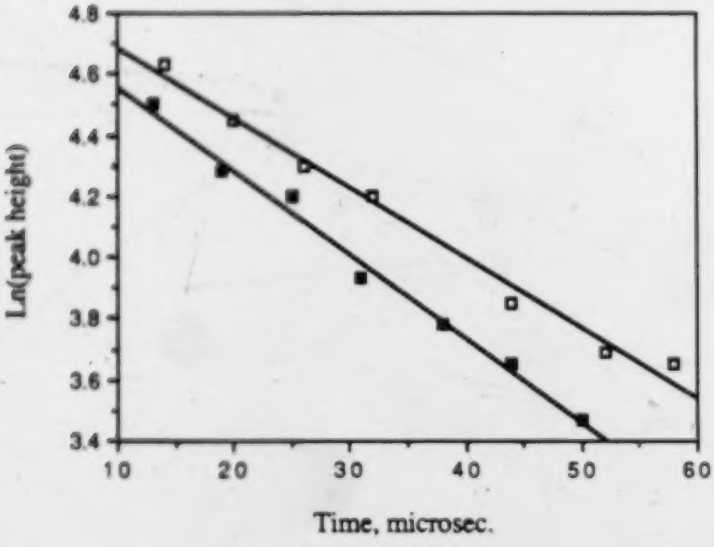

Figure III.24. Decay curves for [$SiCl_2$] in the absence (□) and presence (■) of 0.16 Torr nitrous oxide.

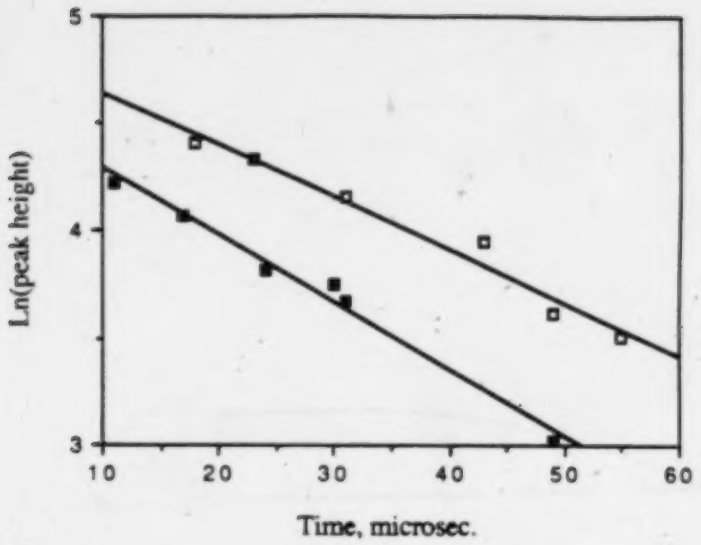

Figure III.25. Decay curves for [$SiCl_2$] in the absence (□) and presence (■) of 0.20 Torr nitrous oxide.

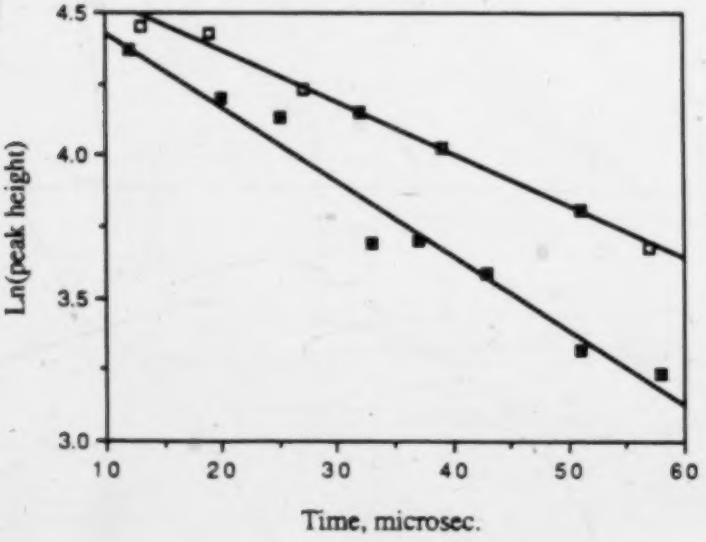

Figure III.26. Decay curves for [$SiCl_2$] in the absence (□) and presence (■) of 0.25 Torr nitrous oxide.

Table III.29: Dependence of the pseudo first-order rate constants of the $SiCl_2 + N_2O$ reaction on nitrous oxide concentration.

$[N_2O]$, Torr	$k[N_2O] \times 10^3$, μs^{-1}	Avg. $k[N_2O] \times 10^3$, μs^{-1}
0.06	2.886	
	1.586	
	2.016	
	1.118	
	2.541	
	2.163	2.05 ± 1.28
0.10	2.971	
	3.077	
	3.592	
	3.405	
	3.885	
	3.939	3.47 ± 0.80
0.12	3.104	
	4.936	
	3.276	
	4.286	
	3.556	3.83 ± 1.53
0.16	5.662	
	5.908	
	5.333	
	4.714	5.40 ± 1.03

Continues on the next page.....

Table III.29.(contd.)

$[N_2O]$, Torr	$k[N_2O] \times 10^3$, μs^{-1}	Avg. $k[N_2O] \times 10^3$, μs^{-1}
0.20	5.242	
	6.850	
	7.388	
	6.288	
	6.082	6.37 ± 1.62
0.25	7.758	
	7.987	
	6.934	7.56 ± 1.11

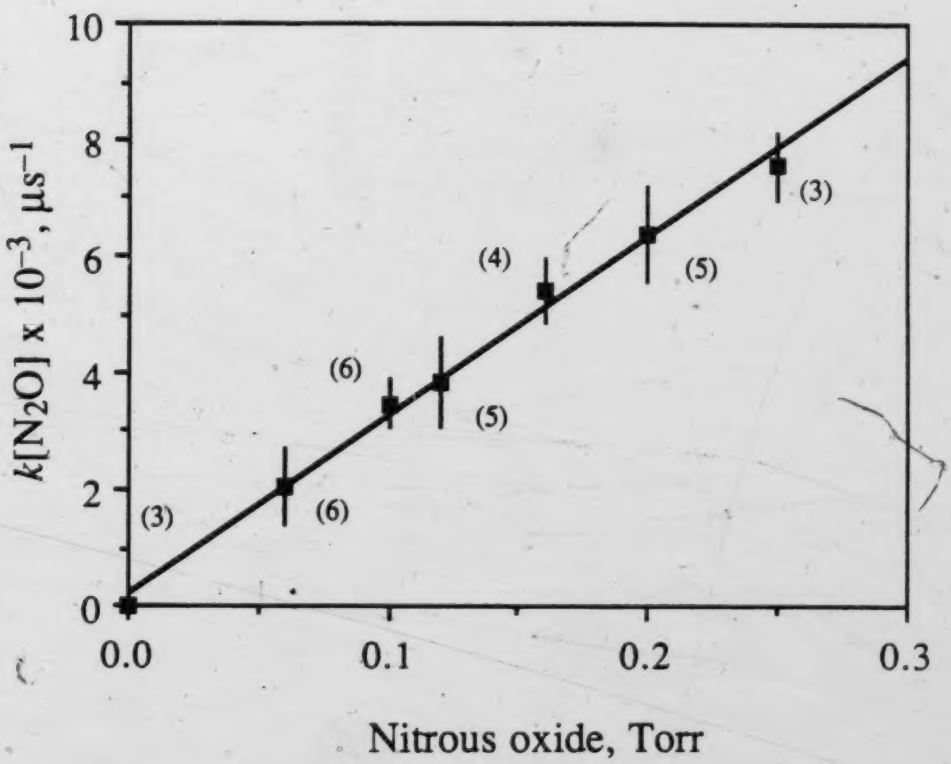

Figure III.27. Dependence of the pseudo first-order rate constants of $SiCl_2 + N_2O$ reaction on the nitrous oxide concentration. Numbers in the parentheses are the number of decay plots with 5 to 8 individual measurements.

III.4.5. The $SiCl_2$ + 1,3-Butadiene Reaction.

The gas-phase reaction of $SiCl_2$ with 1,3-butadiene was studied at five different concentrations of 1,3-butadiene in the 0.04 to 0.20 Torr range. Peak height measurements as a function of time for the decay of $SiCl_2$ in the absence and in the presence of 1,3-butadiene are presented in Tables III.30 to III.34 and the corresponding first-order decay plots are shown in Figures III.28 to III.32. The corrected pseudo first-order rate constants, as obtained from such decay plots as in Figures III.28 to III.32, are listed in Table III.35 and the dependence of these on 1,3-butadiene concentration is shown by the linear plot in Figure III.33. From the slope of this linear plot, the following value for the bimolecular rate constant of the gas-phase reaction between $SiCl_2$ and 1,3-butadiene was obtained (*cf.* Appendix B):

$$k(SiCl_2 + 1,3\text{-}C_4H_6) = (5.4 \pm 0.3) \times 10^8\ M^{-1}s^{-1}.$$

Table III.30. Peak heights as a function of time for the reaction of $SiCl_2$ with 0.04 Torr butadiene.

$[C_4H_6]$ = 0.00 Torr		$[C_4H_6]$ = 0.04 Torr	
Time, μs	Ln(peak height)	Time, μs	Ln(peak height)
09	4.76	12	4.44
15	4.70	21	4.32
21	4.62	26	4.25
25	4.56	33	4.11
35	4.33	38	4.06
40	4.30	42	3.91
44	4.17	47	3.79
49	4.10	53	3.68

Table III.31. Peak heights as a function of time for the reaction of $SiCl_2$ with 0.08 Torr butadiene.

$[C_4H_6]$ = 0.00 Torr		$[C_4H_6]$ = 0.08 Torr	
Time, μs	Ln(peak height)	Time, μs	Ln(peak height)
10	4.71	11	4.28
14	4.67	15	4.14
21	4.59	30	3.90
24	4.50	35	3.82
32	4.47	41	3.76
37	4.19	48	3.49
45	4.02	54	3.28
54	3.99		

Table III.32. Peak heights as a function of time for the reaction of $SiCl_2$ with 0.12 Torr butadiene.

$[C_4H_6]$ = 0.00 Torr		$[C_4H_6]$ = 0.12 Torr	
Time, μs	Ln(peak height)	Time, μs	Ln(peak height)
16	4.26	07	4.32
21	4.22	13	4.08
27	4.03	17	3.97
41	3.74	39	3.53
51	3.58	42	3.47
		46	3.30

Table III.33. Peak heights as a function of time for the reaction of $SiCl_2$ with 0.16 Torr butadiene.

$[C_4H_6]$ = 0.00 Torr		$[C_4H_6]$ = 0.16 Torr	
Time, μs	Ln(peak height)	Time, μs	Ln(peak height)
17	4.53	13	3.99
21	4.49	22	3.64
31	4.32	27	3.58
33	4.26	33	3.33
39	4.08	35	3.40
51	3.85	53	2.77
58	3.58	61	2.64

Table III.34. Peak heights as a function of time for the reaction of $SiCl_2$ with 0.20 Torr butadiene.

$[C_4H_6]$ = 0.00 Torr		$[C_4H_6]$ = 0.20 Torr	
Time, μs	Ln(peak height)	Time, μs	Ln(peak height)
11	4.95	11	3.93
17	4.74	16	3.74
21	4.69	22	3.71
30	4.50	29	3.47
35	4.30	34	3.37
41	4.25	41	3.04
54	4.09	47	2.89
		55	2.77

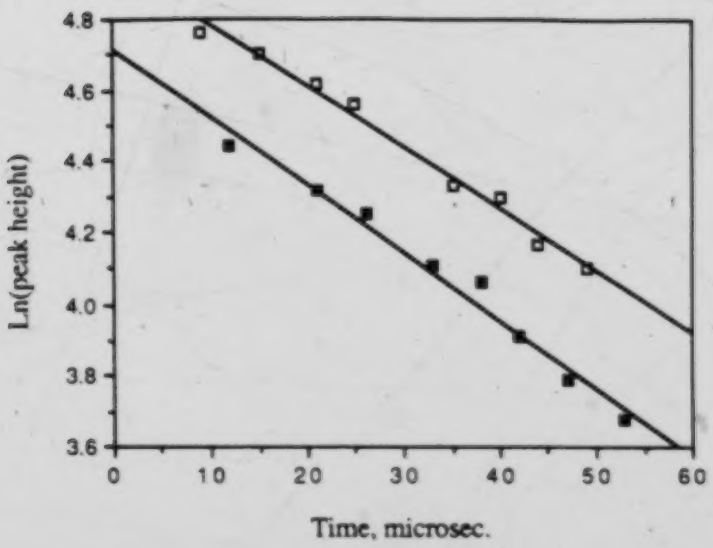

Figure III.28. Decay curves for [$SiCl_2$] in the absence (□) and presence (■) of 0.04 Torr butadiene.

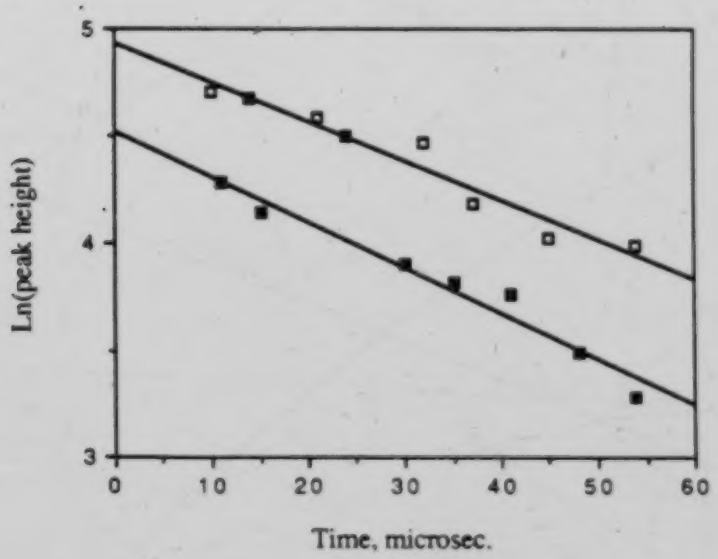

Figure III.29. Decay curves for [$SiCl_2$] in the absence (□) and presence (■) of 0.08 Torr butadiene.

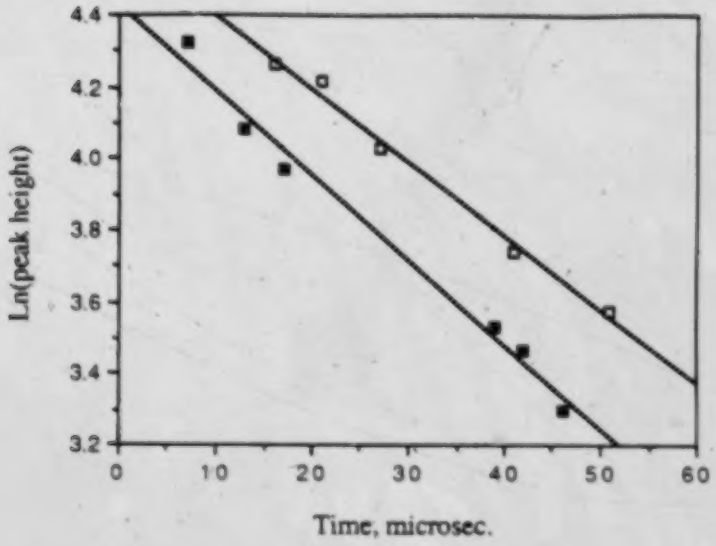

Figure III.30. Decay curves for [$SiCl_2$] in the absence (□) and presence (■) of 0.12 Torr butadiene.

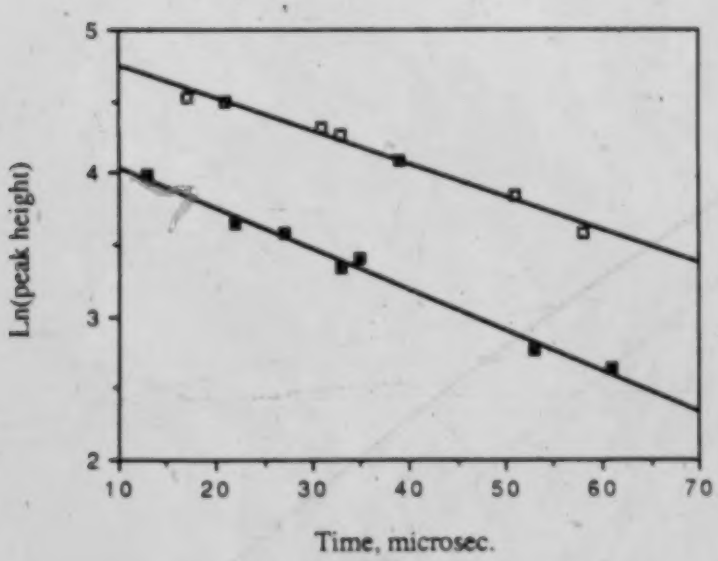

Figure III.31. Decay curves for [$SiCl_2$] in the absence (□) and presence (■) of 0.16 Torr butadiene.

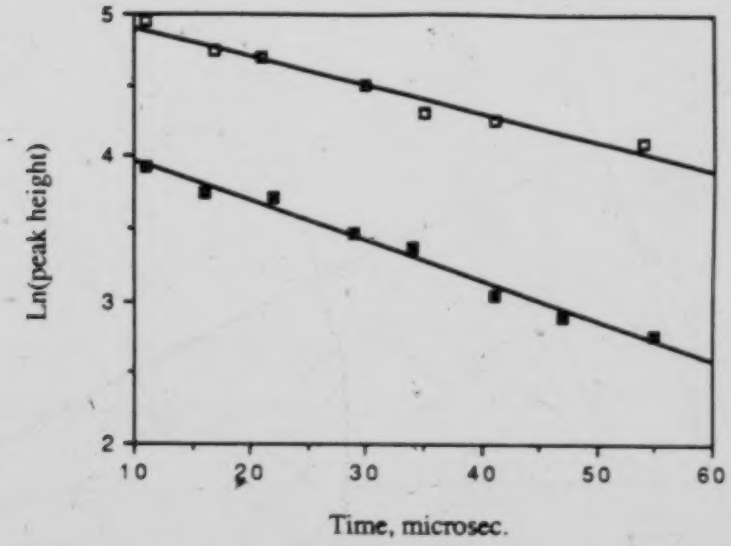

Figure III.32. Decay curves for [$SiCl_2$] in the absence (□) and presence (■) of 0.20 Torr butadiene.

Table III.35: Dependence of the pseudo first-order rate constants of the $SiCl_2 + C_4H_6$ reaction on butadiene concentration.

$[C_4H_6]$, Torr	$k[C_4H_6] \times 10^3$, μs^{-1}	Avg. $k[C_4H_6] \times 10^3$, μs^{-1}
0.04	1.624	
	1.406	
	1.199	
	1.894	1.53 ± 0.60
0.08	2.805	
	2.263	
	1.733	2.27 ± 1.07
0.12	2.836	
	2.474	
	3.329	
	3.639	3.07 ± 1.03
0.16	4.874	
	3.719	
	5.252	
	4.761	4.65 ± 1.31
0.20	5.187	
	5.721	
	6.356	
	7.421	6.17 ± 1.92

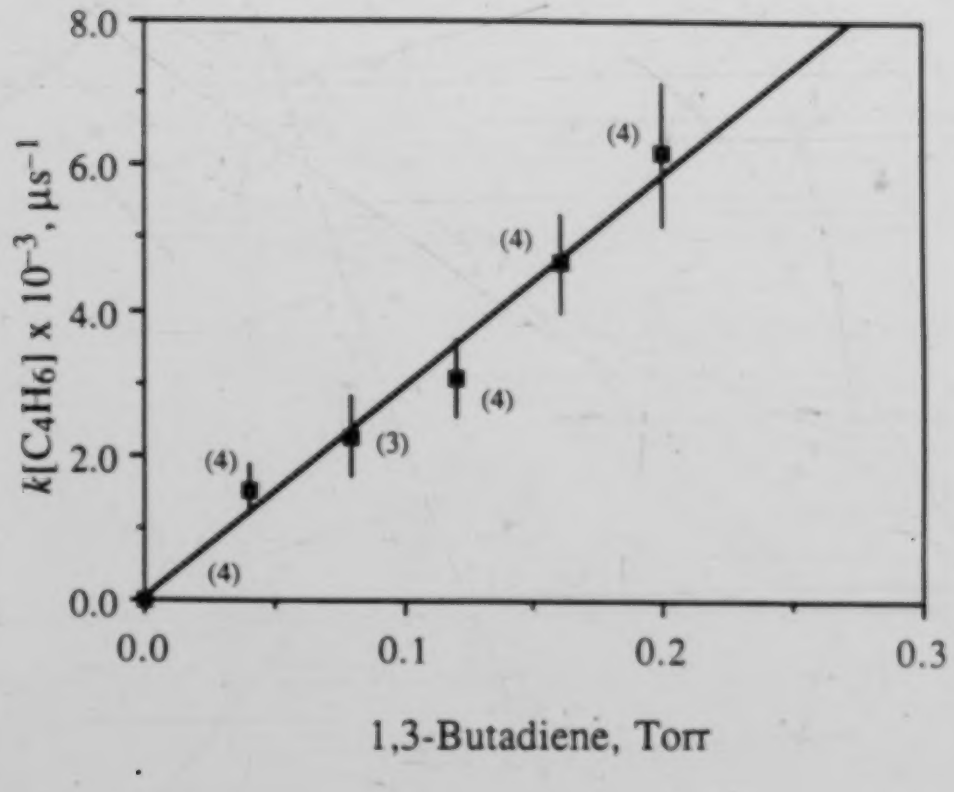

Figure III.33. Dependence of the pseudo first-order rate constants of $SiCl_2$ + 1,3-C_4H_6 reaction on the butadiene concentration. Numbers in the parentheses are the number of decay plots with 5 to 8 individual measurements.

III.4.6. The $SiCl_2$ + Isobutane Reaction.

The decay rates of $SiCl_2$ in the absence and in the presence of 6 Torr isobutane are listed in Table III.36 where it is seen that the peak heights of $SiCl_2$ are smaller in the presence of isobutane, seemingly pointing to an enhanced decay rate, owing to a chemical reaction. However, when these data were plotted to obtained the pseudo first-order rate constant, Figure III.34, the slope of the line corresponding to the $SiCl_2$ + *i*-butane system was less than that of the background decay plot, indicating that isobutane somehow suppresses the rate of decay of $SiCl_2$. No further experiments on this system were carried out.

Table III.36. Peak heights as a function of time for the reaction of $SiCl_2$ with 6.0 Torr isobutane.

$[i\text{-}C_4H_{10}]$ = 0.00 Torr		$[i\text{-}C_4H_{10}]$ = 6.0 Torr	
Time, μs	Ln(peak height)	Time, μs	Ln(peak height)
12	5.08	12	4.19
25	4.80	26	3.94
36	4.61	36	3.70
47	4.44	47	3.56
68	3.95	67	3.12
78	3.78	78	3.07
88	3.76	89	2.82
109	3.30	97	2.67

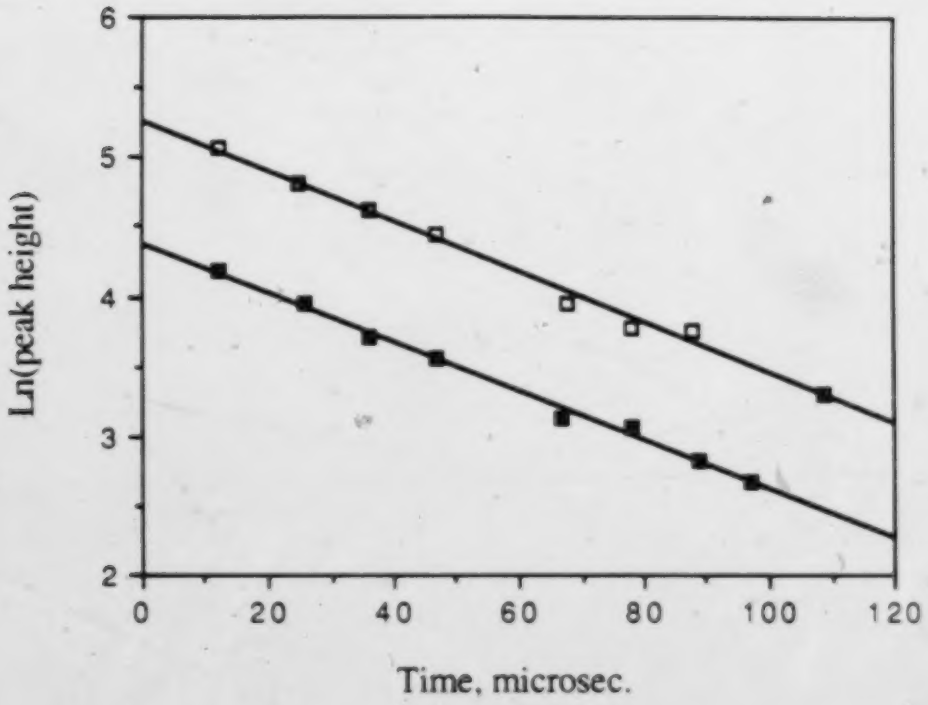

Figure III.34. Decay curves for [$SiCl_2$] in the absence (□) and presence (■) of 6.0 Torr isobutane .

III.5. Reactions of $SiBr_2$.

The gas-phase reactions of $SiBr_2$ were investigated with oxygen and nitric oxide. In all the experiments 0.20 Torr $SiBr_4$ in 40 Torr argon was used as the $SiBr_2$ source. As in the case of the $SiCl_2$ reactions, the background decay of $SiBr_2$ had to be measured before and after each series of decay rate measurements.

III.5.1. The $SiBr_2 + O_2$ Reaction.

The decay of $SiBr_2$ in the presence of O_2, at five different pressures in the 0.06 to 0.20 Torr range, was measured. The rate of decay of $SiBr_2$ was enhanced in the presence of oxygen and followed first-order kinetics. Peak height measurements as a function of time for the decay of $SiBr_2$ in the absence and in the presence of different amounts of oxygen are listed in Tables III.37 to III.41 and Figures III.35 to III.39 display the corresponding first-order decay plots. Such plots yielded the pseudo first-order rate constants which, after being corrected for the background decay of $SiBr_2$, are presented in Table III.42. The plot in Figure III.40 shows the linear relationship between the corrected pseudo first-order rate constants and the O_2 concentration, and the slope of this plot yielded (*cf.* Appendix B) the following value for the bimolecular rate constant of the gas-phase reaction of $SiBr_2$ with oxygen:

$$k(SiBr_2 + O_2) = (5.6 \pm 0.4) \times 10^8\ M^{-1}s^{-1}.$$

Table III.37. Peak heights as a function of time for the reaction of $SiBr_2$ with 0.06 Torr oxygen.

$[O_2]$ = 0.00 Torr		$[O_2]$ = 0.06 Torr	
Time, μs	Ln(peak height)	Time, μs	Ln(peak height)
13	4.06	13	3.74
21	3.92	22	3.43
28	3.86	28	3.52
39	3.71	38	3.23
47	3.64	55	3.09
55	3.58	63	2.89
63	3.36	70	2.80
71	3.23		

Table III.38. Peak heights as a function of time for the reaction of $SiBr_2$ with 0.09 Torr oxygen.

$[O_2]$ = 0.00 Torr		$[O_2]$ = 0.09 Torr	
Time, μs	Ln(peak height)	Time, μs	Ln(peak height)
12	4.28	11	4.19
19	4.10	20	3.92
30	4.00	29	4.00
37	3.98	37	3.77
45	3.81	45	3.66
55	3.78	64	3.38
61	3.62	71	3.20
71	3.46		

Table III.39. Peak heights as a function of time for the reaction of $SiBr_2$ with 0.12 Torr oxygen.

$[O_2]$ = 0.00 Torr		$[O_2]$ = 0.12 Torr	
Time, μs	Ln(peak height)	Time, μs	Ln(peak height)
21	4.68	14	3.73
31	4.59	21	3.56
39	4.52	31	3.45
46	4.48	40	3.39
55	4.43	55	3.18
64	4.25	65	3.06
73	4.26	73	3.06

Table III.40. Peak heights as a function of time for the reaction of $SiBr_2$ with 0.16 Torr oxygen.

$[O_2]$ = 0.00 Torr		$[O_2]$ = 0.16 Torr	
Time, μs	Ln(peak height)	Time, μs	Ln(peak height)
08	4.60	13	3.59
20	4.48	17	3.67
37	4.38	31	3.49
52	4.32	43	3.26
55	4.19	55	3.14
67	4.15	61	3.11
		73	2.93

Table III.41. Peak heights as a function of time for the reaction of $SiBr_2$ with 0.20 Torr oxygen.

$[O_2]$ = 0.00 Torr		$[O_2]$ = 0.20 Torr	
Time, μs	Ln(peak height)	Time, μs	Ln(peak height)
14	4.88	14	3.79
31	4.75	30	3.61
48	4.65	38	3.41
64	4.47	47	3.34
73	4.40	55	3.31
		64	3.05
		72	2.96

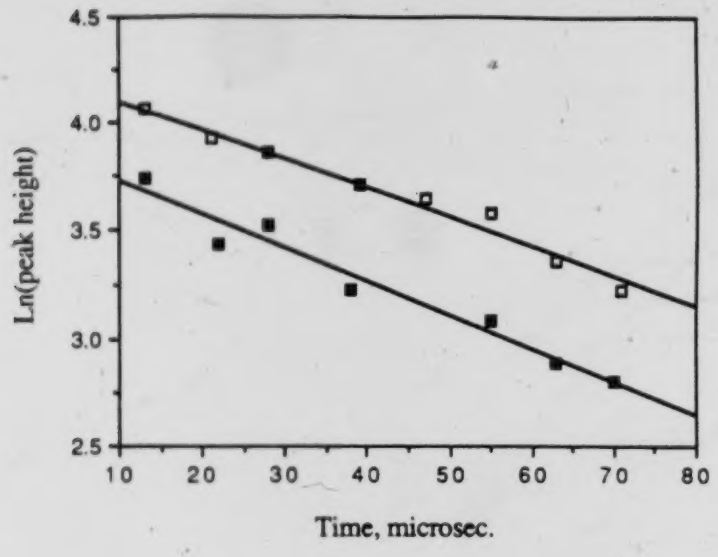

Figure III.35. Decay curves for [$SiBr_2$] in the absence (□) and presence (■) of 0.06 Torr oxygen.

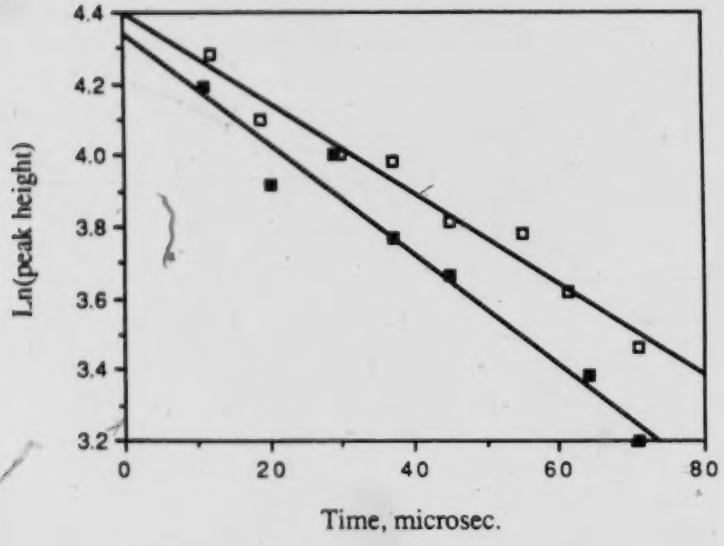

Figure III.36. Decay curves for [$SiBr_2$] in the absence (□) and presence (■) of 0.09 Torr oxygen.

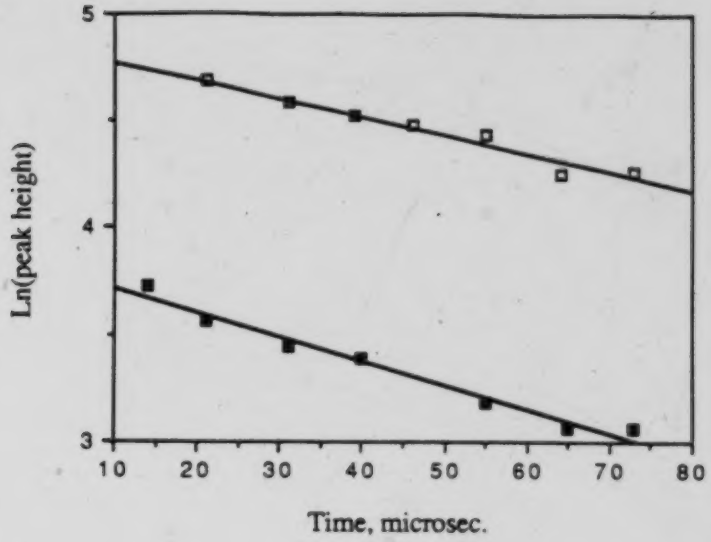

Figure III.37. Decay curves for [$SiBr_2$] in the absence (□) and presence (■) of 0.12 Torr oxygen.

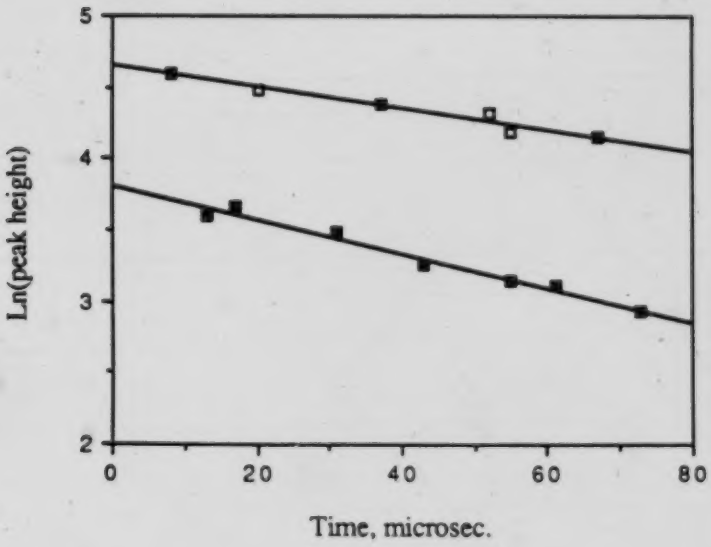

Figure III.38. Decay curves for [$SiBr_2$] in the absence (□) and presence (■) of 0.16 Torr oxygen.

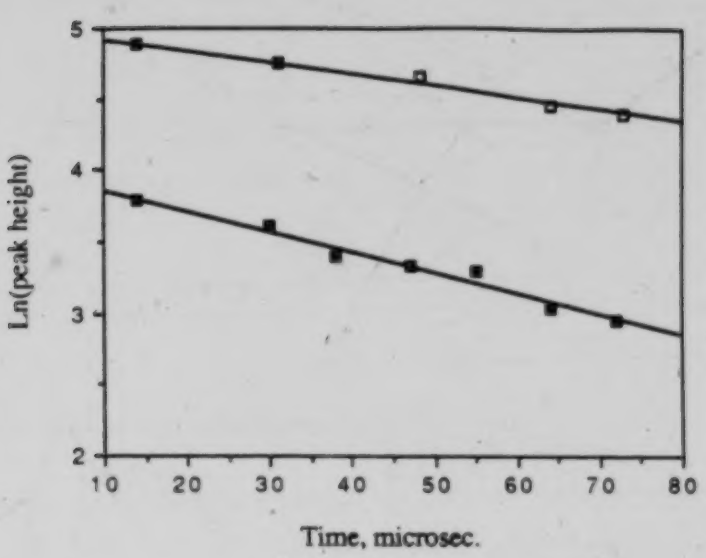

Figure III.39. Decay curves for [$SiBr_2$] in the absence (□) and presence (■) of 0.20 Torr oxygen.

Table III.42. Dependence of the pseudo first-order rate constants of the $SiBr_2 + O_2$ reaction on oxygen concentration.

$[O_2]$, Torr	$k[O_2] \times 10^3$, μs^{-1}	Avg. $k[O_2] \times 10^3$, μs^{-1}
0.06	1.828	
	1.354	1.59 ± 0.47
0.09	2.266	
	2.806	
	2.614	2.56 ± 0.55
0.12	4.571	
	3.182	
	3.548	
	3.696	3.75 ± 1.18
0.16	4.252	
	4.485	
	3.264	
	4.428	4.11 ± 1.14
0.20	6.242	
	5.563	
	6.369	
	6.742	6.23 ± 0.98

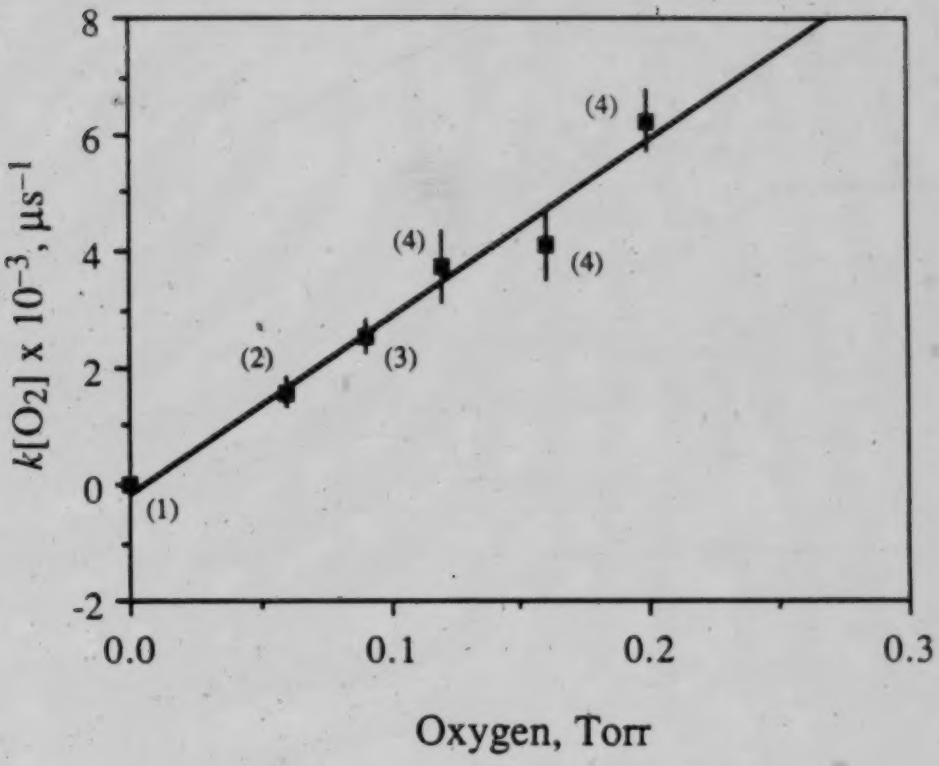

Figure III.40. Dependence of the pseudo first-order rate constants $SiBr_2 + O_2$ reaction on the oxygen concentration. Numbers in the parentheses are the number of decay plots with 5 to 8 individual measurements.

III.5.2. The $SiBr_2$ + NO Reaction.

Only one to three measurements of this reaction, at each of the five different concentrations of nitric oxide in the 0.16 to 0.30 Torr range, were carried out. The data obtained from such measurements are presented in Tables III.43 to III.47 with the corresponding first-order decay plots in Figures III.41 to III.45. The pseudo first-order rate constants as obtained from these plots, after being corrected for the background decay of $SiBr_2$, are listed in Table III.48. The dependence of the corrected pseudo first-order rate constants on the nitric oxide concentration is shown by the linear plot in Figure III.46 whose slope yielded (*cf.* Appendix B) the following bimolecular rate constant for the gas-phase reaction of $SiBr_2$ with NO:

$$k(SiBr_2 + NO) = (2.8 \pm 0.4) \times 10^8\ M^{-1}s^{-1}.$$

Absolute rate constants for the room-temperature gas-phase reactions of $SiCl_2$ and $SiBr_2$ with different substrates as measured in the present study are listed in Table III.49.

Table III.43. Peak heights as a function of time for the reaction of $SiBr_2$ with 0.16 Torr nitric oxide.

[NO] = 0.00 Torr		[NO] = 0.16 Torr	
Time, μs	Ln(peak height)	Time, μs	Ln(peak height)
14	4.79	15	4.50
29	4.69	29	4.35
37	4.63	37	4.28
45	4.53	50	4.20
51	4.50	59	3.99
59	4.44	66	3.98
66	4.37		

Table III.44. Peak heights as a function of time for the reaction of $SiBr_2$ with 0.20 Torr nitric oxide.

[NO] = 0.00 Torr		[NO] = 0.20 Torr	
Time, μs	Ln(peak height)	Time, μs	Ln(peak height)
15	5.25	16	4.57
31	5.16	21	4.52
37	5.14	29	4.48
51	5.10	37	4.43
67	4.92	44	4.34
		59	4.13

Table III.45. Peak heights as a function of time for the reaction of $SiBr_2$ with 0.24 Torr nitric oxide.

[NO] = 0.00 Torr		[NO] = 0.24 Torr	
Time, μs	Ln(peak height)	Time, μs	Ln(peak height)
15	5.26	13	4.64
29	5.22	21	4.59
36	5.19	29	4.62
43	5.11	37	4.55
59	5.06	43	4.46
66	5.02	59	4.24
		67	4.25

Table III.46. Peak heights as a function of time for the reaction of $SiBr_2$ with 0.28 Torr nitric oxide.

[NO] = 0.00 Torr		[NO] = 0.28 Torr	
Time, μs	Ln(peak height)	Time, μs	Ln(peak height)
16	4.84	16	4.08
22	4.76	29	3.92
37	4.70	37	3.88
44	4.68	45	3.75
60	4.49	59	3.63
67	4.48	67	3.50

Table III.47. Peak heights as a function of time for the reaction of $SiBr_2$ with 0.30 Torr nitric oxide.

[NO] = 0.00 Torr		[NO] = 0.30 Torr	
Time, μs	Ln(peak height)	Time, μs	Ln(peak height)
14	5.34	15	4.81
21	5.26	20	4.63
29	5.30	43	4.43
36	5.24	58	4.31
43	5.17	66	4.30
65	5.09		

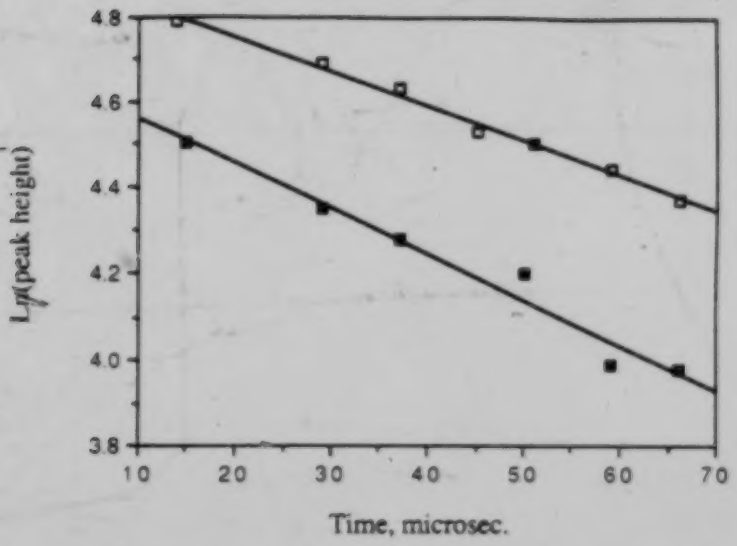

Figure III.41. Decay curves for [$SiBr_2$] in the absence (□) and presence (■) of 0.16 Torr nitric oxide.

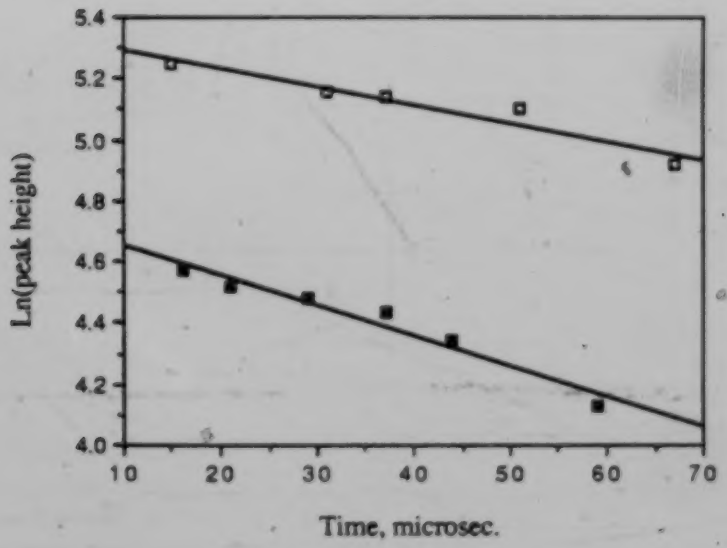

Figure III.42. Decay curves for [$SiBr_2$] in the absence (□) and presence (■) of 0.20 Torr nitric oxide.

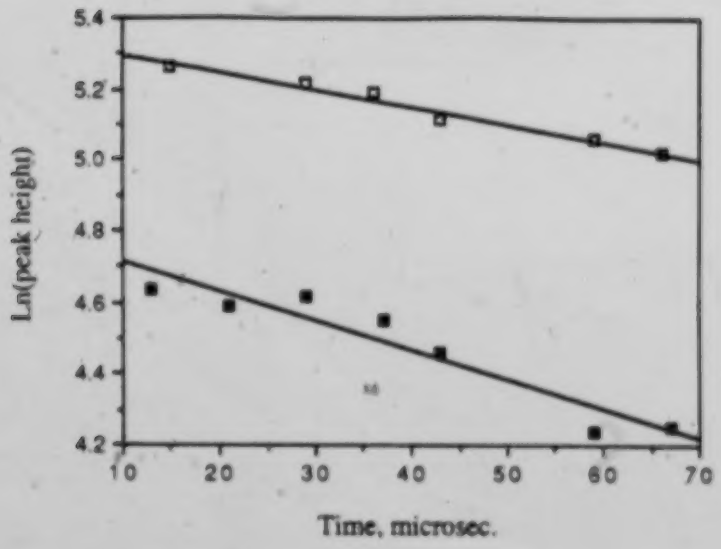

Figure III.43. Decay curves for [$SiBr_2$] in the absence (□) and presence (■) of 0.24 Torr nitric oxide.

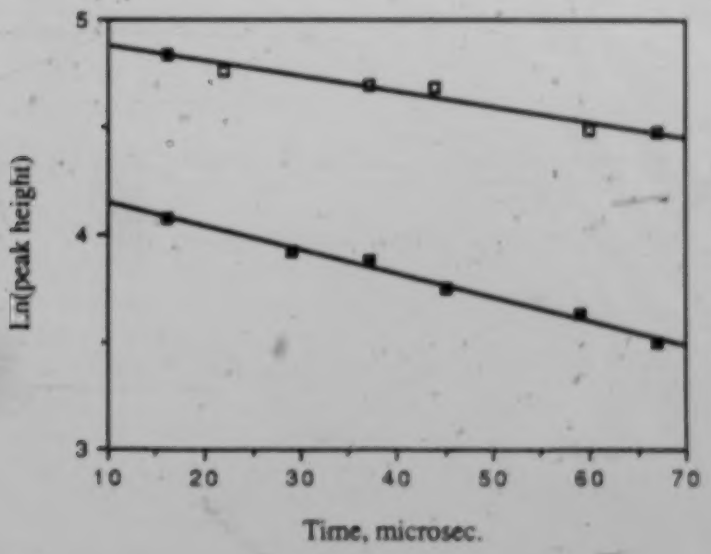

Figure III.44. Decay curves for [$SiBr_2$] in the absence (□) and presence (■) of 0.28 Torr nitric oxide.

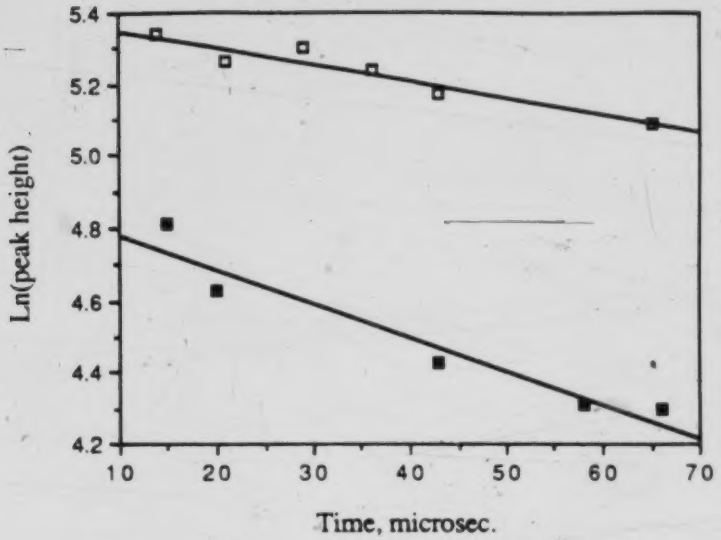

Figure III.45. Decay curves for [$SiBr_2$] in the absence (□) and presence (■) of 0.30 Torr nitric oxide.

Table III.48: Dependence of the pseudo first-order rate constants of the $SiBr_2$ + NO reaction on nitric oxide concentration.

[NO], Torr	k[NO] x 10^3, μs^{-1}	Avg. k[NO] x 10^3, μs^{-1}
0.16	2.246	
	2.586	2.42 ± 0.34
0.20	3.595	
	3.884	
	1.879	3.12 ± 2.17
0.24	3.385	3.38
0.28	3.815	3.82
0.30	4.543	
	4.887	4.72 ± 0.34

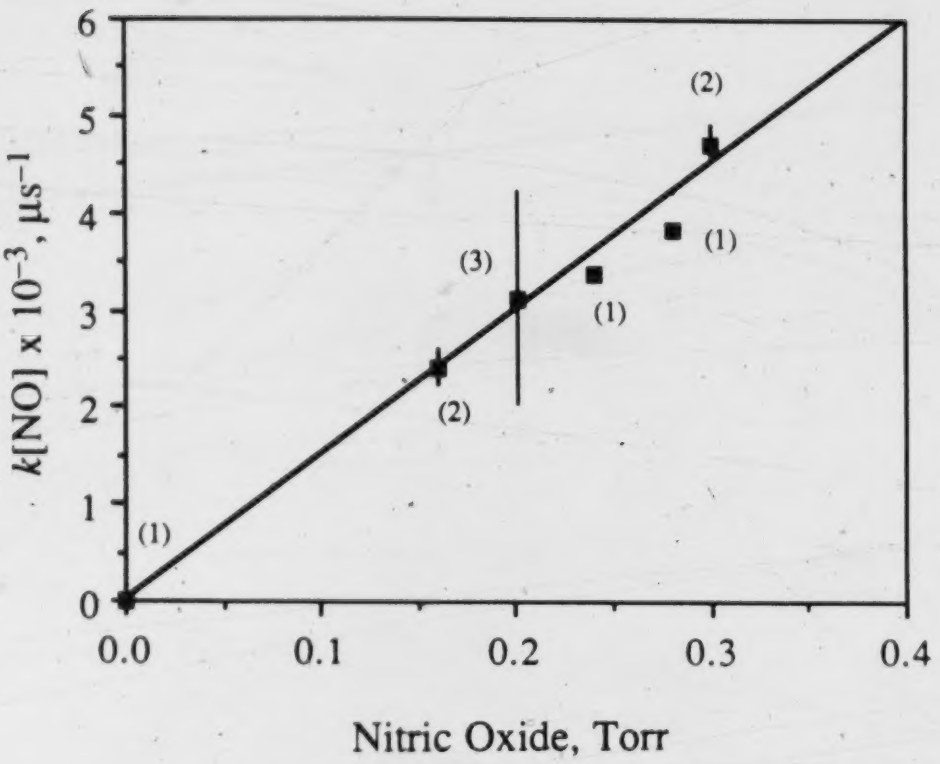

Figure III.46. Dependence of the pseudo first-order rate constants of $SiBr_2$ + NO reaction on the nitric oxide concentration. Numbers in the parentheses are the number of decay plots with 5 to 8 individual measurements.

Table III.49. Absolute rate constants for the gas-phase reactions of $SiCl_2$ and $SiBr_2$ with different substrates R.

R	$k, M^{-1}s^{-1}$	
	$SiCl_2$	$SiBr_2$
O_2	$(3.4 \pm 0.2) \times 10^9$	$(5.6 \pm 0.4) \times 10^8$
NO	$(1.6 \pm 0.1) \times 10^9$	$(2.8 \pm 0.4) \times 10^8$
CO	$(6.3 \pm 0.7) \times 10^8$	——
N_2O	$(5.7 \pm 0.3) \times 10^8$	——
1,3-C_4H_6	$(5.4 \pm 0.3) \times 10^8$	——

Chapter IV

DISCUSSION

IV.1. Argon Pressure Dependence of the Background Decay of $SiCl_2$.

The rate of background decay of $SiCl_2$ was found to increase upon increasing the argon pressure from 50 to 100 Torr (k increased from 7.2×10^3 to 1.5×10^4 M^{-1} s^{-1}) whereas a further increase in argon pressure to 150 Torr showed almost no change in the rate constant value ($k_{avg.} = 1.4 \times 10^4$ $M^{-1}s^{-1}$) (*cf.* Table III.5). In order to explain this behavior, the following mechanism is proposed for the background decay of $SiCl_2$:

$$SiCl_2 + Si_2Cl_6 \xrightarrow{2a} \left[Cl_3Si{-}SiCl_2 \;\; Cl_2Si{\cdots}Cl \right]^{\ddagger} \underset{2c}{\overset{2b}{\rightleftharpoons}} Si_3Cl_8^* \quad (1)$$

$$Si_3Cl_8^* + Ar \xrightarrow{3} Si_3Cl_8 + Ar^*$$

$SiCl_2$ produced from the flash photolysis of Si_2Cl_6, in the absence of any other reactive substrate, would react with excess Si_2Cl_6 *via* insertion into the Si—Cl bond ($SiCl_2$ is known to insert into the Si—Cl bonds of perchloropolysilanes [70] and the reverse of this insertion reaction, *i.e.* one-stage thermal decomposition, has been used as a source of $SiCl_2$ [72]) to give a hot insertion product **1** (reaction 2b). In the absence of a third body, this hot product **1** would decompose reversibly *via* reaction 2c, whereas in the presence of a third body it would be stabilized to the final insertion product Si_3Cl_8 *via* reaction 3. Thus at low argon (third body) pressure, reactions 2c and 3 compete

against each other resulting in an overall slower rate of decay of $SiCl_2$. As the argon pressure is increased, reaction 3 dominates reaction 2c *i.e.* the hot product **1** dissipates its excess energy *via* reaction 3 to yield a stable insertion product and hence the decay rate of $SiCl_2$ increases. However, once the limiting pressure of argon is reached, which is sufficient to accomodate all the excess energy, any further increase in its pressure would not affect the decay rate of $SiCl_2$ (*cf.* Appendix C).

IV.2. Mechanistic Aspects of the Reactions of $SiCl_2$ and $SiBr_2$.

IV.2.1. Reactions with Oxygen.

The room-temperature gas-phase reactions between SiX_2 (X = Cl, Br) and O_2 are found to be first order in both SiX_2 and O_2 concentrations as shown by the linear plots in Figures III.4 to III.8 for X = Cl, and Figures III.35 to III.40 for X = Br. The values of the absolute bimolecular rate constants are

$$k(SiCl_2 + O_2) = (3.4 \pm 0.2) \times 10^9\ M^{-1}s^{-1}$$

$$k(SiBr_2 + O_2) = (5.6 \pm 0.4) \times 10^8 M^{-1}s^{-1}$$

The mechanism of the reaction between SiX_2 (X = Cl, Br) and O_2 is not known. However, for reaction between photochemically generated $SiCl_3$ and O_2 in the liquid phase, Gooden [133] have proposed the following reaction scheme to account for the high quantum efficiency of Cl_3SiOH produced from the photoxidation (λ = 254 nm) of $SiHCl_3$ in $SiCl_4$:

$$SiCl_4 + h\upsilon\ (254\ nm) \longrightarrow SiCl_3 + Cl \qquad (IV.1)$$

$$SiCl_3 + O_2 \longrightarrow Cl_3SiOO \qquad (IV.2)$$

$$2\ Cl_3SiOO \longrightarrow 2\ Cl_3SiO + O_2 \qquad \text{(IV.3)}$$

$$Cl_3SiO + SiHCl_3 \longrightarrow Cl_3SiOH + SiCl_3 \qquad \text{(IV.4)}$$

This mechanism was further supported by the results of Niki *et al.* [134] who studied the Cl-atom initiated gas-phase reactions of $SiHCl_3$ with O_2 using the FTIR spectroscopic technique. They observed the formation of $Cl_3SiOONO_2$ from the Cl-atom initiated oxidation of $SiHCl_3$ in the presence of NO_2 according to following scheme.

$$Cl + SiHCl_3 \longrightarrow HCl + SiCl_3 \qquad \text{(IV.5)}$$

$$SiCl_3 + O_2 \longrightarrow Cl_3SiOO \qquad \text{(IV.6)}$$

$$Cl_3SiOO + NO_2 \xrightarrow{M} Cl_3SiOONO_2 \qquad \text{(IV.7)}$$

Eley *et al.* [135], from relative rate studies of silylene reactions in the gas phase, observed a slow reaction between SiH_2 and O_2, and proposed that it proceeds *via* initial H_2SiO_2 adduct formation with subsequent complex chemistry.

Recently, Gaspar *et al.* [136] suggested that in solution phase, diorganosilylenes SiR_2 (R = Me, t-Bu; R_2 = MePh, 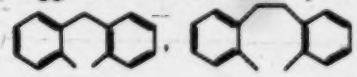) react with O_2 to form a silylene-oxygen adduct which is of either a silanone O-oxide **2** or siladioxirane **3** structure.

$$SiR_2 + O_2 \longrightarrow \underset{\mathbf{2}}{R_2Si{-}\overset{+}{O}{-}\overset{-}{O}} \qquad \underset{\mathbf{3}}{R_2Si\begin{smallmatrix}O\\|\\O\end{smallmatrix}} \qquad \text{(IV.8)}$$

More recently, Akasaka *et al.* [137] reported the first spectroscopic observation of an R_2Si-O_2 (R = H, Mes) adduct from the UV irradiation of the silylene precursor

(trisilane for R = H, and 2,2-dimesityl-1,1,1,3,3,3-hexamethyltrisilane for R = Mes) in an oxygen matrix at 16K. From the FTIR and theoretical studies they concluded that the R_2Si-O_2 adduct has a silanone O-oxide **2** rather than a siladioxirane **3** structure. Upon warming up the matrix above 40K, they observed that the matrix became cloudy and the products at room temperature consisted of polymeric species with Si—O bonds.

The reactions between CF_2, singlet methylene and triplet methylene, and O_2 have also been reported to involve initial CF_2O_2 and CH_2O_2 adduct formation [27, 29, 33].

In view of the consistency among the suggested mechanisms for the reactions of O_2 with trichlorosilyl radicals and divalent Si and C species, and the fact that the gas-phase $SiX_2 + O_2$ (X = Cl, Br) reaction is first order in both SiX_2 and O_2 concentrations as observed from the present study, it is proposed that the gas-phase room-temperature $SiX_2 + O_2$ reactions proceed *via* initial 1:1 adduct formation between SiX_2 (X = Cl, Br) and O_2. This silanone O-oxide type adduct can then react further according to either reactions IV.10a or IV.10b:

$$SiX_2 + O_2 \longrightarrow X_2SiOO \qquad \text{(IV.9)}$$

$$2\ X_2SiOO \longrightarrow 2\ X_2SiO + O_2 \qquad \text{(IV.10a)}$$

or $$X_2SiOO + O_2 \longrightarrow X_2SiO + O_3 \qquad \text{(IV.10b)}$$

The overall reactions can be written as

$$SiX_2 + 1/2\ O_2 \longrightarrow X_2SiO \qquad \text{(IV.11a)}$$

or $$SiX_2 + 2\ O_2 \longrightarrow X_2SiO + O_3 \qquad \text{(IV.11b)}$$

(X = Cl, Br)

Cl_2SiO from the photolysis of a SiO and Cl_2 mixture has been isolated in an Ar matrix [138]. Golovkin *et al.* [139] have also isolated Cl_2SiO in argon and krypton matrices at –78°C, from the thermal decomposition of (benzyloxy)trichlorosilane:

$$C_6H_5CH_2OSiCl_3 \xrightarrow{450-550°C} [Cl_2Si{=}O] + C_6H_5CH_2Cl \qquad (IV.12)$$

These two reports on the isolation of Cl_2SiO lend additional support to the proposed mechanism for the $SiX_2 + O_2$ reactions.

X_2SiO, proposed to form *via* reactions IV.11a' or IV.11b, can undergo oligomerization *i.e.*

$$X_2SiO \longrightarrow (X_2SiO)_n \qquad (IV.13)$$

The isolation of $(X_2SiO)_n$, n = 3,4, polymers has been reported [140 – 144].

Rheinboldt and Wisfeld [140] have examined the thermal oxidation of SiX_4 (X = Cl, Br). From the reaction of $SiCl_4$ with O_2 at 950 – 970°C they obtained a series of siloxy compounds including $Si_4O_4Cl_8$. From the oxidation of $SiBr_4$, the formation of a series of oxybromides was observed at 670 – 695°C, from which crystalline $Si_4O_4Br_8$ was obtained as the major product. The authors suggested a cyclic stucture **4** for $Si_4O_4X_8$ (X = Cl, Br):

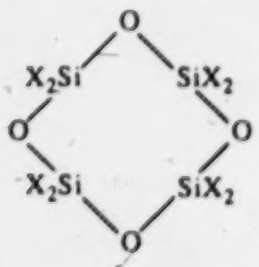

4

Schumb and Klein [141] repeated the experiments of Rheinboldt and Wisfeld on the thermal oxidation of $SiBr_4$ and suggested that the simplest oxybromide, Br_2SiO, would probably be incapable of existence outside the gas phase and that it polymerizes to $(Br_2SiO)_4$ in the liquid phase. A heavy white solid corresponding to empirical formula $(Br_2SiO)_4$, melting to a colorless liquid at ~123°C, was obtained as one of the major products. They also obtained traces of this product from the simultaneous action of O_2 and Br_2 on silicon.

The formation of $(Cl_2SiO)_4$ has also been reported [142] from the photooxidation of trichlorosilane according to the following mechanism:

$$2\ SiHCl_3 + O_2 \xrightarrow{h\upsilon} 2\ Si(OH)Cl_3 \qquad \text{(IV.14)}$$

$$Si(OH)Cl_3 \longrightarrow Cl_2SiO + HCl \qquad \text{(IV.15)}$$

$$4\ Cl_2SiO \longrightarrow (Cl_2SiO)_4 \qquad \text{(IV.16)}$$

$(Cl_2SiO)_4$ was isolated as a viscous, colorless liquid.

Wood *et al.* [143] have also observed the formation of cyclic $Si_4O_4Cl_8$ along with many other higher molecular weight compounds, from the oxidation of $SiCl_4$ at 1100°C. Above 1160°C, only SiO_2 was formed.

Krasnova *et al.* [144] obtained cyclic $(Cl_2SiO)_n$, n = 3, 4, as the final product from the reaction of $SiCl_4$ with lithium in tetrahydrofuran at 35 – 45°C.

$$SiCl_4 + 2\ Li + C_4H_8O \xrightarrow{35-45°C} (Cl_2SiO)_n + 2\ LiCl + C_4H_8 \qquad \text{(IV.17)}$$

$$n = 3 \quad 54\%$$
$$n = 4 \quad 46\%$$

All these reports support the proposed mechanism for the $SiX_2 + O_2$ reaction, as represented by reactions IV.9 to IV.11b and IV.13.

The reaction scheme IV.9 to IV.11b is exothermic. The heats of the overall reactions IV.11a (or IV.11b) are estimated to be –127.4 (or – 97.3) kcal mol^{-1} for X = Cl, and –126.3 (or – 96.2) kcal mol^{-1} for X = Br (*cf.* Appendix D). The activation energy for the primary reaction between SiX_2 and O_2 (*i.e.* recation IV.9) is estimated to be E_a ~3.0 kcal mol^{-1} for X = Cl, and ~4.1 kcal mol^{-1} for X = Br (*cf.* Appendix E).

IV.2.2. Reactions with Nitric Oxide.

The linear plots in Figures III.9 to III.14 and III.41 to III.46 show that both the $SiCl_2 + NO$ and $SiBr_2 + NO$ reactions are first order in both the corresponding silylene and nitric oxide concentrations. Absolute bimolecular rate constants of these gas-phase reactions are:

$$k(SiCl_2 + NO) = (1.6 \pm 0.1) \times 10^9\ M^{-1}s^{-1}$$

$$k(SiBr_2 + NO) = (2.8 \pm 0.4) \times 10^8\ M^{-1}s^{-1}$$

The mechanisms of these reactions have not yet been reported. However, the mechanisms of the reactions of other divalent species such as SiH_2, SiF_2, CF_2 and CH_2, with NO have been studied. For the $SiF_2 + NO$ reaction, Bassler *et al.* [67] reported that in a krypton matrix at 20 – 35K, this reaction yields an adduct containing a single SiF_2 unit and *cis*-dimeric form of NO, which decomposes explosively at –150°C yielding silicon oxyfluoride polymer and nitrous oxide. For such an energetic release of N_2O, the authors proposed that the initial adduct, $SiF_2(NO)_2$, has a cyclic 5 structure

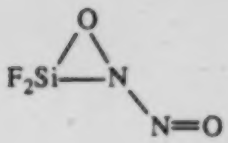

5

Recently, Lampe [145], from IR laser (υ = 944.19 cm^{-1}) photolysis of a SiH_4-NO mixture, observed the formation of N_2O along with H_2, Si_2H_6, Si_3H_8 and Si_4H_{10}, and thus proposed the following reactions to occur (in addition to the formation and subsequent reactions of SiH_3):

$$SiH_4 + n\,h\upsilon \xrightarrow{n \geq 21} SiH_2 + H_2 \qquad \text{(IV.18)}$$

$$SiH_2 + NO \longrightarrow \text{Products} \qquad \text{(IV.19)}$$

Although he could not identify all the products of the above reaction, he noted that they comprise N_2O, solid siloxy compounds and perhaps N_2.

Chu *et al.* [46], using laser resonance absorption flash kinetic spectroscopy, have observed a fast reaction between gas-phase SiH_2 and NO ($k = (1.0 \pm 0.1) \times 10^{10}$ $M^{-1}\,s^{-1}$) and proposed this reaction to proceed *via* initial formation of an H_2SiNO adduct of unspecified molecular structure.

For the similar reaction between $^3CH_2$ and NO, Seidler *et al.* [24] have proposed the initial cyclic adduct **6** formation as a possible channel. However, the details of this reaction mechanism have not yet been elucidated.

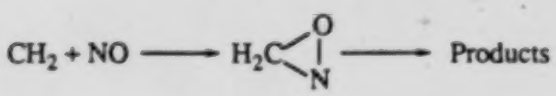

(IV.20)

6

For the analogous reaction of CF_2, two different mechanisms have been proposed. Modica [31] proposed that below 2500K reversible CF_2NO adduct formation is the major reaction,

$$CF_2 + NO \rightleftharpoons CF_2NO \qquad \text{(IV.21)}$$

and above 2500K this adduct reacts further to yield N_2O, CF_2O and N_2 as the final reaction products.

$$2\,CF_2NO \longrightarrow 2\,CF_2O + N_2 \qquad >2500K \qquad \text{(IV.22)}$$

$$CF_2NO + NO \longrightarrow CF_2O + N_2O \qquad \text{(IV.23)}$$

On the other hand, Burks and Lin [32] proposed that CF_2O is formed by simple oxygen abstraction from NO:

$$CF_2 + NO \longrightarrow CF_2O + N \qquad \text{(IV.24)}$$

they also suggested that the formation of N_2O in Modica's high-temperature reaction arises from bimolecular reaction of NO:

$$2\,NO \longrightarrow N_2O + O \qquad \text{(IV.25)}$$

Although no new studies on this reaction have been reported, Modica's mechanism is analogous to those reported for the SiH_2 and SiF_2 + NO reactions, with regard to the formation of N_2O as one of the products.

By analogy with these studies on the reactions of NO with silylenes and carbenes, it is not unreasonable to propose that the room-temperature gas-phase reactions SiX_2 (X = Cl, Br) + NO involve the formation of a X_2SiON adduct which then undergoes further reactions *via* either scheme I or II

$$SiX_2 + NO \longrightarrow X_2SiON \qquad (IV.26)$$

Scheme I:

$$X_2SiON + NO \longrightarrow X_2SiONNO \qquad (IV.27)$$

$$X_2SiONNO \longrightarrow X_2SiO + N_2O \qquad (IV.28)$$

overall reaction:

$$SiX_2 + 2\,NO \longrightarrow X_2SiO + N_2O \qquad (IV.29)$$

Scheme II:

$$2\,X_2SiON \longrightarrow 2\,X_2SiO + N_2 \qquad (IV.30)$$

overall reaction:

$$SiX_2 + NO \longrightarrow X_2SiO + 1/2\,N_2 \qquad (IV.31)$$

The initial adduct formed in reaction IV.26 can be either of cyclic **7** or open **8** geometry:

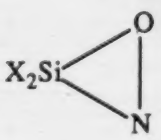

7

$X_2Si - O = N$

8

Very recently, Gosavi and Strausz [146] have carried out molecular orbital studies on the $SiCl_2$ + NO reaction at the SCF level using a 3-21G basis set. From their preliminary calculations on the total energy of both the cyclic **7** and open **8** structures of the initial adduct it appears that the cyclic adduct lies ~3.5 kcal mol^{-1} below the separated reactants, whereas the open adduct lies ~27 kcal mol^{-1} above the reactants.

Thus their calculations support a cyclic geometry **7** for the initial adduct formed in reaction IV.25, similar to the cyclic adduct reported to form from the SiF_2 + NO reaction in a matrix. The calculations of Gosavi and Strausz also indicate that the products of reaction IV.27, *i.e.* Cl_2SiO and N_2O, are ~24 kcal mol^{-1} more stable than the cyclic adduct **7** + NO. Calculations with a larger basis set, 6-31G, yielded even greater stabilization (~48 kcal mol^{-1}) of the final products of scheme I. Thus their calculations show that scheme I is energetically feasible. No such calculations on scheme II have yet been carried out.

A mechanism similar to scheme I for the gas-phase reactions of SiH_3 and $SiCl_3$ with NO, yielding N_2O and the respective oxysilanes, has also been reported [147, 134]; however, the geometries of the initial adducts were not discussed.

$$SiR_3 + NO \longrightarrow R_3SiON \qquad \text{(IV.32)}$$

$$R_3SiON + NO \longrightarrow R_3SiONNO \qquad \text{(IV.33)}$$

$$R_3SiONNO \longrightarrow R_3SiO + N_2O \qquad \text{(IV.34)}$$

R = H, Cl

For the $SiMeR_2$ + NO (R = H, Me) reaction, a mechanism similar to scheme II has been proposed [148]:

$$SiMeR_2 + NO \longrightarrow MeR_2SiON \qquad \text{(IV.35)}$$

$$2\ MeR_2SiON \longrightarrow [MeR_2SiON{=}NOSiR_2Me] \qquad \text{(IV.36)}$$

$$[MeR_2SiON{=}NOSiR_2Me] \longrightarrow 2\ MeR_2SiO + N_2 \qquad \text{(IV.37)}$$

Schemes I and II are both exothermic. For reactions IV.29 and IV.31 $\Delta H_{rxn.}$ is −151 and −149 kcal mol^{-1}, respectively for the reactions of $SiCl_2$, and −149.9 and −147.9 kcal mol^{-1}, respectively for those of $SiBr_2$ (*cf.* Appendix D). An upper limit for the activation energy of the primary reaction IV.26 is estimated to be E_a ~3.5 kcal mol^{-1} for X = Cl and ~4.5 kcal mol^{-1} for X = Br (*cf.* Appendix E).

From the $SiCl_2$ + NO reaction, the formation of a volatile product was observed in both photolyzed and unphotolyzed reaction mixtures. This product was observed as a purple deposit that appeared upon pumping the photolyzed or unphotolyzed reaction mixture through a liquid nitrogen-cooled trap, at the level of the liquid N_2. Upon warming the cold trap, the purple color disappeared *via* following transitions: purple → orange → light yellow with a light blue outer ring → colorless. No product analysis, of this or any other reaction studied in the present work, was carried out. From the observed color change of the product on warming the cold trap the formation of NOCl could be suspected. Crystalline NOCl is yellowish-red and, together with unreacted NO (blue in crystalline form), would give the observed purple color. The formation of NOCl from the photochemical (254 nm, Hg resonance lamp) as well as the dark reaction (24°C, 69 hrs.) between $SiHCl_3$ and NO, has been reported [149]. N_2O and $(SiCl_3)_2O$ were detected in the product mixture from the photochemical reaction but no mechanism was discussed.

IV.2.3. Reaction with Carbon Monoxide.

The absolute bimolecular rate constant for the gas-phase reaction between $SiCl_2$ and CO, which is first order in both $SiCl_2$ and CO concentrations, as evident from the linear plots on Figures III.15 to III.20, is

$$k(SiCl_2 + CO) = (6.3 \pm 0.7) \times 10^8\ M^{-1}s^{-1}$$

The mechanism of this reaction or of any other reaction between divalent silicon or carbon radical and CO has not yet been established. Recently, however, some reports concerning the molecular structure of the initial adduct formed between CO and organosilylenes (SiR_2) in matrices have appeared.

Arrington *et al.* [150] have studied the $SiMe_2$ + CO reaction in low-temperature matrices, and presented spectroscopic evidence for adduct formation between $SiMe_2$ and CO. The IR spectrum of the $SiMe_2$-CO adduct in a solid Ar matrix at 15 – 40K and the UV spectrum in a solid nitrogen matrix at 20 – 40K was recorded. Initially, the authors expected a pyramidal Lewis acid-base type adduct between $SiMe_2$ and CO, in which the lone pair electrons of CO form a coordinate covalent bond with the empty p-orbital on Si. However, their experimental data on the shift of C—O streching frequency in the adduct from that in free CO were in good agreement with theoretical values calculated by AM1 and MNDO methods [151a], both of which predicted the linear silaketene **9** rather than the pyramidal Lewis acid-base **10** type geometry for the Me_2SiCO adduct;

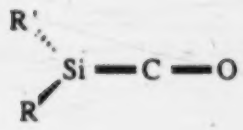

9

10

on the other hand, *ab initio* calculations [151b] predicted the pyramidal acid-base geometry to be more stable. Thus Arrington *et al.* were unable to reach a clear-cut decision with regard to the structure of the Me_2SiCO adduct. They did, however, rule out the possibility of CO bonding to $SiMe_2$ through a Si—O bond, since the energetics of such a reaction would yield a product that is ~49 kcal mol^{-1} less stable than silaketene.

Pearsall and West [152] studied the reactions of diorganosilylenes with CO in frozen hydrocarbon matrices at 77K using UV-visible spectroscopy:

$$SiRR' + CO \longrightarrow R'RSiCO \longrightarrow R'RSi{=}SiRR' \qquad \text{(IV.38)}$$

RR' = Mes, t-butyl; Mes, Mes; Mes, OAr; Me, Me.

Upon warming the matrix they observed depletion of the characteristic silylene band with the concommitant growth of a new band at shorter wavelength, which they attributed to a silylene-CO adduct. Upon further warming of the matrix they observed the formation of stable disilene in each case except for $SiMe_2$. Based on the fact that the silylene-CO adduct behaved in a manner similar to other acid-base complexes of silylenes with other donor molecules in matrices, all yielding disilene upon melting the matrix, Pearsall and West inferred the silylene-CO adduct to be of the pyramidal acid-base **10** type complex rather than silaketene **9**. West and coworkers also suggested [152 – 154] that these acid-base type silylene-CO adducts are formed reversibly and, upon annealing the matrix, dissociate to yield silylene which then dimerize to disilenes.

Hamilton and Schaefer [50], using *ab initio* methods, have calculated the energetics for the formation of the H_2SiCO adduct, in both planar and non-planar geometry, from SiH_2 and CO. They concluded that the equilibrium geometry of

H_2SiCO is indeed pyramidal non-planar, whereas the planar silaketene is the transition state for inversion between the two pyramidal forms. The estimated heat of formation of the non-planar pyramidal geometry is –16 kcal mol^{-1} whereas that of planar silaketene is 18 kcal mol^{-1} higher.

Bassler *et al.* [67], from IR studies of the SiF_2 + CO reaction in an argon matrix, suggested that the reaction proceeds *via* irreversible formation of F_2SiCO which decomposes to volatile silicon oxyfluorides and a carbon-rich polymer at higher temperatures. However, no information concerning the molecular structure of the adduct nor the details of mechanism were given.

On the basis of data reported on the reactions of analogous silylenes with CO and the kinetic measurements of the present study, the following possible routes can be considered for the gas-phase $SiCl_2$ + CO reaction.

Scheme I: $SiCl_2$ reacts with CO to form a silaketene $Cl_2Si{=}C{=}O$ with a subsequent complex chemistry:

$$SiCl_2 + CO \longrightarrow Cl_2Si{=}C{=}O \qquad \text{(IV.39)}$$

The corresponding dichloroketene has been isolated in an argon matrix at 8K [155].

Scheme II: The initial adduct formed between $SiCl_2$ and CO involves Si—O bonding and, upon subsequent reaction with another CO molecule, Cl_2SiO is formed. This mechanism is similar to that proposed for $SiCl_2$ + O_2 and $SiCl_2$ + NO reactions.

$$SiCl_2 + CO \longrightarrow Cl_2SiOC \qquad \text{(IV.40)}$$

$$Cl_2SiOC + CO \longrightarrow Cl_2SiO + C_2O \qquad \text{(IV.41)}$$

The overall reaction is

$$SiCl_2 + 2\,CO \longrightarrow Cl_2SiO + C_2O \qquad \text{(IV.42)}$$

Both these schemes, however, seem unlikely to be involved in the $SiCl_2$ + CO reaction. Scheme I can be ruled out since all the reported data on the reactions of other silylenes with CO favor the pyramidal acid-base type adduct over the silaketene. Scheme II can be discounted since the overall reaction IV.42 is endothermic by 14.4 kcal mol^{-1} (*cf.* Appendix D). Thus scheme III, presented below, seems to be the most probable mechanism for the $SiCl_2$ + CO reaction.

Scheme III: $SiCl_2$ and CO react in the gas-phase to give an initial acid-base type adduct Cl_2SiCO analogous to the one proposed for the SiR_2 + CO (R = H, organo group) reactions [50, 152]. Since the rate of the $SiCl_2$ + CO reaction is moderate ($k = (6.3 \pm 0.7) \times 10^8\ M^{-1}s^{-1}$), the formation of the initial adduct is proposed to be irreversible, as in the SiF_2 + CO reaction [67]. On the basis of Pearsall and West's results [152], the initial adduct is then expected to undergo either reaction IV.44a or IV.44b to yield tetrachlorodisilene:

$$SiCl_2 + CO \longrightarrow Cl_2Si{\leftarrow}CO \qquad \text{(IV.43)}$$

$$2\,Cl_2Si{\leftarrow}CO \longrightarrow Cl_2Si{=}SiCl_2 + 2\,CO \qquad \text{(IV.44a)}$$

or

$$Cl_2Si{\leftarrow}CO + SiCl_2 \longrightarrow Cl_2Si{=}SiCl_2 + CO \qquad \text{(IV.44b)}$$

The overall reaction,

$$2\ SiCl_2 \longrightarrow Cl_2Si{=}SiCl_2 \qquad \text{(IV.45)}$$

is exothermic by –24.3 kcal mol^{-1} (*cf.* Appendix D) and the upper limit of the activation energy for reaction IV.43, is estimated to be ~4.2 kcal mol^{-1} (*cf.* Appendix E)

Tetrachlorodisilene has not yet been isolated, however, from qualitative studies, tetrachlorodisilene has been proposed [76] to be an intermediate in the gas-phase pyrolysis of 1,1-dichlorosilacyclopentene. The formation of the carbon analog of tetrachlorodisilene, tetrachloroethylene (C_2Cl_4), was observed by Torres *et al.* [155] following the thermolysis of the dichloroketene precursor, in an argon matrix at 8K.

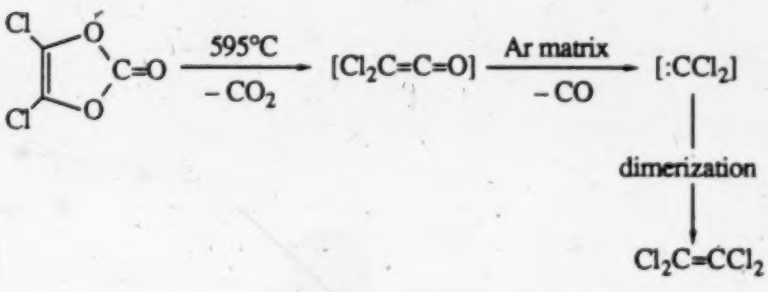

(IV.46)

IV.2.4. Reaction with Nitrous Oxide.

The absolute bimolecular rate constant for the gas-phase $SiCl_2 + N_2O$ reaction, which is first order in both $SiCl_2$ and N_2O concentrations as shown by the linear plots in Figures III.21 to II.27, is:

$$k(SiCl_2 + N_2O) = (5.7 \pm 0.3) \times 10^8\ M^{-1}s^{-1}$$

The mechanism of this reaction is not known. However, the corresponding $SiMe_2 + N_2O$ reaction in an argon matrix at low temperature has been studied by Arrington *et al.* [156] using IR spectroscopy and GC-MS. They concluded that at 35K $SiMe_2$ reacts with N_2O by oxygen abstraction to form $Me_2Si{=}O$ since upon annealing the matrix above 35K, $(Me_2SiO)_3$ was the major product, along with small amounts of $(Me_2SiO)_4$ and $(Me_2SiO)_5$.

$$SiMe_2 + N_2O \xrightarrow{35K} N_2 + Me_2Si{=}O \xrightarrow[n\ Me_2Si{=}O]{> 35K} (Me_2SiO)_{n+1} \qquad n = 2, 3, 4 \qquad \text{(IV.47)}$$

In view of the above study and the observation that: 1) the expected product of the $SiCl_2 + NO$ reaction, the corresponding dichlorosilanone, Cl_2SiO, has been isolated in matrices [138, 139] (*cf.* section IV.2.1.); 2) the Cl_2SiO monomer polymerizes to $(Cl_2SiO)_n$ n = 3, 4 as final products; and 3) the $SiCl_2 + N_2O$ reaction is first order in both $SiCl_2$ and N_2O concentration, it seems reasonable to propose that the room-temperature gas-phase $SiCl_2 + N_2O$ reaction may proceed *via* unimolecular extrusion of N_2:

$$SiCl_2 + N_2O \longrightarrow Cl_2SiO + N_2 \qquad \text{(IV.48)}$$

The resulting Cl_2SiO probably further oligomerizes.

Silyl and alkyl radicals have also been reported to react with N_2O *via* N_2 extrusion. The $SiH_3 + N_2O \rightarrow H_3SiO + N_2$ reaction has been reported to proceed very slowly at 500K with an upper limit for the rate constant estimated to be $k < 3 \times 10^6\ M^{-1}\ s^{-1}$ [157]. Other radicals which have been reported to react with N_2O to form N_2 below 400° *via* oxygen abstraction [158] include the ethyl, methyl and trifluoromethyl radicals:

$$R + N_2O \longrightarrow RO + N_2 \qquad \text{(IV.49)}$$

$(R = CH_3, C_2H_5, CF_3)$

For $R = CF_3$, the rate constant at 400°C is ~4 x 10^2 $M^{-1}s^{-1}$ and the estimated Arrhenius parameters are: E_a ~ 24 kcal mol^{-1} and A ~10^{10} $M^{-1}s^{-1}$.

For the gas-phase reaction of $SiCl_2$ with N_2O *i.e.* reaction IV.48, $\Delta H_{rxn.}$ is calculated to be –147 kcal mol^{-1} (*cf.* Appendix D) and an upper limit for the activation energy is estimated to be E_a ~4.3 kcal mol^{-1} (*cf.* Appendix E).

IV.2.5. Reaction with 1,3-Butadiene.

The $SiCl_2$ + 1,3-C_4H_6 reaction is also first order in silylene and butadiene concentration as shown by the linear plots of Figures III.28 to III.33. The bimolecular rate constant is:

$$k(SiCl_2 + 1,3\text{-}C_4H_6) = (5.4 \pm 0.3) \times 10^8\ M^{-1}s^{-1}$$

Butadiene and substituted butadienes have been used as trapping agents for $SiCl_2$ and other silylenes and the mechanism of these reactions has been explored by different workers.

Chernyshev *et al.* [123], from their qualitative studies, initially proposed that at 500°C $SiCl_2$ adds to butadienes to give silacyclopentenes in 90 – 95% yield, which appear to be formally 1,4-addition products. However, they also suggested that these products could also have been formed through initial 1,2-addition followed by the fast isomerization of the vinylsilacyclopropane intermediate:

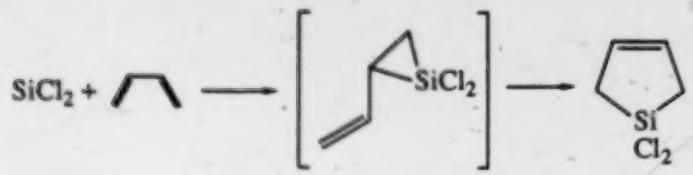

(IV.50)

Later on, based on the results of the thermal decomposition of 1,1-dichloro-1-silacyclo-3-pentene in the presence of 2,3-dimethyl-1,3-butadiene at 500°C, which generated butadiene and 1,1-dichloro-1-silacyclo-2,3-dimethyl-3-pentene and the fact that copyrolysis of the products regenerated the starting materials, they concluded that the addition of $SiCl_2$ to butadiene occurs *via* concerted 1,4-cycloaddition [76]:

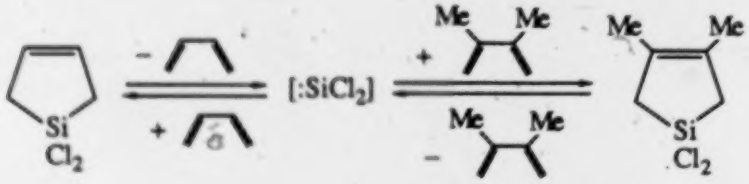

(IV.51)

From the pyrolysis of disilane (a SiH_2 precursor) in the presence of 1,4-substituted butadiene (hexa-2,4-diene) at 420°C, Gaspar and Hwang [159] observed the formation of both *cis*- and *trans*- isomers of the corresponding silacyclopentene in equal amounts (10%) and thus they suggested initial 1,2-addition (reaction IV.52) instead of 1,4-concerted addition (reaction IV.53) which would only give the *cis* product:

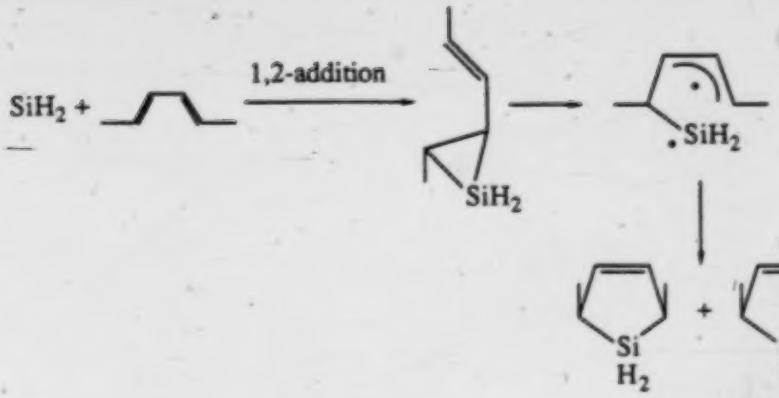

(IV.52)

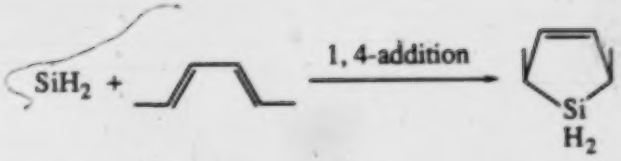

(IV.53)

Lei *et al.* [160] have also proposed initial 1,2-addition for the high-temperature reaction of $SiMe_2$ with 1,4-dimethyl-1,3-butadiene, followed by rearrangement of the vinylsilacyclopropane intermediate to yield the final products:

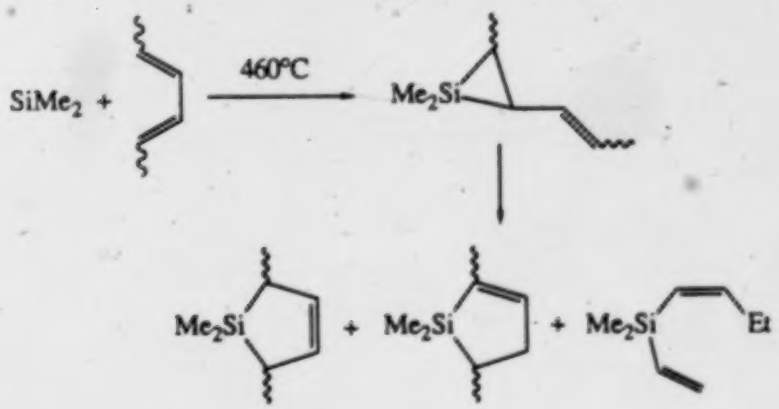

(IV.54)

Clark and Davidson [161], based on their qualitative studies of the reactions of SiMeX (X = H, Cl, Me) with 1,3-butadiene at 430° – 520°C, have also proposed 1,2-addition rather than 1,4-addition for these reactions:

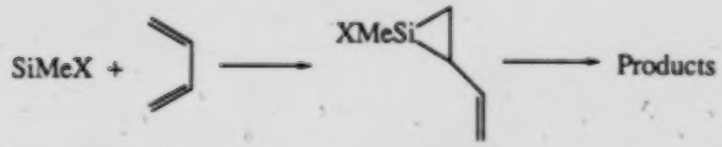

(IV.55)

Baggott *et al.* [162] studied the room-temperature gas-phase reaction between $SiMe_2$ and 1,3-butadiene using the time-resolved flash photolysis method. They observed a fast reaction ($k = (4.5 \pm 0.3) \times 10^9\ M^{-1}s^{-1}$) but were unable to detect

significant amounts of the expected 3,3-dimethyl-3-silacyclopentene product (which is known to form as a stable product from the same reaction under pyrolysis conditions at 370°C) even upon raising the temperature to 100°C. Thus they suggested that $SiMe_2$ reacts with 1,3-butadiene *via* initial 1,2-addition yielding vinylsilacyclopropane, which is either stable to rearrangement to the corresponding silacyclopentene at temperatures below 100°C or is lost *via* a different channel.

(IV.56)

From the above reports it is obvious that for the high-temperature (400 – 520°C) addition of silylenes to butadienes, the reaction mechanism is controversial since the products can be explained *via* either 1,2- or 1,4-addition. For the room temperature reaction, although only 1,2- addition has been proposed [162], the 1,4-addition route cannot be ruled out either since neither the silirane intermediate nor the final

silacyclopentene products could be isolated in the photolysis experiment of Baggott *et al.*

Ioffe *et al.* [163] have used the intermolecular orbital theory of interactions to examine the reaction of CCl_2, $SiCl_2$ and $GeCl_2$ with 1,3-butadiene and concluded that the probability of 1,4-addition increases on going from CCl_2 to $SiCl_2$ to $GeCl_2$.

Neither the value of the absolute rate constant for the $SiCl_2$ + 1,3-C_4H_6 reaction, nor the fact that $SiCl_2$ is an electrophilic species (see Section IV.3.2), make it possible to differentiate between 1,2- and 1,4-addition:

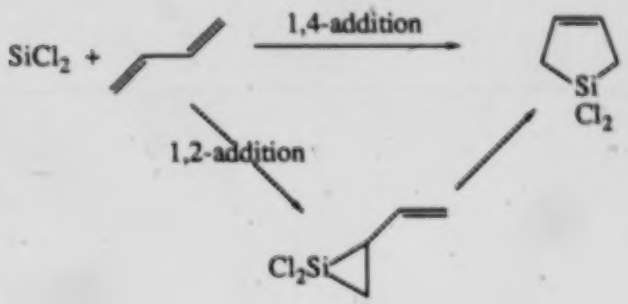

(IV.57)

Reaction IV.57 is calculated to be exothermic by 105 kcal mol^{-1} (*cf.* Appendix D) and an upper limit for its activation energy is estimated to be E_a ~3.8 kcal mol^{-1} (*cf.* Appendix E).

IV.3. Chemical Reactivities of the Ground State Singlet $SiCl_2$ and $SiBr_2$.

IV.3.1. Reactions with Inorganic Substrates.

Absolute rate constants of the room-temperature gas-phase reactions of $^1SiCl_2$ and $^1SiBr_2$ as obtained from the present study are compiled in Table IV.1 along with the available data on similar reactions of $^1SiH_2$, $^1SiF_2$, $^1CH_2$, $^1CCl_2$ and $^1CF_2$.

Toward O_2 and NO, both silylenes and carbenes follow a similar reactivity trend. The reactivity of MX_2 (M = Si, C) follow the order X = H > Cl > F, *i.e.* the reactivity of divalent species MX_2 decreases with increasing electronegativity of the substituent X. For carbenes it has been proposed [16] that the more electronegative substituents would increase its stability, and thus decrease its reactivity, through such canonical forms as:

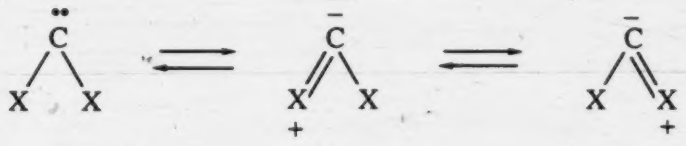

The same electronegativity effect also seems to be operative in SiX_2 (X = H, Cl) + NO and SiX_2 (X = Cl, F) + O_2 reactions. For SiX_2 (X = H, Cl) + O_2 reactions the rate constants are too similar to observe any electronegativity effect which may exist as in the cases of X = Cl, F. The reactivity of $SiBr_2$ is less than that of $SiCl_2$, contrary to that expected on the basis of the electronegativity effect. It should be noted, however, that the decrease in electronegativity between Cl and Br is very small (3.0 *vs* 2.8) as compared to that between Cl and F (3.0 *vs* 4.0) whereas the corresponding increase in atomic size between Cl and Br is twice as much as between Cl and F {F(9), Cl(17), Br(35)}. Since the electronegativities of Cl and Br are very similar, the increase in

Table IV.1. Absolute rate constants of reactions of divalent species MX_2 with various inorganic substrates.

Substrate	k, $M^{-1}s^{-1}$			
	SiH_2 [a]	$SiBr_2$ [b]	$SiCl_2$ [b]	SiF_2 [c]
O_2	$(4.6 \pm 0.6) \times 10^9$	$(5.6 \pm 0.4) \times 10^8$	$(3.4 \pm 0.2) \times 10^9$	$< 1.2 \times 10^4$
NO	$(1.0 \pm 0.1) \times 10^{10}$	$(2.8 \pm 0.4) \times 10^8$	$(1.6 \pm 0.1) \times 10^9$	
CO	$< 6 \times 10^7$		$(6.3 \pm 0.7) \times 10^8$	
N_2O			$(5.7 \pm 0.3) \times 10^8$	

Substrate	k, $M^{-1}s^{-1}$			
	$^1CH_2$ [d]	CBr_2	CCl_2 [e]	CF_2 [f]
O_2	4.5×10^{10}		$\leq 1.8 \times 10^6$	1.2×10^1
NO	9.6×10^{10}		1.8×10^8	
CO	2.9×10^{10}		3.0×10^7	
N_2O				

[a] Reference 46; [b] Present work; [c] Reference 68; [d] Reference 18; [e] Reference 34; [f] Reference 33.

molecular size of the silylene (*i.e.* the increased steric hindrance to the approaching reactive molecules) on going from Cl to Br may therefore be the dominating factor in determining the reactivity of $SiBr_2$ and thus may wholly or in part be responsible for the slower reactions of $SiBr_2$ than those of $SiCl_2$. On the other hand, for the reactivity of $SiCl_2$ *vs* SiF_2, the large difference in the electronegativities of Cl and F seems to be the dominant factor.

No absolute rate constant data for the reactions of CBr_2 are yet available for comparison. Although it has been reported [15] from qualitative studies that CBr_2 is less selective and thus more reactive than CCl_2 toward olefins, the chemistry involved in the reactions with olefins is different from that in the reactions with inorganic compounds, and it cannot be assumed, in the absence of any quantitative or qualitative data, that the reactivity of CBr_2, relative to other carbenes, towards inorganic species would follow the same trend as that towards olefins. A more comprehensive set of quantitative data on the reactions of MX_2 (M = Si, C; X = Cl, Br) with various substrates is required to establish the exact position of MBr_2 (M = Si, C) on the reactivity ladder $MH_2 > MCl_2 > MBr_2$ (?) $> MF_2$.

The reactions of SiH_2, $^1CH_2$ and CCl_2 are faster with NO than with O_2, whereas the present study has shown that the reactions of $SiCl_2$ and $SiBr_2$ with NO are about twice as slow as that with O_2. In the case of the $SiCl_2$ + NO reaction, as mentioned earlier, the formation of a volatile product from some dark reaction was observed. Since the extent of the dark reaction was not known, no correction was applied to accomodate the decrease in the NO concentration due to the occurrence of the dark reaction. Thus the NO concentration used in the calculation of $k(SiCl_2 + NO)$ could have been higher than the NO concentration actually present in the reaction

could have been higher than the NO concentration actually present in the reaction mixture. Therefore the reported value of $k(SiCl_2 + NO)$ might be a lower limit. A similar dark reaction might have been operative in case of $SiBr_2$-NO system.

From Table IV.1 it is seen that the reactivity of carbenes with O_2, NO and CO follows the trend $CH_2 >> CCl_2 >> CF_2$, as expected on the basis of increasing electronegativity of the halogen substituents. On the other hand, with the exception of the single reported rate constant for SiF_2, no clear trend can be discerned in the reactivities of silylenes.

Inspection of the data in Table IV.1 reveals the following trends:

$k(^1CH_2 + NO, CO) > k(CCl_2 + NO, CO)$;

$k(SiH_2 + NO) > k(SiCl_2 + NO)$;

however,

$k(SiH_2 + CO) < k(SiCl_2 + CO)$.

A possible explanation for the reverse trend in the reactivity of SiH_2 *vs* $SiCl_2$ compared to that of $^1CH_2$ *vs* CCl_2 toward CO could be provided by considering the following two observations.

First, the large difference between $k(SiH_2 + CO)$ and $k(^1CH_2 + CO)$ is significant and must be due to totally different reaction paths for these two reactions. The $^1CH_2$ + CO reaction leads to the formation of ground-state ketene $^1(CH_2=C=O)$, whereas for the SiH_2 + CO reactions, the theoretical calculations of Hamilton and Schaefer [50] have predicted the silaketene to be less stable than the Lewis acid-base type adduct $H_2Si\leftarrow CO$. Thus the SiH_2 + CO reaction path, unlike that of $^1CH_2$ + CO,

would not yield a silaketene product and therefore different rate constants can be expected for the two reactions. On the other hand for the reactions of SiH_2 and $^1CH_2$ with O_2 and NO, the formation of similar initial adducts has been proposed and their rate constants are similar as well.

The second point to be noted is the lower rate constant of the SiH_2 + CO reaction compared to that of the $SiCl_2$ + CO reaction for which an initial Lewis acid-base type adduct ($Cl_2Si\leftarrow CO$), similar to that predicted for the SiH_2 + CO reaction, is proposed to be the most probable mechanism. From qualitative investigations, the $Si(Mes)_2$ + CO reaction (Mes = mesityl) in a hydrocarbon matrix has been proposed [153] to yield an acid-base type adduct in a reversible manner. The lower rate constant reported by Chu *et al.* [46] for the SiH_2 + CO reaction could be due to the reversible formation of such an adduct at the low (5 Torr) total pressure used. It is important to note that Chu *et al.* [46] reported that the SiH_2 + O_2 and SiH_2 + NO reactions are slightly pressure dependent. Although these authors did not give many details of the SiH_2 + CO system, it is possible that this reaction is also pressure dependent. Thus at the 5 Torr total pressure used in their measurements, reversible decomposition of the initial weak acid-base type adduct ($H_2Si\leftarrow CO$) could compete with pressure stabilization and thus a slow reaction would be observed. On the other hand, for the $SiCl_2$ + CO reaction, irreversible formation of a $Cl_2Si\leftarrow CO$ adduct, analogous to the irreversible SiF_2CO adduct formation from the SiF_2 + CO reaction in a low-temperature matrix [67], is proposed. In the present study the total pressure used was 100 Torr, enough to stabilize the adduct and thus to reduce and perhaps eliminate the reverse decomposition of the adduct. Therefore the present rate constant value for the $SiCl_2$ + CO reaction is probably accurate and $k(SiH_2 + CO)$ should be re-evaluated at higher pressures.

Another trend worth noting is that the reactivity of $SiCl_2$ is higher than that of CCl_2 whereas that of SiH_2 is slightly lower than that of $^1CH_2$. The slightly higher reactivity of $^1CH_2$ compared with SiH_2 (except for the reaction with CO) could be due to the fact that all the reported rate constants for $^1CH_2$ reactions include the rate of its physical quenching to the ground state, $^3CH_2$, whereas in the case of SiH_2 there is no such physical quenching and the rate constant values are the rates of chemical reactions. Thus, after applying corrections for physical quenching to the overall $^1CH_2$ rate constants, the SiH_2 *vs* $^1CH_2$ reactivity might follow the same trend as that of $SiCl_2$ *vs* CCl_2 , *i.e.* $SiX_2 > CX_2$ (X = H, Cl), since the difference between $k(SiH_2)$ and $k(^1CH_2)$ is very small. The faster reactions of SiX_2 species compared to those of CX_2 toward O_2 and NO, could be due to the stronger Si—O bond compared to the C—O bond {D(C—O) = 84 kcal mol^{-1}; D(Si—O) is not known but the comparison of their double bond energies, *i.e.* D(Si=O) = 187 kcal mol^{-1} *vs* D(C=O) = 174 kcal mol^{-1}, indicates D(Si—O) to be larger than D(C—O)} since mechanisms involving initial adducts containing Si—O and C—O bonds have been proposed for the reactions of $^1CH_2$, SiH_2, $SiCl_2$ and $SiBr_2$ with O_2 and NO. No information is available on the mechanisms of CCl_2 reactions with these molecules but they could be expected to follow similar pathways involving adducts with C—O bonds, as has been proposed for the $CF_2 + O_2$ and $CF_2 + NO$ reactions [31 – 33].

For reaction with N_2O no comparison can be made at present due to the unavailabilty of kinetic data on the reactions of N_2O with any other divalent species.

IV.3.2. Reactions with Unsaturated Hydrocarbons.

The absolute rate constant for the room-temperature gas-phase reaction of $SiCl_2$ with 1,3-butadiene along with previously reported data for reactions with other olefins and acetylenes are presented in Table IV.2. Data for SiH_2 and $SiMe_2$ are also listed.

Among the olefins, the $SiCl_2$ rate constants follow the order $C_2H_4 < C_3H_6 <$ t-$C_4H_8 <$ 1,3-C_4H_6. Thus $SiCl_2$ acts as an electrophile towards addition to olefins. The rate constants for the SiH_2 and $SiMe_2$ reactions also show a trend similar to that of $SiCl_2$. The reactivity of $SiCl_2$ is lower than that of SiH_2, which is consistent with the electronegativity effect of the halogen substituent. The selectivity of $SiCl_2$ is about twice as high as that of SiH_2. This parallels the selectivity of CH_2 *vs* CCl_2, proposed on the basis of qualitative measurements. Only kinetic data available on reactivity of carbenes towards unsaturated hydrocarbons is that for the reactions of $^1CH_2$ with C_2H_2, C_2H_4, C_3H_6, *i*-C_4H_8 and 1,3-C_4H_6 [17]. All these reactions are very fast (rate constants are of the order of $10^{11}\ M^{-1}s^{-1}$, an order of magnitude higher than those of SiH_2 reactions) and shows almost no selectivity among olefins. The faster reactions of $^1CH_2$ than those of SiH_2 with unsaturated hydrocarbons could be due to the formation of stable cylcopropane from the reactions of $^1CH_2$, whereas the corresponding silacyclopropanes have not yet been isolated. The almost similar reactivity of SiH_2 and $SiMe_2$ could be due to the almost similar polarities of Si—H and Si—CH_3 bonds. Both H and CH_3, when bonded to Si, act as weak electronegative substituents.

Table IV.2. Absolute rate constants of the reactions of divalent species MX_2 with various unsaturated hydrocarbons.

Substrate	k, $M^{-1}s^{-1}$		
	$SiCl_2$ [a]	SiH_2 [b]	$SiMe_2$ [c]
C_2H_4	$(7.8 \pm 2.0) \times 10^7$	$(3.2 \pm 0.3) \times 10^{10}$	$(1.3 \pm 0.7) \times 10^{10}$
C_3H_6	$(2.3 \pm 0.6) \times 10^8$	$(7.2 \pm 0.6) \times 10^{10}$	$(2.2 \pm 0.2) \times 10^{10}$
t-C_4H_8	$(3.1 \pm 0.8) \times 10^8$	—	$(2.7 \pm 0.1) \times 10^{10}$
1,3-C_4H_6	$(5.4 \pm 0.3) \times 10^8$ [d]	$(1.1 \pm 0.1) \times 10^{11}$	$(4.5 \pm 0.3) \times 10^{10}$
C_2H_2	$(4.3 \pm 1.1) \times 10^7$	$(5.9 \pm 0.7) \times 10^{10}$	$(2.8 \pm 0.1) \times 10^{10}$
1-C_4H_6	$(7.9 \pm 1.9) \times 10^8$	—	—

[a] Reference 125.

[b] Reference 45.

[c] Reference 162.

[d] Present work.

SUMMARY AND CONCLUSIONS

Dihalosilylenes are important from the technical as well as chemical point of view. Thus, $SiCl_2$ has been found to play an important role in the chemical vapor deposition (CVD) of thin Si films, in the growth of epitaxial Si films on which integrated circuits are fabricated, and it is also one of the products of the etching of Si surfaces by Cl_2 gas and chlorine-containing compounds. $SiBr_2$ is also anticipated to be an intermediate of the CVD and etching of Si surfaces when bromine or bromine-containing Si compounds are used for etching or CVD.

The fabrication of integrated circuits is a key process in the fast-growing micro and submicro electronic industries.

In both CVD and chemical etching a detailed knowledge of the chemical processes involved is essential in the control of the technological processes and in the developement of new improved technologies.

From the chemical point of view $SiCl_2$ is also important in the synthesis of new novel organosilicon compounds. Qualitative investigations of the reactions of thermally-generated $SiCl_2$ have shown that, like carbenes, $SiCl_2$ is capable of insertion into various bonds such as Si—Cl, Si—H, C—H, O—H, O—C, C—Cl, B—Cl, P—Cl etc. and, addition, to the double and triple bonds of unsaturated hydrocarbons. However, quantitative data on the reactions of $SiCl_2$ are scarce and none have been reported for the reactions of $SiBr_2$. Recently, absolute rate constants of $SiCl_2$ reactions, in the gas phase, with a set of unsaturated hydrocarbons have been reported. On the other hand no quantitative information on its reactions with inorganic substances like

O_2, NO, CO or N_2O, had been available. On the reactions of $SiBr_2$, as mentioned before, no data whatsoever had been reported prior to the present study.

The present research was, therefore, undertaken in order to obtain quantitative data on the reactions of SiX_2 (X = Cl, Br) with various inorganic substrates and to probe into their mechanisms.

Absolute rate constants of the room-temperature gas-phase reactions of $SiCl_2$ with O_2, NO, CO, N_2O and 1,3-butadiene, and those of $SiBr_2$ with O_2 and NO, were measured using the flash photolysis-kinetic absorption spectroscopic technique. This technique employs a high energy (2900J) light flash to photolyze the silylene precursor, thus generating a high initial concentration of the silylenes SiX_2 (X = Cl, Br), whose absorption spectra were recorded at various times during their decay. These absorption spectra were used to monitor the SiX_2 concentrations during their reactions with different substrates.

All the reactions investigated were found to follow second-order kinetics — first-order in SiX_2 and first-order in substrate concentration, and proceeded at moderate to high velocity. The results provide the first and the only set of absolute rate constants for the (gas-phase room-temperature) reactions of $SiCl_2$ and $SiBr_2$ with inorganic molecules and 1,3-butadiene. Similar data on the reactions of dihalocarbenes CX_2 (X = Cl, Br), whose spectra have been known for many years and which are much easier to handle than silylenes, are very limited. Absolute rate constants for the gas-phase room-temperature reactions of CCl_2 with O_2, NO and CO have been reported, whereas none are available for the reactions of CBr_2. Therefore, from the kinetic point of view, knowledge of chemical reactivities of $SiCl_2$ and $SiBr_2$, whose spectra have only recently been discovered, is a step ahead of that of their carbene analogs.

On the basis of the present rate constant measurements and the other available reports on the mechanisms of similar reactions of other Si and C divalent species, silyl and alkyl radicals, mechanisms have been proposed for the reactions of SiX_2 with O_2, NO, CO and N_2O, which involve the following primary steps:

$$SiX_2 + O_2 \longrightarrow X_2SiOO \qquad (X = Cl, Br)$$

$$SiX_2 + NO \longrightarrow X_2Si\begin{matrix}O\\|\\N\end{matrix} \qquad (X = Cl, Br)$$

$$SiCl_2 + CO \longrightarrow Cl_2Si{\leftarrow}CO$$

$$SiCl_2 + N_2O \longrightarrow Cl_2SiO + N_2$$

No product analyses were carried out in the present study. However, for the case of the $SiCl_2$ + NO reaction, additional support for the proposed mechanism is provided by recent molecular orbital studies. $\Delta H^{\circ}_{rxn.}$ values for the overall reactions have been calculated which show that all the proposed schemes are exothermic, *i.e.* energetically feasible. Using the present rate constant data and the gas-kinetic collision frequencies upper limits for the Arrhenius parameters of all the primary reactions have been estimated. All these reactions feature a slight activation energy barrier (3 – 5 kcal mol^{-1}).

Based on the present kinetic measurements, a comparison of the reactivities of $SiCl_2$ and $SiBr_2$ with those of SiH_2, SiF_2 and carbenes was made in order to see whether dihalosilylenes follow a trend similar to the one proposed for carbenes. From qualitative work it has been suggested that the reactivity of carbenes towards unsaturated hydrocarbons increases in the order $CF_2 < CCl_2 < CBr_2 < CH_2$, *i.e.* the reactivity decreases with increasing electronegativity of the halogen substituents. However, there

are not enough quantitative data available to support this postulate. The very limited quantitative data thus far reported on the reactions of carbenes with inorganic substrates show that $^1CH_2$ reacts much faster than CCl_2 with O_2, NO and CO. CF_2 reacts very slowly with O_2. Among silylenes, SiF_2, like CF_2, is almost inert towards O_2, and, SiH_2 and $SiCl_2$ are about equally reactive ($k \sim 10^9\ M^{-1}s^{-1}$). For reactions with NO, SiH_2 and $SiCl_2$ follow the same reactivity trend as that of the corresponding carbenes, *i.e.* $k(SiH_2) > k(SiCl_2)$. Towards CO, however, the SiH_2 *vs* $SiCl_2$ reactivity shows a trend opposite to that of $^1CH_2$ *vs* CCl_2 *i.e.* $k(SiH_2) < k(SiCl_2)$. This may be attributed to the reversibility of the postulated initial Lewis acid-base type $H_2Si{\leftarrow}CO$ adduct formed in the SiH_2 reaction. Such reversible decomposition of the initial adduct could be a competetive route for its disappearence at the low total pressure (5 Torr) employed in the rate measurements. On the other hand, the similar adduct formed from $SiCl_2$ reaction ($Cl_2Si{\leftarrow}CO$) is proposed to be irreversible since at the high total pressure (100 Torr) used in the present study, the initial adduct would be collisionally stabilized and the reverse decomposition, if any, would be suppressed. Thus, the rate constant of the $SiCl_2$ + CO reaction should be more reliable and the SiH_2 + CO reaction should be reinvestigated at higher pressures.

The reactivity of $SiBr_2$ is found to be lower than that of $SiCl_2$, which is the opposite to that expected on the basis of the electronegativities of the substituents. Since no comparable data for the reactions of CBr_2 are available, it is not known whether the reactivity of CBr_2 *vs* CCl_2 towards inorganic substrates follows the same trend as that reported for their reactions with unsaturated hydrocarbons. The lower reactivity of $SiBr_2$ may be a consequence of steric hindrance, due to the increased size of the bromine substituents, to the approaching substrate molecules.

The faster rates of the reactions of $SiCl_2$ with O_2 and NO as compared to those of CCl_2 are attributed to the stronger Si—O, than C—O bonds (the reactions of $SiCl_2$ with O_2 and NO are proposed to proceed *via* initial adducts containing Si—O bonds). The mechanisms of the reactions of CCl_2 with O_2 and NO are not yet known but they could be expected to involve adducts containing C—O bonds, as has been proposed for the $CF_2 + O_2$ and CF_2 + NO reactions. The reactions of SiH_2 with O_2 and NO, on the other hand, are slightly slower than those involving $^1CH_2$. This could be due to the fact that the rate measurements for the $^1CH_2$ reactions may also contain a physical quenching component.

Towards unsaturated hydrocarbons, $SiCl_2$ exhibits an electrophilic nature like other silylenes, SiH_2 and $SiMe_2$, and dihalocarbenes. For its reactions with olefins the rate constant increases in the order $C_2H_4 < C_3H_6 < t\text{-}C_4H_8 < 1,3\text{-}C_4H_6$. The reactions of $SiCl_2$ with unsaturated hydrocarbons are slower than those of SiH_2, as expected on the basis of the high electronegativity of the halogen substituent and the consequent resonance stabilization of $SiCl_2$. Toward olefins, $SiCl_2$ is twice as selective as SiH_2, which parallels the trend in the reactivity of CCl_2 *vs* CH_2, observed in qualitative studies.

Thus, from these comparisons, some trends in the reactivities of silylenes and carbenes have been delineated. However, no extended meaningful correlations could be formulated at this stage due to the lack of, or very limited data available, on other silylene and carbene reactions. More quantitative data on the reactions of both silylenes and carbenes with various substrates is desired in order to infer more significant trends in their reactivities and to deduce any correlation between them. In addition, qualitative work on all the reactions examined in the present study would facilitate the establishment of the mechanism of these reactions.

REFERENCES

1. "Carbene Chemistry" W. Kirmse, vol.1, 2nd ed., Academic press, New York, 1971; "Carbenes" vol.2, eds. M. Jones, Jr. and R.A. Moss, Wiley, New York, 1975; R.A. Moss and M. Jones, Jr., in Reactive Intermediates, vol.3, eds. M. Jones, Jr.; A.H. Laufer, Rev. Chem. Intermediates, 4 (1981) 225 and R.A. Moss, Wiley, New York (1985) p.45.

2. F.W. Kirkbride and R.G.W. Norrish, J. Chem. Soc., Part I (1933) 119.

3. R.G.W. Norrish, H.G. Crone and O. Saltmarsh, J. Chem. Soc., Part II (1933) 1533.

4. G. Herzberg and J. Shoosmith, Nature, 183 (1959) 1801.

5. P.P. Gaspar and G.S. Hammond, in Carbenes, vol.2, eds. R.A. Moss and M. Jones, Jr., Wiley, New York (1975) p.207.

6. G. Herzberg and J.W.C. Johns, J. Chem. Phys., 54 (1971) 2276.

7. D.G. Leopold, K.K. Murray and W.C. Lineberger, J. Chem. Phys., 81 (1984) 1048.; D.G. Leopold, K.K. Murray, A.E.S. Miller and W.C. Lineberger, J. Chem. Phys., 83 (1985) 4849.; P.R. Bunker and T.J. Sears, J. Chem. Phys., 83 (1985) 4866.; P.R. Bunker, P. Jensen, W.P. Kraemer and R. Beardsworth, J. Chem. Phys., 85 (1986) 3724.

8. E.A. Carter and W.A. Goddard III, J. Chem. Phys., 88 (1988) 1752.

9. J.F. Harrison, R.C. Liedtke and J.F. Liebman, J. Am. Chem. Soc., 101 (1979) 7162.

10. C.W. Bauschlicher, Jr., J. Am. Chem. Soc., 102 (1980) 5492.

11. P.C. Jordan, J. Chem. Phys., 44 (1966) 3400.

12. W.H. Kirchoff, D.R. Lide and F.X. Powell, J. Mol. Spectrosc., 47 (1973) 491.; H. Shoji, T. Tanka and E. Hirota, J. Mol. Spectrosc., 47 (1973) 268.; H. Takeo, R.F. Curl, Jr. and P.W. Wilson, J. Mol. Spectrosc., 38 (1971) 464.

13. V.A. Svyatkin, A.K. Maltsev and O.M. Nefedov, Izv. Akad. Nauk SSSR, Ser. Khim., No.10 (1977) 2236.

14. R.C. Ivey, P.D. Schulze, T.L. Leggett and D.A. Kohl, J. Chem. Phys., 60 (1974) 3174.

15. R.A.Moss, Accounts Chem. Res., 13 (1980) 58.

16. P.S. Skell and A.Y. Garner, J. Am. Chem. Soc., 78 (1956) 5430.

17. W. Hack, M. Koch, R. Wagner and H.Gg. Wagner, Ber. Bunsenges. Phys. Chem., 93 (1989) 165.

18. A.O. Langford, H. Petek and C.B. Moore, J. Chem. Phys., 78 (1983) 6650.

19. R.A. Moss, Accounts Chem. Res., 22 (1989) 15.

20. A.H. Laufer and A.M. Bass, J. Phys. Chem., 78 (1974) 1344.

21. M.J. Pilling and J.A. Robertson, J. Chem. Soc. Farad. Trans. I, 73 (1977) 968.

22. C. Vinckier and W. Debruyn, J. Phys. Chem., 83 (1979) 2057.

23. D.C. Darwin, A.T. Young, H.S. Johnston and C.B. Moore, J. Phys. Chem., 93 (1989) 1074.

24. V. Seidler, F. Temps, H.Gg. Wagner and M.Wolf, J. Phys. Chem., 93 (1989) 1070.

25. T. Bohland, F. Temps and H.Gg. Wagner, Ber. Bunsenges. Phys. Chem., 88 (1984) 455.

26. R.L. Russell and F.S. Rowland, J. Am. Chem. Soc., 90 (1968) 1671.

27. D.C. Montague and F.S. Rowland, J. Am. Chem. Soc., 93 (1971) 5381.

28. D.S.Y. Hsu and M.C. Lin, Int. J. Chem. Kinet., 9 (1977) 507.

29. M.N.R. Ashfold, M.A. Fullstone, G. Hancock and G.W. Ketley, Chem. Phys., 55 (1981) 245.

30. F.S. Rowland, P.S.-T. Lee, D.C. Montague and R.L. Russell, Farad. Disc. Chem. Soc., 53 (1972) 111.

31. A.P. Modica, J. Chem. Phys., 46 (1967) 3663.

32. T.L. Burks and M.C. Lin, J. Chem. Phys., 64 (1976) 4235.

33. F.W. Dalby, J. Chem. Phys., 41 (1964) 2297.

34. J.J. Tiee, F.B. Wampler and W.W. Rice, Jr., Chem. Phys. Lett., 73 (1980) 519.

35. P.P. Gaspar and J. Herold, in Carbene Chemistry, vol.1, 2nd ed., W. Kirmse, Academic press, Wiley, New York (1971) p.504.

36. P.P. Gaspar, in Reactive Intermediates, vol.1, eds. M. Jones, Jr. and R.A. Moss, Wiley, New York (1978) p.229.

37. P.P. Gaspar, in Reactive Intermediates, vol.2, eds. M. Jones, Jr. and R.A. Moss, Wiley, New York (1981) p.335.

38. Y.-N. Tang, in Reactive Intermediates, vol.2, ed. R.A. Abramovitch, Plenum press, New York (1982) p.297.

39. P.P. Gaspar, in Reactive Intermediates, vol.3, eds. M. Jones, Jr. and R.A. Moss, Wiley, New York (1985) p.333.

40. I. Dubois, G. Herzberg and R.D. Varma, J. Chem. Phys., 47 (1967) 4262.

41. O.F. Zeck, Y.Y. Su, G.P. Gennaro and Y.-N. Tang, J. Am. Chem. Soc., 96 (1974) 5967.

42. G. Herzberg and J.W.C. Johns, Proc. Roy. Soc. A, 295 (1966) 107.

43. W. Hack, H.Gg. Wagner and A. Wilms, Ber. Bunsenges. Phys. Chem., 92 (1988) 620.

44. J.M. Jasinski and J.O. Chu, J. Chem. Phys., 88 (1988) 1678.

45. J.O. Chu, D.B. Beach and J.M. Jasinski, J. Phys. Chem., 91 (1987) 5340.

46. J.O. Chu, D.B. Beach, R.D. Estes and J.M. Jasinski, Chem. Phys. Lett., 143 (1988) 135.

47. G. Inoue and M. Suzuki, Chem. Phys. Lett., 122 (1985) 361.

48. R. Walsh, Accounts Chem. Res., 14 (1981) 246.

49. S. Yamabe and K. Morokuma, J. Am. Chem. Soc., 100 (1978) 7551.

50. T.P. Hamilton and H.F. Schaefer III, J. Chem. Phys., 90 (1989) 1031.

51. S. Koda, Chem. Phys. Lett., 55 (1978) 353.

52. A. Kasdan, E. Herbst and W.C. Lineberger, J. Chem. Phys., 62 (1975) 541.

53. D.R. Rao, J. Mol. Spectrosc., 34 (1970) 284.

54. M.E. Colvin, R.S. Grev, H.F. Schaefer III and J. Bicerano, Chem. Phys. Lett., 99 (1983) 399.

55. J.M. Coffin, T.P. Hamilton, P. Pulay and I. Hargittai, Private communication.

56. J.L. Margrave and P.W. Wilson, Accounts Chem. Res., 4 (1971) 145.

57. C.-S. Liu, J.L. Margrave, J.C. Thompson and P.L. Timms, Can. J. Chem., 50 (1972) 459.

58. C.-S. Liu, J.L. Margrave and J.C. Thompson, Can. J. Chem., 50 (1972) 465.

59. J.L. Margrave and D.L. Perry, Inorg. Chem., 16 (1977) 1820.

60. D.L. Perry and J.L. Margrave, J. Chem. Ed., 53 (1976) 696.

61. D. Seyferth and D.P. Duncan, J. Am. Chem. Soc., 100 (1978) 7734.

62. J.C. Thompson, A.P.G. Wright and W.J. Reynolds, J. Am. Chem. Soc., 101 (1979) 2236.

63. T.-L. Hwang and C.-S. Liu, J. Am. Chem. Soc., 102 (1980) 385.

64. C.-S. Liu and T.-L. Hwang, in Advan. Inorg. Chem. Radiochem., vol.29, eds. H.J. Emeleus and A.G. Sharpe, Academic press, New York (1985) p.1.

65. O.F. Zeck, Y.Y. Su, G.P. Gennaro and Y.-N. Tang, J. Am. Chem. Soc., 98 (1976) 3474.

66. E.E. Siefert, S.D. Witt and Y.-N. Tang, J. Chem. Soc. Chem. Commun. (1981) 217.

67. J.M. Bassler, P.L. Timms and J.L. Margrave, Inorg. Chem., 5 (1966) 729.

68. A. Freedman, K.E. McCurdy, J. Wormhoudt and P.P. Gaspar, Chem. Phys. Lett., 142 (1987) 255.

69. C. Sosa and H.B. Schlegel, J. Am. Chem. Soc. , 106 (1984) 5847.

70. W.H. Atwell and D.R. Weyenberg, Angew. Chem. Int. Ed., 8 (1969) 469, and references therein.

71. W.H. Atwell and D.R. Weyenberg, Intra-science Chem. Rept., 7 (1973) 139.

72. E.A. Chernyshev, N.G. Komalenkova and S.A. Bashkirova, Zh. Obshch. Khim., 41 (1971) 1175.

73. A.M. Doncaster and R. Walsh, J. Chem. Soc. Farad. I, 76 (1980) 272.

74. N.D. Kagramanov, A.K. Maltsev, M.Y. Dubinskii and O.M. Nefedov, Izv. Akad. Nauk. SSSR, Ser. Khim. No.3 (1983) 536.

75. I. Hargittai, G. Schultz, J. Tremmel, N.D. Kagramanov, A.K. Maltsev and O.M. Nefedov, J. Am. Chem. Soc., 105 (1983) 2895.

76. E.A. Chernyshev, N.G. Komalenkova and S.A. Bashkirova, J. Organomet. Chem., 271 (1984) 129, and references therein.

77. L.E. Guselnikov, V.M. Sokolova, E.A. Volnina, Z.A. Kerzina, N.S. Nametkin, N.G. Komalenkova, S.A. Bashkirova and E.A. Chernyshev, Dokl. Akad. Nauk. SSSR, 260 (1981) 348.

78. E.A. Chernyshev, N.G. Komalenkova, D.A. Zagorets and M.Y. Kelman, Zh. Obshch. Khim., 57 (1987) 2732.

79. B.P. Ruzsicska, A. Jodhan, I. Safarik, O.P. Strausz and T.N. Bell, Chem. Phys. Lett., 113 (1985) 67.

80. N. Washida, Y. Matsumi, T. Hayashi, T. Ibuki, A. Hiraya and K. Shobatake, J. Chem. Phys., 83 (1985) 2769.

81. R.C. Sausa and A.M. Ronn, Chem. Phys., 96 (1985) 183.

82. M. Suzuki, N. Washida and G. Inoue, Chem. Phys. Lett., 131 (1986) 24.

83. B.P. Ruzsicska, A. Jodhan, I. Safarik, O.P. Strausz and T.N. Bell, Chem. Phys. Lett., 139 (1987) 72.

84. R.J. Madix and J.A. Schwarz, Surf. Sci., 24 (1971) 264.

85. V.N. Bochkarev, A.N. Polivanov, T.F. Slyusarenko, A.A. Bernadskii, N.N. Silkina and B.N. Klimantov, Zh. Obs. Khim., 51 (1981) 824.

86. D. Sameith, J.P. Monch, H.-J. Tiller and K. Schade, Chem. Phys. Lett., 128 (1986) 483.

87. H. Bock, B. Solouki and G. Maier, Angew. Chem. Int. Ed., 24 (1985) 205.

88. R.K. Asundi, M. Karim and R. Samuel, Proc. Phys. Soc. London, 50 (1938) 581.

89. H. Burger and R. Eujen, in Topics in Current Chemistry, vol.50, ed. F.L. Boschke, Springer, Berlin (1974) p.1.

90. K. Weiland and M. Heise, Angew. Chem., 63 (1951) 438.

91. D.E. Milligan and M.E. Jacox, J. Chem. Phys., 49 (1968) 1938.

92. G. Maass, R.H. Hauge and J.L. Margrave, Z. Anorg. Allg. Chem., 392 (1975) 295.

93. R. Cornet and I. Dubois, J. Phys, B: Atom. Molec. Phys., 10 (1977) L69.

94. H. Remy, Treatise on Inorganic Chemistry, Elsevier, Amsterdam, 1956.

95. S. Ghosh, S. Nagraj and R.D. Verma, Can. J. Phys., 54 (1976) 695.

96. B. Rosen, Tables Internationales de Constantes Selectionnées, Pergamon press, Oxford, 1970.

97. R.D. Verma and S.R. Singhal, Can. J. Phys., 53 (1975) 411.

98. R.D. Verma, Can. J. Phys., 48 (1970) 2391.

99. R.D. Verma and H.P. Broida, Can. J. Phys., 48 (1970) 2991.

100. R.K. Gosavi and O.P. Strausz, Chem. Phys. Lett., 123 (1986) 65.

101. T.-K. Ha, M.T. NGuyen, M.C. Kerins and J. Fitzpatrick, Chem. Phys., 103 (1986) 243.

102. L.A. Kuznetsova and Y.Y. Kuzyakov, J. Appl. Spectrosc., 10 (1969) 278.

103. K. B. Rao and P.B.V. Haranath, J. Phys.B: Atom. Molec. Phys. ser.2, 2 (1969) 1381.

104. G. Bosser, J. Lebreton and J. Rostas, J. Chim. Phys., 78 (1981) 787.

105. V.E. Bondybey and J.H. English, J. Mol. Spectrosc., 79 (1980) 416.

106. R.H. Hauge, V.M. Khanna and J.L. Margrave, J. Mol. Spectrosc., 27 (1968) 143.

107. J.W. Hastie, R.H. Hauge and J.L. Margrave, J. Mol. Spectrosc., 29 (1969)152.

108. R.H. Hauge, J.W. Hastie and J.L. Margrave, J. Phys. Chem., 72 (1968) 350.

109. J. Maya, J. Chem. Phys., 67 (1977) 4976.

110. M. Tanimoto, H. Takeo and C. Matsumura, Proc. 49th Spring Conf. Chem. Soc. Jpn., No.1 (1984) 6.

111. JANAF Thermochemical Tables, 1982 Supplement, J. Phys. Chem. Ref. Data 11 (1982) 695.

112. H. Schaefer, H. Bruderseek and B. Morcher, Z. Anorg. Chem., 352 (1967) 122.

113. M. Farber and R.D. Srivastave, J. Chem. Soc. Farad. Trans. I, 73 (1977) 1672.

114. J.B. Pedley and B.S. Iseard, "CATCH Tables" Univ. of Sussex, 1972 and 1976 (available from NTIS, No. AD-773-468).

115. P. Ho, M.E. Coltrin, J.S. Binkley and C.F. Melius, J. Phys. Chem., 89 (1985) 4647.

116. E. Wolf and C. Herbst, Z. Anorg. Allg. Chem., 317 (1966) 113.

117. M. Farber and R.D. Srivastava, High Temp. Sci., 12 (1980) 21.

118. R. Walsh, J. Chem. Soc. Farad. Trans. I, 79 (1983) 2233.

119. P.L. Timms, Inorg. Chem., 7 (1968) 387.

120. E.A. Chernyshev, N.G. Komalenkova and S.A. Bashkirova, Zh. Obshch. Khim., 46 (1976) 1286.

121. E.A. Chernyshev, N.G. Komalenkova, T.A. Klochkova, S.A. Shchepinov and A.M. Mosin, Zh. Obshch. Khim., 41 (1971) 122.

122. V.I. Zubkov, M.V. Tikhomirov, K.A. Andrianov and S.A. Golubustov, Dokl. Akad. Nauk. SSSR, 188 (1969) 594.

123. E.A. Chernyshev, N.G. Komalenkova, S.A. Bashkirova and V.V. Sokolov, Zh. Obshch. Khim., 48 (1978) 830.

124. E.A. Chernyshev, N.G. Komalekova and S.A. Bashkirova, Dokl. Akad. Nauk. SSSR, 205 (1972) 868.

125. I. Safarik, B.P. Ruzsicska, A. Jodhan, O.P. Strausz and T.N. Bell, Chem. Phys. Lett., 113 (1985) 71.

126. J.E. Smith, Jr. and T.O. Sedgwick, Thin Solid Films, 40 (1977) 1.

127. T.O. Sedgwick, G.V. Arbach and R. Ghez, Proc. Electrochem. Soc. (Proc. 6th Int. Conf. Chem. Vapor Deposition), 77-5 (1977) 79.

128. T.O. Sedgwick and G.V. Arbach, NBS Special Publ. 561, Proc. 10th Mater. Res. Symp. on Characterization of Vapors and Gases, Gaithersburg, Maryland (1979) p.885.

129. V.S. Ban, Proc. Electrochem. Soc. (Proc. 6th Int. Conf. Chem. Vapor Deposition), 77-5 (1977) 66.

130. J.-I. Nishizawa and M. Saito, Proc. 8th Intn. Conf. Chem. Vapor Deposition, The Electrochem. Soc. Inc., Pennington, NJ, (1981) p.317.

131. Y.-L. Li, Z.-J. Zhang, Q.-K. Zheng, Z.-K. Jin, Z.-K. Wu and Q.-Z. Qin, Appl. Phys. Lett., 53 (1988) 1955.

132. R.G.W. Norrish and G. Porter, Nature, London, 164 (1949) 658.

133. R. Gooden, Inorg. Chem., 22 (1983) 2272.

134. H. Niki, P.D. Maker, C.M. Savage, L.P. Breitenbach and M.D. Hurley, J. Phys. Chem., 89 (1985) 3725.

135. C.D. Eley, M.C.A. Rowe and R. Walsh, Chem. Phys. Lett., 126 (1986) 153.

136. P.P. Gaspar, D. Holten, S. Konieczny and J.Y. Corey, Accounts Chem. Res., 20 (1987) 329.

137. T. Akasaka, S. Nagase, A. Yabe and W. Ando, J. Am. Chem. Soc., 110 (1988) 6270.

138. H. Schnockel, Z. Anorg. Allg. Chem., 460 (1987) 37.

139. A.V. Golovkin, N.A. Mudrova, T.L. Krasnova, L.V. Serebrennikov, V.S. Nikitin and E.A. Chernyshev, Zh. Obshch. Khim., 55 (1985) 2802.

140. H. Rheinboldt and W. Wisfeld, Ann. Chem., 517 (1935) 197.

141. W.C. Schumb and C.H. Klein, J. Am. Chem. Soc., 59 (1937) 261.

142. H.J. Emeleus and A.J.E. Welch, J. Chem. Soc., (1939) 1928.

143. D.L. Wood, J.B. Macchesney and J.P. Luongo, J. Mater. Sci., 13 (1978) 1761.

144. T.L. Krasnova, N.A. Mudrova, V.N. Bochkarev and A.V. Kisin, Zh. Obshch. Khim., 55 (1985) 1528.

145. F.W. Lampe, Spectrochim. Acta, 43A (1987) 257.

146. R.K. Gosavi and O.P. Strausz, to be published.

147. E. Kamaratos and F.W. Lampe, J. Phys. Chem., 74 (1970) 2267.

148. M.A. Nay, G.N.C. Woodall, O.P. Strausz and H.E. Gunning, J. Am. Chem. Soc., 87 (1965) 179.

149. R. Varma, P. Orlander and A.K. Ray, J. Inorg. Nucl. Chem., 37 (1975) 1797.

150. C.A. Arrington, J.T. Petty, S.E. Payne and W.C.K. Haskins, J. Am. Chem. Soc., 110 (1988) 6240.

151.(a) J.J.P. Stewart, QCPE no. 455 (Version 4.0).

(b) M.J. Frisch, J.S. Binkley, H.B. Schlegel, K. Ragahavachari, C.F. Melius, R.L. Martin, J.J.P. Stewart, F.W. Bobrowicz, C.M. Rohlfing, L.R. Kahn, D.J. Defrees, R. Seeger, R.A. Whiteside, D.J. Fox, E.M. Fleuder and J.A. Pople, GAUSSIAN 86, Carnegie-Mellon Quantum Chemistry Publishing Unit, Pittsburgh, PA, 1984.

152. M.-A. Pearsall and R. West, J. Am. Chem. Soc., 110 (1988) 7228.

153. M.-A. Pearsall and R. West, Abstracts, XXI Organosilicon Symp., Montreal, Canada, (1988) P32.

154. R. West, M.J. Fink and J. Michl, Science, 214 (1981) 1343.

155. M. Torres, J. Ribo, A. Clement and O.P. Strausz, Nouv. J. Chim., 5 (1981) 351.

156. C.A. Arrington, R. West and J. Michl, J. Am. Chem. Soc., 105 (1983) 6176.

157. I.R. Slagle, J.R. Bernhardt and D. Gutman, Chem. Phys. Lett., 149 (1988) 180.

158. T.N. Bell and K.O. Kutschke, Can. J. Chem., 42 (1964) 2713.

159. P.P. Gaspar and R.-J. Hwang, J. Am. Chem. Soc., 96 (1974) 6198.

160. D. Lei, R.-J. Hwang and P.P. Gaspar, J.Organomet. Chem., 271 (1984) 1.

161. M.P. Clarke and I.M.T. Davidson, J. Chem. Soc. Commun., (1988) 241.

162. J.E. Baggott, M.A. Blitz, H.M. Frey, P.D. Lightfoot and R. Walsh, J. Chem. Soc. Farad. Trans. II, 84 (1988) 515.

163. A.I. Ioffe, L.I. Korzhenevich, S.P. Kolesnikov and O.M. Nefedov, Izv. Akad. Nauk SSSR, Ser. Khimi., No.2 (1976) 343.

Appendix A.

Relationship Between Concentration and Absorption Peak Height:

Shape of a typical SiX_2 absorption band is shown in Figure A.1.

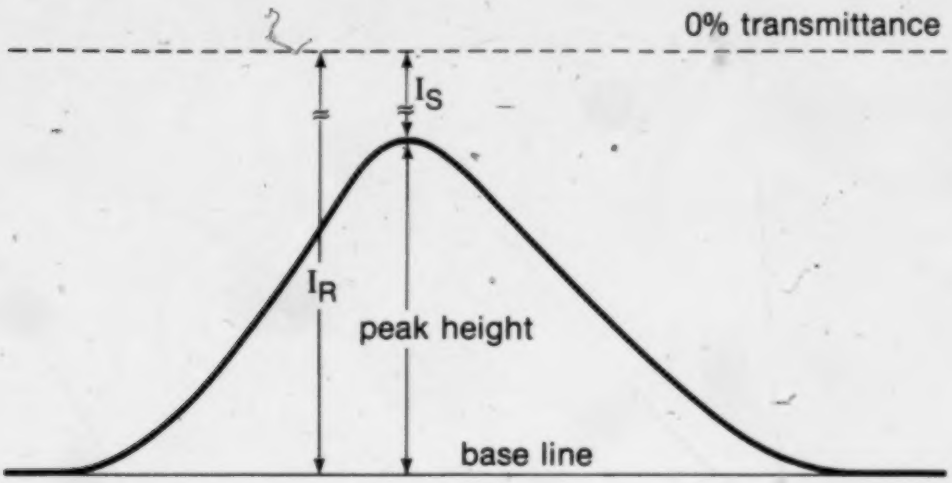

Figure A.1. Trace of SiX_2 absorption band.

where I_R is the lamp intensity reaching the spectrograph through the empty cell; and

I_S is the lamp intensity reaching the spectrograph in the presence of the sample.

From Figure A.1 the peak height of the absorption band is given by:

$$\text{peak height} = I_R - I_S$$

$$= I_R(1 - t)$$

$$= I_R(x) \qquad \text{(A.1)}$$

where t is the transmittance = I_S / I_R; and x is the absorption = 1 – t

Thus peak height $\propto$ absorption x

$\propto I_R$, *i.e.* the lamp intensity for that particular flash

According to Beer-Lambert's law,

$$\text{absorbance} = -\log_{10}(I_S / I_R) = acl \qquad \text{(A.2)}$$

where a (litre mol^{-1} cm^{-1}) is the molar extinction coefficient; $c(M)$ is the concentration; and l(cm) is the path length.

$$\log_{10}(I_S / I_R) = \log_{10} t = \log_{10}(1 - x) = -x \qquad \text{if } x << 1 \qquad \text{(A.3)}$$

Combining equations A.2 and A.3 yields:

$$x = acl \qquad \text{if } x << 1$$

Thus peak height $= acl(I_R)$ if $x << 1$,

i.e. at a constant l and I_R, peak height of the absorption spectrum of species SiX_2 is directly proportional to its concentration provided that the absorption $x << 1$.

Appendix B.

Calculation of the Absolute Rate Constant of the SiX_2 + S (X = Cl, Br; S = reactive substrates) Reaction:

A sample calculation of an absolute rate constant (*e.g.* of the $SiCl_2 + O_2$ reaction) is shown below.

Peak heights of the absorption profile of $SiCl_2$ recorded at different times during its decay in the absence and in the presence of a known concentration of O_2 were measured relative to the base line as shown in Figure B.1. The base line refers to the absorption profile of the empty cell.

Ln(peak height) was then plotted against time to obtain the decay curves of $SiCl_2$ in the absence and in the presence of O_2 as shown in Figure B.2.

Slope of the decay curve (1) = $-k_1$, the first-order rate constant for the decay of $SiCl_2$ in the absence of O_2; and

Slope of the decay curve (2) = $-k_2 = -(k_1 + k[O_2])$, the pseudo first-order rate constant for the decay of $SiCl_2$ in the presence of 0.06 Torr O_2, where k is the second-order rate constant for the reaction $SiCl_2 + O_2 \rightarrow$ Products.

Subtraction of the slope of the decay curve (1) from that of (2) gives $k[O_2]$, the corrected pseudo first-order rate constant for the decay of $SiCl_2$ in the presence of 0.06 Torr O_2. Such corrected pseudo first-order rate constants were obtained at different O_2 pressures and when plotted against $[O_2]$ yielded a linear plot as shown in Figure B.3,

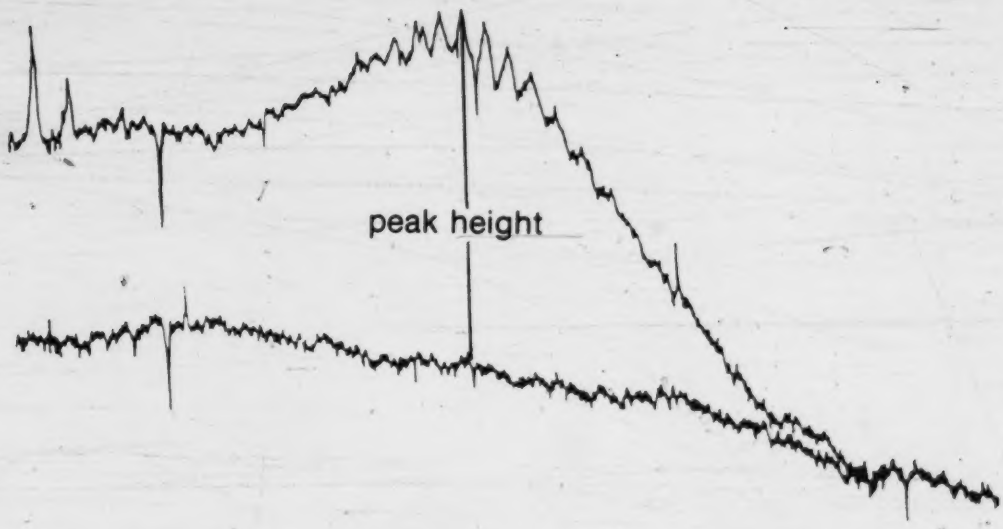

Figure B.1. Measurement of the peak height of the absorption profile of $SiCl_2$.
(Si_2Cl_6 = 0.2 Torr, O_2 = 0.06 Torr and Ar = 100 Torr, Time = 11μs)

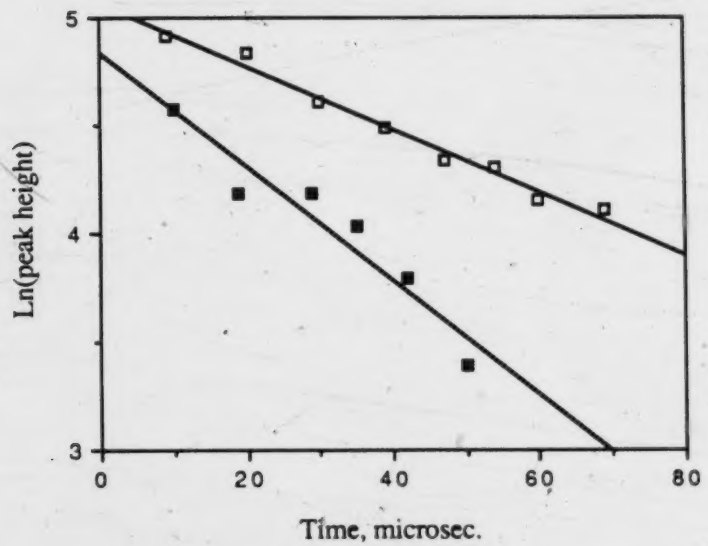

Figure B.2. Decay curves for [$SiCl_2$] in the absence (□) and presence (■) of 0.06 Torr oxygen.

which shows that the $SiCl_2 + O_2$ reaction is first order in $[O_2]$. The slope of this linear plot is k — the second-order rate constant of the reaction $SiCl_2 + O_2 \rightarrow$ Products.

$$k(SiCl_2 + O_2) = (3.4 \pm 0.2) \times 10^9\ M^{-1}s^{-1}.$$

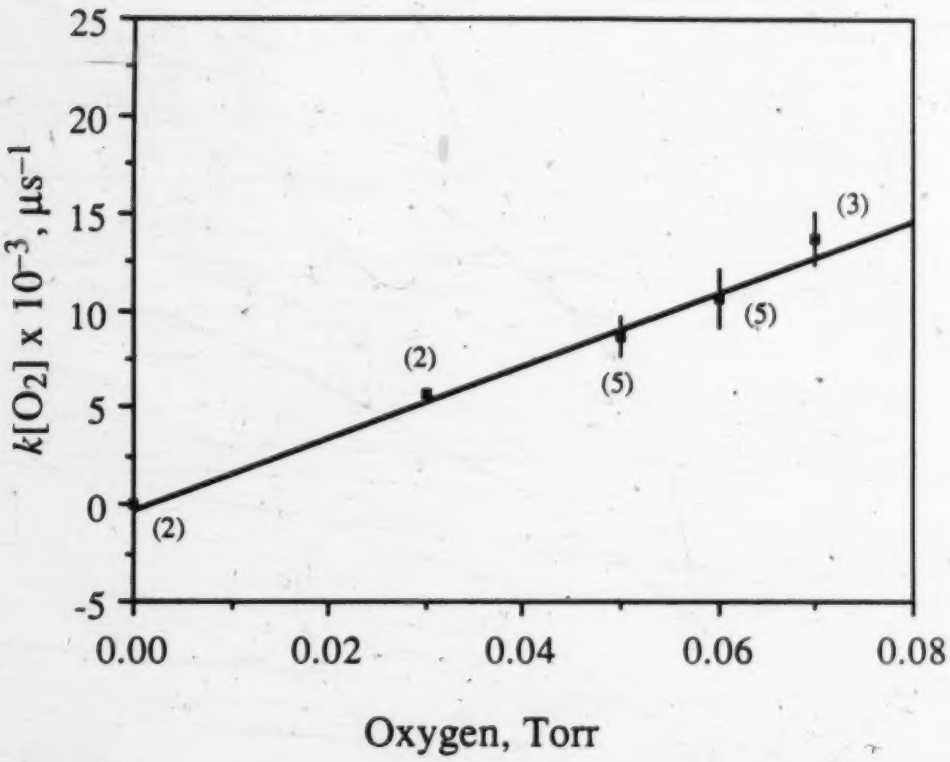

Figure B.3. Dependence of the pseudo first-order rate constants of $SiCl_2 + O_2$ reaction on the oxygen concentration. Numbers in the parentheses are the number of decay plots with 5 to 8 individual measurements.

Appendix C.

$SiCl_2$ Background Decay as a Function of Ar Pressure.

The background decay of $SiCl_2$ can be represented by the following reactions:

$$SiCl_2 + Si_2Cl_6 \longrightarrow Si_3Cl_8^* \qquad (C.1)$$

$$Si_3Cl_8^* \longrightarrow SiCl_2 + Si_2Cl_6 \qquad (C.2)$$

$$Si_3Cl_8^* + Ar \longrightarrow Si_3Cl_8 + Ar^* \qquad (C.3)$$

The observed rate of the background decay is a ratio of the rates of reactions C.2 and C.3:

$$R_2 = k_2[Si_3Cl_8^*]$$

$$R_3 = k_3[Si_3Cl_8^*][Ar]$$

$$R_{obs} = \frac{R_3}{R_2 + R_3} = \frac{k_3[Si_3Cl_8^*][Ar]}{(k_2 + k_3[Ar])[Si_3Cl_8^*]}$$

$$= \frac{k_3[Ar]}{k_2 + k_3[Ar]}$$

Since $k_{obs} \propto R_{obs}$, where k_{obs} is the observed rate constant for the background decay of $SiCl_2$, therefore

$$k_{obs} \propto k_3[Ar] / (k_2 + k_3[Ar]) \qquad (C.4)$$

In the absence of argon $k_{obs} = 0$ and in the presence of large pressures of argon, k_{obs} is constant.

Thus at low Ar pressure, Eq. C.4 predicts that k_{obs} should increase linearily with [Ar], but at high Ar pressure, k_{obs} should reach a plateau, in agreement with experimental observation.

Appendix D.

Calculation of Heat of Reaction:

All the heat of reaction values ($\Delta H^{\circ}_{rxn.}$) presented in this thesis were calculated from the standard heats of formation (ΔH°_{f}) of reactants and products using equation (D.1):

$$\Delta H^{\circ}_{rxn.} = \Sigma \Delta H^{\circ}_{f}(\text{products}) - \Sigma \Delta H^{\circ}_{f}(\textit{reactants}) \qquad \text{(D.1)}$$

when ΔH°_{f} values were not available, bond energies (D) were used to calculate $\Delta H^{\circ}_{rxn.}$ using

$$\Delta H^{\circ}_{rxn.} = \begin{pmatrix}\text{Total energy required}\\ \text{to break all bonds in}\\ \text{reactants)}\end{pmatrix} - \begin{pmatrix}\text{Total energy evolved}\\ \text{in forming all the}\\ \text{bonds in products)}\end{pmatrix} \qquad \text{(D.2)}$$

The thermochemical data used in the calculations are listed in Table D.1 and the calculated $\Delta H^{\circ}_{rxn.}$ values, for each reaction system, are presented in Table D.2.

Sample calculations of $\Delta H^{\circ}_{rxn.}$ using equations D.1 (*e.g.* for the $SiCl_2 + O_2$ reaction) and another using equation D.2 (*e.g.* for the $SiCl_2$ + 1,3-C_4H_6 reaction) are shown below.

(i) The $SiCl_2 + O_2$ Reaction:

$$SiCl_2 + O_2 \longrightarrow SiCl_2O_2 \qquad \text{(D.3)}$$

$$SiCl_2O_2 + O_2 \longrightarrow SiCl_2O + O_3 \qquad \text{(D.4)}$$

Table D.1. Thermochemical data used in the present study.

Species	ΔH_f°, kcal mol^{-1}	Reference
$SiCl_2$ (g)	-40.3 ± 0.8	[1]
$SiCl_2O$(g)	-167.7[a]	[2]
Si_2Cl_4 (g)	-129.5 ± 10	[3]
O_3 (g)	30.1[a]	[4]
NO(g)	21.6[a]	[4]
N_2O(g)	19.6[a]	[4]
CO(g)	-26.4[a]	[4]
C_2O(g)	89.0 ± 3	[5]
$SiBr_2$ (g)	-11 ± 2	[6]
$SiBr_2O$(g)	-137.3[a]	[2]

Bond	D, kcal mol^{-1}	Reference
C—C	82.9[a]	[7]
C=C	147.9[a]	[7]
Si—C	85.04[a]	[8]

[a] No uncertainity limits have been reported for these values.

The overall reaction is

$$SiCl_2 + 2O_2 \longrightarrow SiCl_2O + O_3 \qquad (D.5)$$

and $\Delta H^{\circ}_{rxn.}$ of reaction D.5 is given by

$$\Delta H^{\circ}_{rxn.} = \Delta H^{\circ}_f(SiCl_2O) + \Delta H^{\circ}_f(O_3) - \{\Delta H^{\circ}_f(SiCl_2) + 2\Delta H^{\circ}_f(O_2)\}$$

Substituting the ΔH°_f values from Table D.1 into the above equation gives

$$\Delta H^{\circ}_{rxn.} = (-167.7 + 30.1) - (-40.3)$$

$$= -97.3 \text{ kcal mol}^{-1}.$$

(ii) The $SiCl_2$ + 1,3-butadiene Reaction:

(D.6)

$\Delta H^{\circ}_{rxn.}$ for reaction D.6 can be obtained using equation D.2. In going from reactants to products, two C=C bonds are converted into two C—C bonds and one C—C bond is converted to a C=C bond; in other words, one C=C double bond is broken and one C—C single bond is formed. Two C—Si bonds are also formed in the products. Hence

$$\Delta H^{\circ}_{rxn.} = D(C{=}C) - \{D(C{-}C) + 2D(C{-}Si)\}$$

$$= 147.9 - \{82.9 + 2(85)\}$$

$$= -105 \text{ kcal mol}^{-1}.$$

Table D.2. Heats of reaction ($\Delta H^{\circ}_{rxn.}$) for SiX_2 + S systems (X = Cl, Br; S = O_2, NO, CO, N_2O and 1,3-C_4H_6).

System	Overall Reaction	$\Delta H^{\circ}_{rxn.}$, kcal mol^{-1} *
$SiCl_2$ / O_2	$SiCl_2 + 1/2\ O_2 \rightarrow Cl_2SiO$	− 127.4 ± 0.8
	$SiCl_2 + 2O_2 \rightarrow Cl_2SiO + O_3$	− 97.3 ± 0.8
$SiCl_2$ / NO	$SiCl_2 + 2NO \rightarrow Cl_2SiO + N_2O$	− 151.0 ± 0.8
	$SiCl_2 + NO \rightarrow Cl_2SiO + 1/2\ N_2$	− 149.0 ± 0.8
$SiCl_2$ / CO	$SiCl_2 + 2CO \rightarrow Cl_2SiO + C_2O$	14.4 ± 3.8
	$SiCl_2 \rightarrow 1/2\ Cl_2Si{=}SiCl_2$	− 24.3 ± 10.8
$SiCl_2$ / N_2O	$SiCl_2 + N_2O \rightarrow Cl_2SiO + N_2$	− 147.0 ± 0.8
$SiCl_2$ / 1,3-C_4H_6	$SiCl_2$ + 1,3-C_4H_6 → 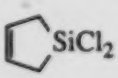	− 105.0 ± 0.8
$SiBr_2$ / O_2	$SiBr_2 + 1/2\ O_2 \rightarrow Br_2SiO$	− 126.3 ± 2
	$SiBr_2 + 2O_2 \rightarrow Br_2SiO + O_3$	− 96.2 ± 2
$SiBr_2$ / NO	$SiBr_2 + 2NO \rightarrow Br_2SiO + N_2O$	− 149.9 ± 2
	$SiBr_2 + NO \rightarrow Br_2SiO + 1/2\ N_2$	− 147.9 ± 2

* Uncertainities correspond to those in the ΔH°_{f} data.

References:

1. JANAF Thermochemical Tables, 1982 Supplement, J. Phys. Chem. Ref. Data 11 (1982) 695.

2. G. Dittmer and U. Niemann, Philips J. Res., 37 (1982) 1.

3. T.N. Bell, A.F. Kieran, K.A. Perkins and P.G. Perkins, J. Phys. Chem., 88 (1984) 1334.

4. The NBS Tables of the Chemical Thermodynamic Properties, J. Physical and Chemical Ref. Data, ACS Publication, vol. 11, Supplement No. 2 (1982).

5. S.P. Walch, J. Chem. Phys., 72 (1980) 5679.

6. R. Walsh, J. Chem. Soc. Farad. Trans. I, 79 (1983) 2233.

7. Standard Value.

8. T.N. Bell, K.A. Perkins and P.G. Perkins, J. Chem. Soc. Farad. Trans. I, 77 (1981) 1779.

Appendix E.

Estimation of E_a Values:

The activation energies (E_a) of all the reactions studied in the present work were estimated using the Arrhenius equation.

$$\log k = \log A - \frac{E_a}{2.303\ RT} \qquad \text{(E.1)}$$

where k is the absolute rate constant in $M^{-1}s^{-1}$;

R is the gas constant = 1.987×10^{-3} kcal mol^{-1} K^{-1};

T is temperature (K);

and A is the pre-exponential factor, whose value can be estimated from the gas-kinetic expression:

$$A = \pi(r_A + r_B)^2 \sqrt{\frac{8kT}{\mu\pi}} \qquad \text{(E.2)}$$

where μ is the reduced mass and is given by $1/\mu = 1/m_A + 1/m_B$ (m_A and m_B are masses of reactants A and B), r_A and r_B are the molecular radii of colliding molecules A and B, assumed to be solid spheres, and k is Boltzman's constant = 1.38066×10^{-23} $J.K^{-1}$.

Values of the molecular radii r_A (of silylene SiX_2) and r_B (of the reactive substrate) used in these calculations are listed in Table E.1 and the values of the A-factors and E_a's obtained from such calculations are listed in Table E.2. A sample calculation of the A-factor and E_a for the $SiCl_2 + O_2 \rightarrow SiCl_2O_2$ reaction, is shown below.

Table E.1. Molecular radii used in the estimation of *A*-factors.

Species	r, Å	Reference
$SiCl_2$	2.20	[a]
$SiBr_2$	2.39	[a]
O_2	1.48	[4]
NO	1.50	[b]
CO	1.90	[4]
N_2O	2.5	[b]
1,3-C_4H_6	3.0	[5][c]

[a] Estimated values using equation E.3 and following values of Si—X bond distances r"(Si—X), and θ(XSiX):

for X = Cl: r" = 2.083Å [1], θ = 103.3° [1, 2, 3]; for X = Br: r" = 2.243Å [1], θ = 105.9 [1, 3]

[b] Assumed value from the periodic trend of atomic radii.

[c] Distance of closest approach between 1,3-butadiene and $SiCl_2$.

$k(SiCl_2 + O_2) = (3.4 \pm 0.2) \times 10^9\ M^{-1}s^{-1}$

T = 298K; $1/\mu = 0.0414$; $r_{O_2} = 1.48$Å [1]

$r_{SiCl_2} = 2.20$Å — was estimated as follows:

Since $SiCl_2$ is bent (θ(ClSiCl) = 103.3°) and was assumed to be solid sphere, $r_{SiCl_2} = 2.20$Å represents the effective collisional molecular radius instead of the molecular radius and was estimated using equation E.3.

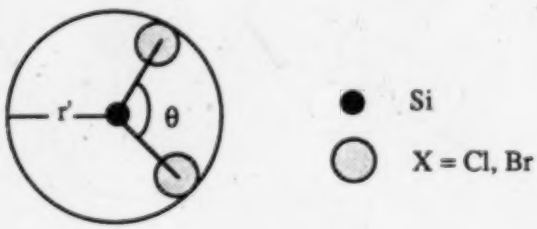

$$r_{SiCl_2} = r'_{SiCl_2} \times \left(\frac{360 - \theta}{360}\right) \qquad \text{(E.3)}$$

r'_{SiCl_2} = molecular radius of $SiCl_2$, approximately equal to the sum of the Si—Cl bond distances and the atomic radius of chlorine: = (2.083 + 1.0) = 3.083Å.

Substitution of these values in equation E.2 gives

$$A = 5.35 \times 10^{11}\ M^{-1}s^{-1}$$

which, along with the value of $k(SiCl_2 + O_2)$ obtained from the present work, yields the following value as an upper limit of E_a:

$$E_a \sim 3.0 \text{ kcal mol}^{-1}.$$

Table E.2. Arrhenius parameters for SiX_2 + S reactions.

Reaction	k, $M^{-1}s^{-1}$	A x 10^{-11}, $M^{-1}s^{-1}$	Ea, kcal mol^{-1}
$SiCl_2 + O_2$	$(3.4 \pm 0.2) \times 10^9$	5.35	~3.0
$SiCl_2 + NO$	$(1.6 \pm 0.1) \times 10^9$	5.53	~3.5
$SiCl_2 + CO$	$(6.3 \pm 0.7) \times 10^8$	6.98	~4.2
$SiCl_2 + N_2O$	$(5.7 \pm 0.3) \times 10^8$	7.76	~4.3
$SiCl_2 + 1,3\text{-}C_4H_6$	$(5.4 \pm 0.3) \times 10^8$	3.07	~3.8
$SiBr_2 + O_2$	$(5.6 \pm 0.4) \times 10^8$	5.56	~4.1
$SiBr_2 + NO$	$(2.8 \pm 0.4) \times 10^8$	5.77	~4.5

References:

1. I. Hargittai, G. Schultz, J. Tremmel, N.D. Kagramanov, A.K. Maltsev and O.M. Nefedov, J. Am. Chem. Soc., 105 (1983) 2895.

2. V.A. Svyatkin, A.K. Maltsev and O.M. Nefedov, Izv. Akad. Nauk SSSR, Ser. Khim., No. 10 (1977) 2236.

3. G. Maass, R.H. Hauge and J.L. Margrave, Z. Anorg. Allg. Chem., 392 (1975) 295.

4. "Physical Chemistry" J. Moore, 2nd ed., Englewood Cliffs, N.J., (1956) p. 179.

5. A.I. Ioffe, L.I. Korzhenevich, S.P. Kolesnikov and O.M. Nefedov, Izv. Akad. Nauk SSSR, Ser. Khim., No. 2 (1976) 343.